STRUCTURAL RELIABILITY ASSESSMENT UNDER FIRE

by

Qianru Guo

A dissertation submitted in partial fulfillment
of the requirements for the degree of
Doctor of Philosophy
(Civil Engineering)
in the University of Michigan
2015

Doctoral Committee:

Assistant Professor Ann E. Jeffers, Chair
Professor Sherif El-Tawil
Professor Krishnakumar R. Garikipati
Associate Professor Jeffrey T. Scruggs

DEDICATION

This work is dedicated to my husband, Xiaohu,
and parents, Jian and Li, for their support,
encouragement, and love.

ACKNOWLEDGEMENT

Throughout my study at University of Michigan, I have been fortunate to get mentorship, friendship, and love in addition to a doctoral degree. I would like to thank everyone at University of Michigan who has contributed to my research, my education, and my life. In particular, I am grateful that I met a great advisor and person, Dr. Ann E. Jeffers, who has offered me continuous mentorship, guidance, and friendship. It was her encouragement and support that helped me through the many times when I doubted myself. Her competency, passion, and high standards on work and research had a deep impact on shaping the scholar that I am today. I would also like to acknowledge Dr. El-Tawil, Dr. Garikipati, and Dr. Scruggs for their commitment and their helpful comments and suggestions. I would also like to acknowledge the U.S. National Science Foundation (Grant No. CMMI-1032493) for supporting this study.

TABLE OF CONTENTS

LIST OF FIGURES

LIST OF TABLES

ABSTRACT

Structural safety under fire has received significant attention in recent years. Current approaches to structural fire design are based on prescriptive codes that emphasize insulation of steel members to achieve adequate fire resistance. The prescriptive approach fails to give a measure of the true performance of structural systems in fire and gives no indication of the level of reliability provided by the structure in the face of uncertainty. The performance-based design methodology overcomes many of the limitations of the prescriptive approach. The quantification of the structural reliability is a key component of performance-based design as it provides an objective manner of comparing alternative design solutions. In this study, a probabilistic framework is established to evaluate the structural reliability under fire considering uncertainties that exist in the system. The structural performance subjected to realistic fires is estimated by numerical simulations of sequentially coupled fire, thermal, and structural analyses. In this dissertation, multiple reliability methods (i.e., Latin hypercube simulation, subset simulation, and the first/second order reliability methods) are extended to investigate the structural safety under fire.

The reliability analysis of structures in fire involves (i) the identification and characterization of uncertain parameters in the system, (ii) a probabilistic analysis of the thermo-mechanical response of the structure, and (iii) the evaluation of structural reliability based on a suitable limit state function. Several applications are considered involving the response of steel and steel-concrete composite structures subjected to natural fires. Parameters in the fire, thermal, and structural models are characterized, and an improved fire hazard model is proposed that accounts for fire spread to adjacent rooms. The importance of various parameters is determined by considering the response sensitivity, which is determined by finite difference and direct differentiation methods. The accuracy and efficiency of the various reliability methods, as applied to structures in fire, are compared, and the strengths and weaknesses of each approach are identified.

Latin hypercube simulation is found to provide an accurate estimate of the reliability, although the method requires significant computational expense. The gradient-based first-order and second-order reliability methods are applied to the structural fire problem, and an in-depth analysis is conducted to evaluate the response surface. It is found that the first-order reliability method provides a rapid estimation of the component-level reliability but has limited applicability to structures in fire due to the nonlinear response surface. The subset simulation methodology is applied to determine the response of a steel-concrete composite floor system, and it is found that the methodology yields acceptable accuracy and results in significant cost-savings over the Latin hypercube simulation. The analyses presented herein give a better understanding of the uncertainties that exist in the structural fire problem and their influence on the structural performance.

CHAPTER 1 : INTRODUCTION

Building fire protection systems are typically a combination of active and passive fire protection systems. The active fire protection system includes the automatic fire detection and sprinkler systems, which actively detect fires, control fire spread, and alert building occupants in the case of fire. On the other hand, the passive fire protection system helps to control the spread of fire and ensure structural integration. The current design of structural fire protection mainly follows the prescriptive requirements given by the International Building Code (IBC 2006) and NFPA 5000 Building Construction and Safety Code (NFPA 2005). A minimum fire resistance rating is given for each structural member based on the building use, and the fire protection material needed to achieve the fire resistance rating is specified based on the qualification testing under a standard fire exposure (e.g., ASTM E 119). This prescriptive approach ensures that buildings provide at least a minimum level of safety; however, this design philosophy has been criticized in recent years as it limits the application of new fire protection technologies and ignores the true performance of structures under elevated temperature. To address the limitations of prescriptive design, the performance-based design methodology is receiving more attention in both the structural engineering and fire protection engineering communities. Performance-based design has been widely applied in earthquake engineering and wind engineering. However, more research is needed to understand the structural response under realistic fire conditions before performance-based design can be confidently applied in structural fire engineering. This is one of the major motivations behind the recent interest in structural-fire research in the United States.

The work described herein is meant to contribute to this widespread effort to develop a framework to quantify the structural reliability level under fire. Although this dissertation covers a wide range of topics, the central theme of this study is to establish a framework to evaluate structural reliability under a potential post-flashover fire by considering

possible uncertainties within the analytical system. Under this general theme, we see the development of the proposed reliability analysis framework and its application.

The first section of this chapter provides an overview of the framework to the structural reliability analysis under fire and defines the scope of the project. The organizational structure of the dissertation is described in the second section.

1.1 Overview and Scope of the Project

In prescriptive design, neither the deterministic safety factor nor the probability-based reliability index can be quantified as the design is based solely on the fire resistance rating of isolated structural members under the standard fire exposure. On the other hand, the performance-based fire resistance design has shown the potential to apply more flexible design strategies and to determine the safety margin of a building. The reliability evaluation plays an important role in determining how well the performance goals are achieved for a specified design strategy; however, there is no well-established framework for the structural reliability assessment under fire.

The proposed reliability analysis framework involves the simulation of structural systems in fire and the related reliability analysis methods. The multi-physics simulations involve fire simulation, thermal analysis, and structural analysis. Various fire models, heat transfer analysis methods, and structural analysis methods have been involved in this study, and they have been sequentially-coupled together by the transfer of temperature data of structural members to simulate the structural performance under realistic fire scenarios. Both statistical reliability methods and analytical methods have been applied in the framework to check their applicability, accuracy, and efficiency for the multi-physics problem.

The scope of this study focuses on calculating the failure probability of a structure when a flashover fire occurs. The reliability values reported in this study are conditional values. They contribute to the holistic risk assessment, giving decision makers more comprehensive information of the potential for major structural failure due to fire. The following main tasks are conducted to achieve the goal of this research:

Task 1 – Numerical Modelling of Structures under Fire:

- Conduct realistic fire simulation based on the parametric fire curve and the zone fire model
- Apply analytical method and finite element method for the thermal analysis of structural members under fire
- Analyze the structural performance under elevated temperature for structural members and structural systems using the finite element method
- Sequentially couple the fire simulation, thermal analysis, and mechanical analysis
- Validate the numerical models through comparison with the experimental tests results reported in literatures

Task 2 –Reliability Assessment of Structures under Fire:

- Identify uncertainties that exist in the structural-fire simulation
- Introduce the direct differentiation method to the sequentially coupled thermo-structural model with nonlinear, temperature-dependent material properties for sensitivity analysis and gradient-based reliability analysis
- Extend existing reliability methods (Latin Hypercube simulation, subset simulation, and first/second order reliability methods) to the structural-fire problem
- Compare the advantages and disadvantages of different methods in the context of structural fire engineering

1.2 Organization

The organizational structure of this dissertation follows the manuscript format, in which the standard dissertation chapters are replaced by manuscripts that will be submitted or have already been published in refereed technical journals. This dissertation consists of the following chapters:

Chapter 1 provides a brief introduction of the background and motivation for this research on the structural reliability assessment under fire.

Chapter 2 is a journal paper entitled "Probabilistic Evaluation of Structural Fire Resistance", which has been published in *Fire Technology* journal. This paper establishes the reliability evaluation framework for structures under fire. The reliability of a protected beam under realistic fire exposure has been assessed by the Latin Hypercube method.

Chapter 3 is a journal paper entitled "Direct Differentiation method for response sensitivity analysis of structures in fire", which has been published in *Engineering Structures*. The direct differentiation method has been introduced to calculate response sensitivity and gradient in the thermo-mechanical simulation.

Chapter 4 is a journal paper entitled "Finite-Element Reliability Analysis of Structures Subjected to Fire", which has been published in *Journal of Structural Engineering*. The first-order reliability method and second-order reliability method have been extended to the structural reliability problem under fire to perform efficient calculations of structural reliability.

Chapter 5 is a manuscript entitled "Evaluating the Reliability of Structural Systems in Fire using Subset Simulation", which will be submitted for publication in the *Fire Safety Journal*. A comprehensive fire model accounting for fire spread is included along with a 3D model of a composite floor system. Both Latin Hypercube method and subset sampling method have been applied in this study.

Chapter 6 summarizes the findings of this research and discusses directions for future work.

Reference

IBC (2006). International Building Code, Falls Church, VA.

NFPA (2005). *NFPA 5000: Building Construction and Safety Code*, National Fire Protection Association, Quincy, MA.

CHAPTER 2 : PROBABILISTIC EVALUATION OF STRUCTURAL FIRE RESISTANCE USING LATIN HYPERCUBE SIMULATION[1]

2.1 Introduction

Regardless of whether a structural design is prescriptive or performance-based, it is essential that the designer has a sense of the level of risk associated with the design. However, current design practices that are deeply rooted in the standard fire test fail to yield any information about the reliability of the structure, particularly because all that is gained from the test is the time duration to failure under standard fire exposure. Although the prescriptive method is generally considered to be overly conservative (Bailey 2006), there is no way to actually quantify the level of conservatism in existing designs. The prescriptive methodology has thus resulted in a practice in which structural reliability is indeterminate (Fellinger and Both 2000, Lange et al. 2008) and inconsistent with the design for other hazards such as wind and earthquake (Ellingwood 2005). Research that has led to performance-based methods of structural fire design has provided an improved understanding of structural fire resistance, and it could be argued that recent advances have finally made possible the in-depth exploration of the reliability of structures in fire.

Aside from the philosophical basis for a reliability-based design methodology, the probabilistic treatment of structural performance in fire is matter of practicality in understanding structural responses observed in fire resistance tests. For instance, even in standard fire tests, a large amount of scatter can be observed in results from different testing facilities due to variations in the heating conditions, material properties of the specimens, magnitudes of applied loads, and the degree of restraint provided by the

[1] Contents of this chapter have been published as Guo, Q., Shi, K., Jia, Z., and Jeffers, A.E, "Probabilistic Evaluation of Structural Fire Resistance," *Fire Technology*, 49, 793-811, 2012. Co-author Kaihang Shi conducted a preliminary analysis that helped form the basis of this research. Co-author Zili Jia assisted with the program realization on the Flux system.

surrounding structure (Witteveen and Twilt 1981/1982). Additionally, the fire resistance of steel structures is heavily dependent on the level of fire protection that is present, yet cementitious spray-applied fire resistant materials (SFRMs) and intumescent coatings have large variability due to the nature of the materials, the manner in which they are applied in the field, and their adhesion and durability characteristics (Ryder et al. 2002).

The topic of structural reliability in fire is not new, but a review of literature reveals that coverage of the topic is incomplete at this point in time. Early works (e.g., Magnusson and Pettersson 1980/81) provided fundamental insight and demonstrated that the subject was certainly worthy of contemplation; however, progress was limited to the rudimentary technology of the time. More recently, reliability theory has been applied to the structural fire problem, specifically, to derive load and resistance factors for inclusion in structural specifications (Ellingwood 2005, Iqbal and Harichandran 2010, and Iqbal and Harichandran 2011, Vaidogas and Juocevicius 2008, Huang and Delichatsios 2010, and Khorasani et al. 2012), to account for high levels of uncertainty observed in experimental tests (Hietaniemi 2007, Sakji et al. 2008, Jensen et al. 2010, and Van Coile et al. 2011), and to enable risk-informed decision-making (Fellinger and Both 2000, Lange et al. 2008, Vaidogas and Juocevicius 2008, Huang and Delichatsios 2010, and Khorasani et al. 2012). Research to date has addressed a range of issues concerning the probabilistic modeling of structures in fire but has not fully addressed the multi-physical nature of the problem and the high order of dimensionality.

The work described herein seeks to utilize probabilistic methods to evaluate the fire resistance of structures given uncertainties in key model parameters. The proposed methodology accounts for uncertainty stemming from the fire exposure and structural resistance parameters. The approach is capable of providing a quantitative measure of the structure's reliability, thus giving designers the ability to rationally evaluate the robustness provided by various design options. Prior research has provided little guidance in the selection of parameters to be treated as probabilistic and the definition of suitable limit state functions for various types of structures. In this study, the model dimensionality (i.e., the number of probabilistic parameters) is reduced using a sensitivity

analysis and limit state functions are defined based on deflection criteria used in fire resistance tests.

The probabilistic framework is demonstrated through an analysis of a protected steel beam given uncertainties in the fire load and structural resistance parameters. Analyses were conducted via a sequentially coupled, stochastic finite element simulation embedded within a Monte Carlo simulation. The research demonstrates that a probabilistic treatment of the structural fire problem yields a wealth of data that may lead to a better understanding of the factors affecting structural fire resistance. Furthermore, reliability-based assessments of structural performance in fire provide necessary data that enables risk-informed decision making, which is an essential component of performance-based design.

2.2 Background

A reliability-based methodology for engineering design requires consideration for uncertainty in the system parameters $\boldsymbol{X} = (X_1, X_2, \ldots X_n)$. Structural resistance R and load demand S are both random variables, which are dependent on $\boldsymbol{X}$ and characterized by statistical properties such as the mean μ, standard deviation σ, and probability distribution f. To determine the reliability of the system, one needs to define a performance function $G(\boldsymbol{X}) = R(\boldsymbol{X}) - S(\boldsymbol{X})$ to evaluate the limit of resistance. Failure is said to occur when the demand S exceeds the capacity R of the system, i.e., when $G(\boldsymbol{X}) < 0$, as illustrated by the shaded region in Fig. 2-1.

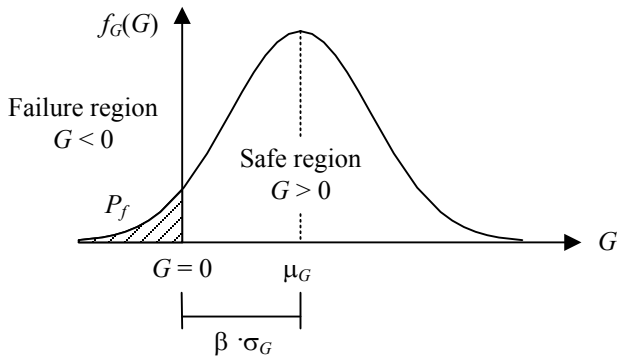

Figure 2-1 Characteristics of performance function *G* (adapted from Choi et al. 2007)

The failure probability P_f is defined as the probability that $G(\boldsymbol{X}) < 0$, or

$$P_f = P[G(\boldsymbol{X}) < 0]. \tag{1}$$

Failure can also be expressed in terms of a reliability index β, which denotes the distance the failure surface, as shown in Fig. 2-1. If the probability density function f_X for the random variables X_i are known, then the failure probability can be determined by integrating the joint probability density functions over the failure region (Puatatsananon and Saouma 2006), i.e.,

$$P_f = \int_{g(\mathbf{X})<0} f_{\boldsymbol{X}}(\boldsymbol{X}) d\boldsymbol{X}. \tag{2}$$

In most applications, Eq. (2) is too complex to be evaluated analytically and so numerical methods are generally employed to conduct the reliability analysis. Existing methods include the first-order and second-order reliability methods, the response surface method, and Monte Carlo simulation. Most methods for reliability analysis are well-established and used in a range of engineering fields (Huang and Delichatsios 2010, Nowak and Collins 2000, and Singh et al. 2007).

A safe design is achieved by ensuring that the probability of failure is acceptably small. This is often realized in industry through the use of safety factors. For example, in current codes for structural design (e.g., AISC 2005), load and resistance factors alter the design load S and structural capacity R such that the chances of failure are suitably small given expected uncertainty in the system.

Alternatively, a reliability analysis can be carried out to evaluate a system's reliability under an anticipated load event. The latter forms the basis for risk-based engineering, which allows trade-offs in cost and utility to be explored to identify the best engineered solution given a target performance level (Singh et al. 2007).

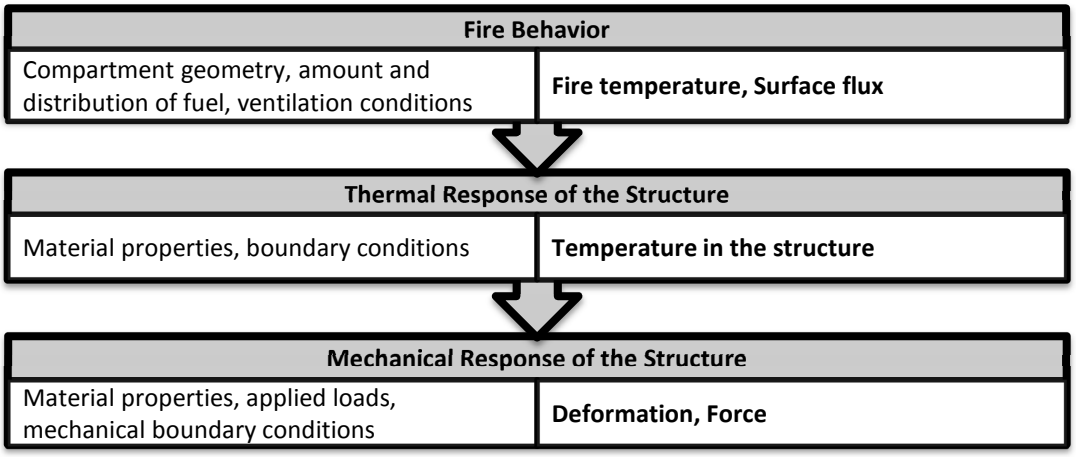

Figure 2-2 Propagation of uncertainty in the structural fire simulation

In the context of fire safety engineering, a reliability-based methodology can be employed; however, additional work is needed to extend the theory to account for the interdependencies between multiple physical domains. This interdependency is illustrated in Fig. 2-2, in which structure-fire interaction is shown as a sequentially coupled process. Model inputs are shown in the left column, while model outputs are shown on the right. A stochastic analysis of the system involves a propagation of uncertainty that affects each stage of the response. For example, uncertainty in the compartment geometry, type and distribution of fuel, ventilation conditions, and performance of fire protection measures lead to an uncertain fire load, which influences the temperature distribution in the structure and ultimately affects the mechanical response of the structure. Additional uncertainty associated with the material properties of the structure, the thermal and structural boundary conditions, and magnitude of mechanical loads are introduced at subsequent stages of the analysis and further affect the structural response.

Probabilistic simulation of fire-structure interaction can be rather involved due to the multi-physical nature of the problem and the high order of dimensionality. A probabilistic treatment of the problem requires: (1) the identification and characterization of the sources of uncertainty in the model, (2) the definition of appropriate performance function(s) by which failure can be evaluated, (3) the development of a stochastic model for the system that captures the propagation of uncertainty illustrated in Fig. 2-2, and (4)

the quantification of the system reliability, which is generally expressed in terms of a failure probability P_f or reliability index β.

In the present study, a response sensitivity analysis was conducted to identify the factors which have the greatest effect on the mechanical response of the structure. Probabilistic characteristics were then defined for parameters whose uncertainty had a strong influence on the response. A stochastic simulation was subsequently carried out to evaluate the response of the system given uncertainty in key model parameters. Based on a prescribed performance function, the system reliability was then quantified. For stochastic modeling, the Monte Carlo simulation technique was chosen due to its versatility and ability to account for the propagation of uncertainty from the fire to the thermal and structural models. The methodology is demonstrated by an application in which the reliability of a protected steel beam is evaluated given uncertainty in the fire load and structural resistance parameters.

2.3 Application: Protected Steel Beam Exposed to Compartment Fire

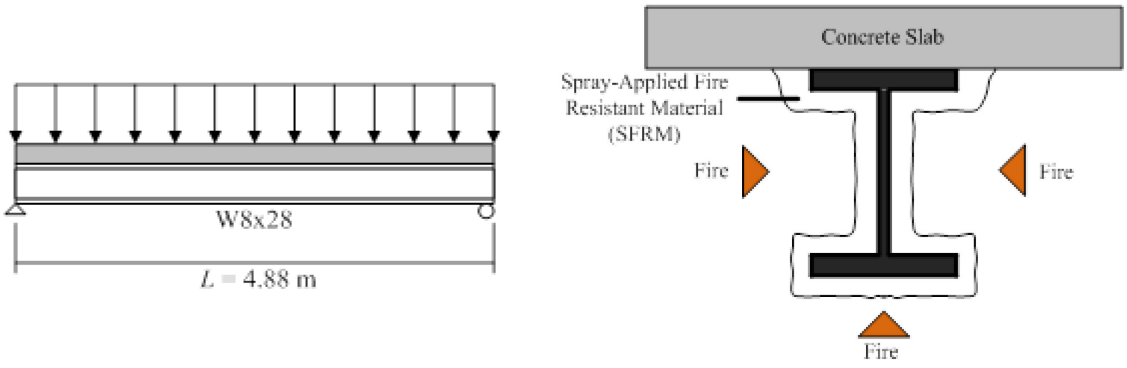

(a) (b)

Figure 2-3 Protected steel beam exposed to fire: (a) loading, and (b) cross-section

To illustrate the proposed framework, numerical simulations were conducted for a protected steel beam exposed to natural fire. As illustrated in Fig. 2-3a, the beam was simply supported and carried a uniformly distributed load w, which contained both dead and live load components of 5.15 kN/m and 3.65 kN/m, respectively. The beam supported a concrete slab, which was assumed to act non-compositely with the beam. Thus, the concrete slab influenced the temperature profile in the section but did not

contribute to the structural performance. The steel had a nominal yield strength of 345 MPa and a cross-section of W8x28. Based on the loading, a smaller section could have been used to satisfy the strength requirement according to the AISC design specification (AISC 2005). However, a minimum section of W8x28 was required to meet the ANSI/UL 263 listed fire protection. As shown in Fig. 2-3b, the beam was protected by a cementitious spray-applied fire resistant material with 11.1mm thickness such that the beam achieved a 1 h fire resistance rating.

Natural fire exposure was modeled using the Eurocode parametric fire (EC1 2005). Specifically, the fire temperature T_f (ºC) is given as

$$T_f = 20 + 1325(1 - 0.324e^{-0.2t^*} - 0.204e^{-1.7t^*} - 0.472e^{-19t^*}) \tag{3}$$

where t^* is a fictitious time given by

$$t^* = \Gamma t \,. \tag{4}$$

Here, t is the time (hours) and Γ is given as

$$\Gamma = \frac{(O/b)^2}{(0.04/1160)^2}, \tag{5}$$

where O is the opening factor and b is the thermal inertia of the surroundings. Knowing the fire load per total surface area $q_{t,d}$, the duration of burning $t^*_{\max}$ can be calculated as

$$t^*_{\max} = \max\left(0.2\times10^{-3}\cdot\frac{q_{t,d}}{O},\quad t_{\lim}\right). \tag{6}$$

The limiting temperature $t_{\lim}$ is taken as 20 min, assuming a medium growth fire (Lennon et al. 2007). After time $t^*_{\max}$ the fire is assumed to decay according to the rate defined in (EC1 2005), i.e.,

$$T_f = \begin{cases} T_{\max} - 625(t^* - t^*_{\max}) & \text{for } t^*_{\max} \le 0.5 \\ T_{\max} - 250(3 - t^*_{\max})(t^* - t^*_{\max}) & \text{for } t^*_{\max} \le 2 \\ T_{\max} - 250(t^* - t^*_{\max}) & \text{for } t^*_{\max} > 2 \end{cases} . \quad (7)$$

Note that the Eurocode fire model accounts for some of the parameters that are expected to introduce uncertainty in the fire behavior such as the compartment geometry and the amount of fuel, but it cannot capture effects such as the spatial distribution in the fuel.

The objective of the analysis was to evaluate the performance of the beam under a natural fire given uncertainty in the fire load and structural resistance parameters. The stochastic model for the system was based on the Monte Carlo method, in which a large number of deterministic simulations were carried out for a representative population of the random parameters. The number of simulations needed to accurately predict the failure probability is dependent on the magnitude of the failure probability. However, it is not possible to know the magnitude of the failure probability prior to running the simulation. Using classical Monte Carlo sampling, a failure probability of 0.01 can be calculated with 20 percent error using 10,000 samples (Haldar and Mahadevan 2000). A preliminary analysis demonstrated that the failure probability was likely to be greater than 0.01 in the present study, indicating that 10,000 sample values would allow the failure probability to be calculated with sufficient accuracy (i.e., an error of less than 20 percent). For a system with n random parameters, classical Monte Carlo sampling would have required $10{,}000^n$ simulations. In the present study, Latin hypercube sampling (Helton and Davis 2003) was used to reduce the total number of simulations to 10,000.

Each Monte Carlo calculation required a sequentially coupled thermo-mechanical analysis of the system, which was conducted in a finite element code that was programmed in Matlab (MATLAB, v.7.11 2010). Heat transfer over the cross-section was modeled using a fiber-based heat transfer element formulated by (Jeffers and Sotelino 2009). The mechanical response was subsequently modeled using two-dimensional beam elements. Temperatures in the flanges and web were obtained from the heat transfer analysis and transferred directly into the structural model. It should be noted that simplifications in the thermal and structural models were introduced to keep the analysis within a reasonable bounds. For example, in the heat transfer analysis, the

concrete slab was conservatively treated as an insulated boundary at the steel-concrete interface to reduce the total number of parameters in the model. This simplification resulted in somewhat higher temperatures in the upper flange than if the concrete slab had been modeled explicitly in the heat transfer analysis.

2.3.1 Deterministic analysis

The beam shown in Fig. 2-3 was first modeled deterministically to evaluate the response (a) under standard fire exposure, and (b) under natural fire exposure. For standard fire exposure, the standard ISO 834 (ISO 1999) temperature-time curve was imposed. For natural fire exposure, the fire temperature was calculated according to Eqs. (3)-(7). The opening factor O was assumed to be 0.04 $m^{1/2}$ to ensure that the fire was ventilation-controlled (Buchanan 2001). The thermal inertia b of 432.5 $Ws^{1/2}/m^2K$ was used based on the assumption that the walls and ceiling were lined with gypsum board (Iqbal and Harichandran 2011). A fuel load density of 564 MJ/m^2 per unit floor area was chosen based on the mean value reported by (Culver 1976). The fuel load density was transformed to total surface area based on an assumed compartment that was 6.1m wide, 4.9m deep, and 3m high.

In the heat transfer analysis, the exposed surfaces were heated by convection and radiation assuming that the convection heat transfer coefficient h was 25 W/m^2K under standard fire exposure and 35 W/m^2-K under natural fire exposure, and the effective emissivity ε of the structural surface was 0.80 (EC1 2005). The SFRM had a nominal thickness of 11.1 mm to achieve a 1-hour rating. The nominal thickness was used under standard fire exposure assuming controlled testing conditions. However, the design thickness was increased by 1.6 mm under natural fire exposure based on the fact that the SFRM thickness in the field is generally higher than the design thickness (Iqbal and Harichandran 2010). The SFRM was assumed to have a density of 300 kg/m^3, a conductivity of 0.12 W/m-K, and a specific heat capacity of 1200 J/kg-K (Buchanan 2001). The temperature-dependent thermal and mechanical properties for steel were taken from the Eurocode (EC3 2005).

In the structural model, the design dead and live loads of 5.15 kN/m and 3.65 kN/m, respectively, were combined to determine the total distributed load acting on the beam. Under standard fire exposure, the total distributed load (6.98 kN/m) was obtained by adding the dead load and half of the live load according to standard testing procedures. Under natural fire exposure, arbitrary-point-in-time dead and live loads were used to simulate the actual load that might be acting on the structure in the rare event of a fire. To get the arbitrary-point-in-time dead w_{DL} and live w_{LL} loads, the design dead load was multiplied by a factor of 1.05 (Iqbal and Harichandran 2010) and the design live load was multiplied by a factor of 0.24 (Ellingwood 2005 and Iqbal and Harichandran 2010). The total distributed load w was calculated according to

$$w = E(Aw_{DL} + Bw_{LL}), \tag{8}$$

where A, B, and E are stochastic parameters that account for variability in the loads (Iqbal and Harichandran 2010 and Ravindra and Galambos 1978). Parameters A, B, and E have mean values of 1.0 (Iqbal and Harichandran 2010 and Ravindra and Galambos 1978). For deterministic analysis under natural fire exposure, the applied load was therefore taken as 6.28 kN/m.

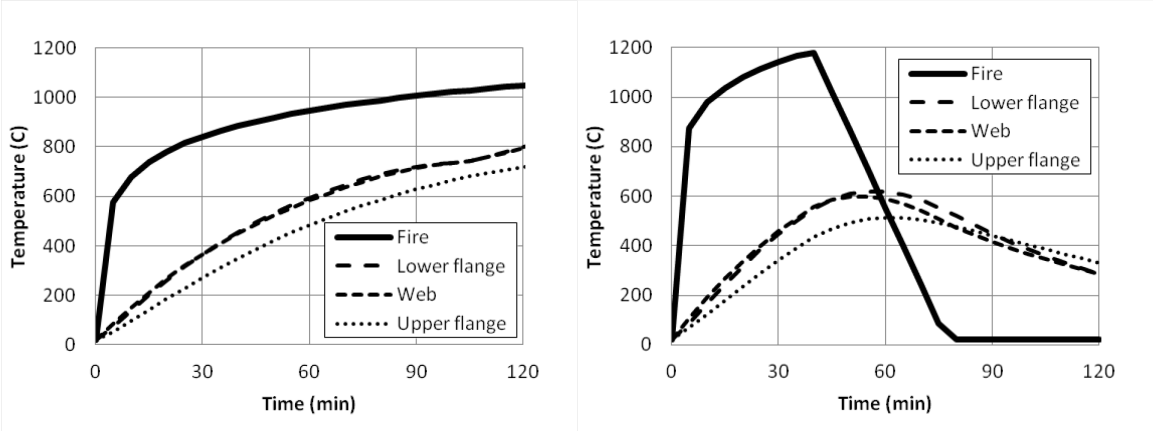

Figure 2-4 Thermal response based on deterministic analysis: (a) standard fire exposure, and (b) natural fire exposure

The yield strength used in the deterministic analysis was assumed to be greater than the nominal yield strength of 345 MPa due to the fact that the actual yield strength of steel tends to exceed the nominal value that is assumed in design. A statistical analysis was

conducted for the data published by (Wainman and Kirby 1988), and it was found that steel of this grade has a mean yield strength of 380 MPa.

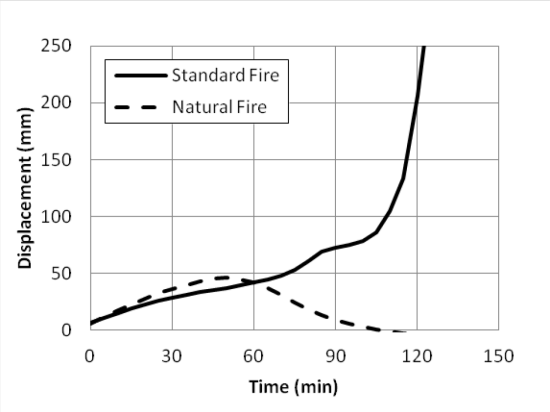

Figure 2-5 Mechanical response based on deterministic analysis

Results from the deterministic analyses are shown in Figs. 2-4 and 2-5. Specifically, the fire and steel temperatures are shown in Fig. 2-4, and the mid-span deflection is plotted in Fig. 2-5 for both standard fire and natural fire exposures. Under standard fire exposure, the beam reaches an average temperature of 600 C around 70 min and a maximum temperature of 700 C around 85 min, indicating that the beam has failed according to limiting temperature criteria imposed by the ASTM E-119 standard used in the U.S. (ASTM E119 1999) and therefore achieves a 1-hour fire rating. As shown in Fig. 2-5, the beam maintains structural stability for approximately 2 hours despite temperatures exceeding 700 C, most likely due to the relatively small load that is applied (i.e., the applied load is 30 percent of the ultimate load capacity of the beam). Under natural fire exposure, the beam heats up to a maximum temperature around 50 min, after which the temperature decreases as the fire cools. The beam reaches a maximum mid-span deflection of 46 mm around the time that the maximum temperature is reached. The deformation then decreases due to cooling. The beam does not lose stability during this time, which is expected due to the fact that the maximum beam temperature is less than the temperature at which the beam fails under standard fire exposure. Note that the beam artificially bows upward occurs during cooling due to the assumed insulated boundary condition at the steel-concrete interface.

2.3.2 Identification and characterization of the sources of uncertainty

As described previously, the problem comprises three sequentially coupled processes, each of which involves some level of uncertainty. In the fire model, there is uncertainty associated with the occurrence of a fire event as well as the nature of the temperature evolution. In the thermal and structural models, uncertainty appears in the material properties, the thermal and structural boundary conditions, and the applied loads, as well as the temperatures associated with the fire. At all stages, there is additional model uncertainty due to assumed simplifications in the fire, thermal, and structural behaviors. The present study seeks to evaluate the probability of structural failure given a natural fire event. Therefore, the probability of fire occurrence is treated as 1.0. Model uncertainty was not calculated in this study. Thus, the results shown here account solely for randomness in the input parameters associated with the fire, thermal, and structural behaviors.

A large number of parameters exist despite the simplifications in the numerical models. The fire model is dependent on the opening factor O, the thermal inertia b of the surroundings, and the fire load density $q_{t,d}$, which are also reliant on the compartment geometry. The thermal model is dependent on the fire temperature T_f, the convection heat transfer coefficient h, the surface emissivity ε, the thickness t_{sfrm} of the spray-applied fire resistant material (SFRM), and the thermal properties (i.e., density, thermal conductivity, and specific heat) for the SFRM and steel. The structural model depends on the temperature T of the steel, which varies spatially over the depth and is time-dependent, as well as the mechanical properties of the steel and the magnitude of the applied load w, which contains dead and live load components. Table 2-1 contains a list of the candidate parameters, the mean values assumed in the present study, and the statistical properties reported in the literature. Statistical data for some of the model parameters has been reported in the literature, while data for other parameters is missing, incomplete, or outdated. It is important to note that lack of statistical data is not an acceptable reason to avoid such calculations, particularly because statistical methods can be used to provide a reasonable prediction of the response (Magnusson and Pettersson 1980/81).

Table 2-1 Properties for parameters

Parameter	Mean	COV	Distribution	References	Sensitivity Coefficient	Stochastic?
Fire model:						
Opening factor, O	0.04 $m^{1/2}$	--	Unknown	Culver 1976, Iqbal and Harichandran 2010	--	N
Fire load density	564 MJ/m^2	0.62	Extreme I		**0.931**	**Y**
Thermal inertia, b	423.5 $Ws^{1/2}/m^2K$	0.09	Normal		**-0.233**	**Y**
Thermal model:						
Emissivity, ε	0.80	--	Unknown	Iqbal and Harichandran 2010	0.013	N
Heat transfer coeff., h	35 W/m^2K	--	Unknown		0.001	N
Thickness, t_{sfrm}	Nominal + 1.6mm	0.20	Lognormal		**-0.702**	**Y**
Density, ρ_{sfrm}	300 kg/m^3	0.29	Normal		-0.061	N
Conductivity, k_{sfrm}	0.120 W/m-K	0.24	Lognormal		**0.690**	**Y**
Specific heat, c_{sfrm}	1200 J/kg-K	--	Unknown		-0.061	N
Density, ρ_{steel}	EC3	--	Unknown		-0.407	N
Conductivity, k_{steel}	EC3	--	Unknown		-0.236	N
Specific heat, c_{steel}	EC3	--	Unknown		-0.407	N
Structural model:						
Dead load, w_{DL}	1.05 x Nominal	0.10	Normal	Iqbal and Harichandran 2010, Ravindra and Galambos 1978	**0.269**	**Y**
Live load, w_{LL}	0.24 x Nominal	0.80	Gamma		**0.044**	**Y**
A	1.0	0.04	Normal		**--**	**Y**
B	1.0	0.20	Normal		**--**	**Y**
E	1.0	0.05	Normal		**--**	**Y**
Yield strength, F_y	380 MPa	0.08	Normal	*	0.000	N

*Statistical analysis of Wainman and Kirby 1988

To reduce the dimensionality, a sensitivity study was conducted to identify the parameters that have the strongest influence on the system response. Given that the structure consists of a simply supported beam, it is well-known that the beam will fail by the formation of a plastic hinge at mid-span. Structural resistance can be defined in terms of the strength of the section (i.e., the plastic moment capacity). Due to its strong dependence on temperature, however, a close-formed statement for the plastic moment capacity is difficult to express, particularly when the temperature over the section varies non-proportionally. Alternatively, failure can be defined in terms of a limiting deformation, as is often done in fire resistance tests. In the present study, the deformation criteria in the BS 476 standard (BS 476 2008) were used. Specifically, failure was assumed to occur (a) when the maximum displacement exceeded $L/20$ (mm), or (b) when the rate of deformation exceeded $L^2/9000d$ (mm/min), where L = beam length in mm and d = beam depth in mm. The BS 476 failure criteria are intended to signify the point at

which the structure has reached its plastic limit and can no longer sustain the fire load. Because failure was defined in terms of a limiting deformation, the sensitivity of the mid-span displacement U was calculated with respect to each model parameter X_i in the sensitivity analysis.

To conduct the sensitivity study, the thermo-mechanical response was evaluated using the mean (expected) values for all input parameters and then computed for a small perturbation of 0.1 percent in a parameter X_i about its mean value. A first-order finite difference approximation was used to evaluate the response gradient. For example, sensitivity of the deformation U was calculated as

$$\frac{\partial U}{\partial X_i} \approx \frac{\Delta U}{\Delta X_i}. \tag{9}$$

For comparison, the sensitivity coefficients were normalized based on the mean value $\overline{X}_i$ of each parameter and on the maximum mid-span displacement $U_{\max}$, i.e., $(\partial U / \partial X_i) \cdot (\overline{X}_i / U_{\max})$. A negative value for a sensitivity coefficient means that an increase in parameter X_i improves the structural performance, while a positive value for a sensitivity coefficient means that an increase in parameter X_i worsens the structural performance.

Sensitivity coefficients are presented in Table 2-1 along with the available statistical information for each parameter. From the presented data, it is clear that the fire load density and the thermal inertia have a significant influence on the response due to the relatively high sensitivity coefficients. The thickness and conductivity of the SFRM and the thermal properties for the steel also have relatively high sensitivity coefficients. The magnitude of the applied load is also found to have a relatively high influence on the response.

When deciding whether a parameter should be treated as stochastic in the following simulation, the variability of the parameter was taken into consideration along with its sensitivity. For instance, the thermal properties in the steel resulted in high sensitivity coefficients but it was assumed that these properties would exhibit low variability and therefore could be treated as deterministic. Similarly, the sensitivity coefficient for the

live load was relatively small, but the parameter had a relatively high coefficient of variation (0.80). Therefore the live load was treated as stochastic. Sensitivity coefficients were not calculated for the load parameters A, B, and E because these parameters are considered part of the stochastic model for applied load. It was noted that the coefficient of variation reported by (Iqbal and Harichandran 2010) for the thermal inertia was relatively small (0.09). However, this parameter was included in the stochastic model.

2.3.3 Stochastic model

As described previously, 10,000 Monte Carlo simulations were conducted using Latin hypercube sampling to reduce the total number of analyses. To run the large number of finite element simulations, two parametric studies (i.e., one for the heat transfer analysis, one for the structural analysis) were run using a finite element code that was programmed in Matlab (MATLAB, v.7.11 2010). Random values for each parameter were generated in Matlab using the appropriate mean, covariance, and probability distribution, which were then input into the thermo-structural model.

Due to the large computational demand, analyses were conducted in parallel on the `flux` system housed at the University of Michigan's Center for Advanced Computing. As shown in Fig. 2-6, the total number of simulations was divided into smaller batches of jobs that were submitted to the queue and then distributed to one of four nodes that were assigned to the analysis. Each node contained dual socket six core Intel I7 CPUs, yielding in an average of 4GB RAM per node. The clustering of jobs maximized the capabilities of each node so as to improve the computational efficiency of the total analysis. Once each batch of jobs was completed, output data was transferred from the local memory to the hard drive to enable the compilation of the results. The total simulation required 5.34 hours.

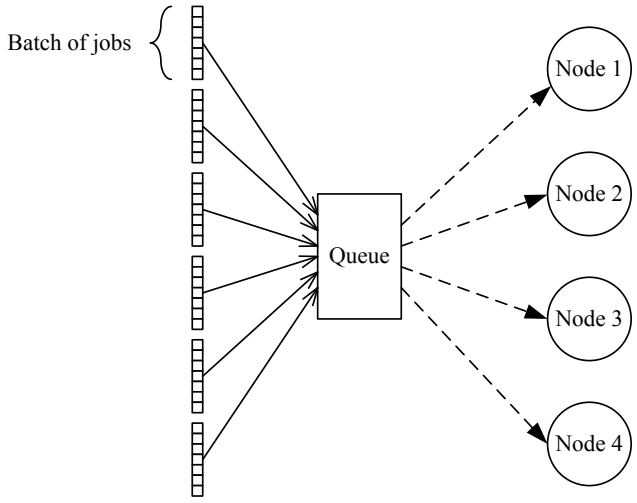

Figure 2-6 Schematic of parallel computing algorithm

2.4 Results and Discussion

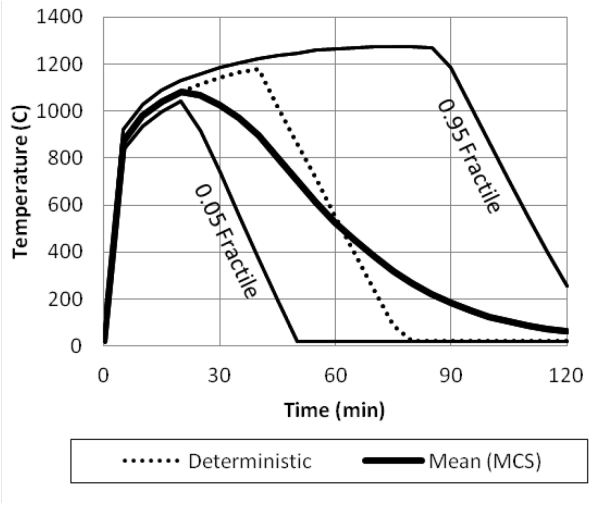

Figure 2-7 Calculated fire temperatures with 0.05 and 0.95 fractiles

Based on the assumed statistical distributions for the fire parameters, a series of natural fire curves were obtained. The mean fire load is shown in Fig. 2-7 along with the 0.05 and 0.95 fractiles. As illustrated, a range of fire curves was obtained with varying intensities and durations. The mean response was similar to the fire curve used in the deterministic analysis, although the maximum temperatures were slightly less severe. Nevertheless, maximum fire temperatures exceeded 1200 C in several instances.

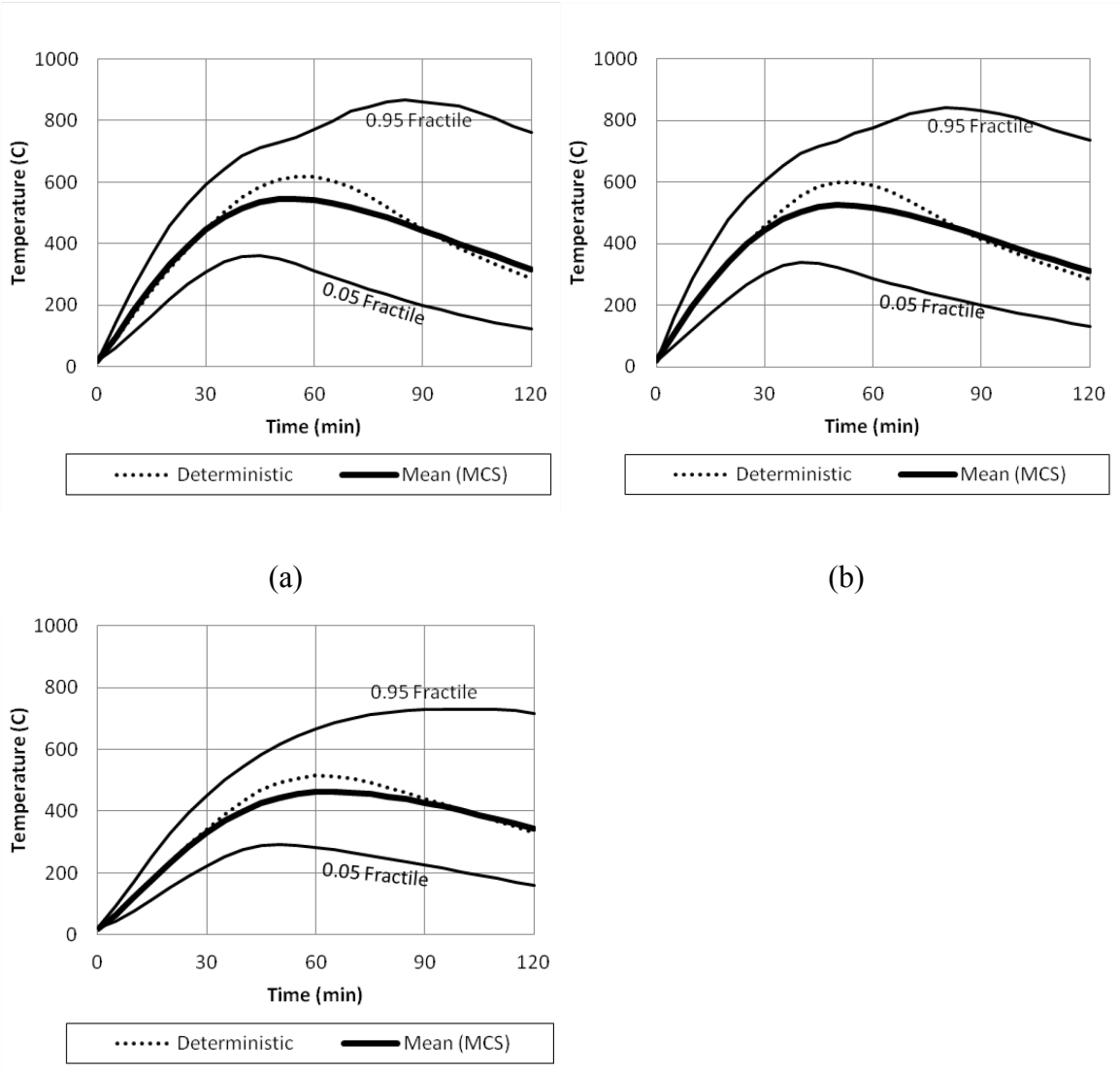

Figure 2-8 Calculated steel temperature with 0.05 and 0.95 fractiles: (a) lower flange, (b) web, (c) upper flange

Using the fire curves obtained from the stochastic model along with random values for the SFRM thickness and conductivity, the thermal response was modeled stochastically through a series of 2D heat transfer analyses conducted in Matlab. The calculated mean and 0.05 and 0.95 fractiles for the lower flange, web, and upper flange temperatures are shown in Fig. 2-8. While the mean temperatures were slightly less than those obtained in the deterministic analysis, the stochastic simulation resulted in a number of cases in

which the steel temperature exceeded 800 C, thus indicating that there was a significant chance that the beam may fail in some instances.

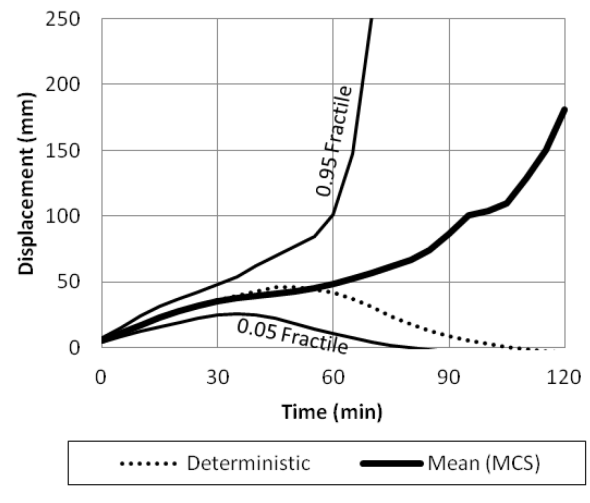

Figure 2-9 Calculated deformation response with 0.05 and 0.95 fractiles

The temperatures were entered into the structural model along with random values for the applied dead and live loads to evaluate the mechanical response of the beam. The mid-span displacement is plotted in Fig. 2-9 for the mean response as well as the 0.05 and 0.95 fractiles. The mean deformation continuously increases with time whereas the deterministic simulation reaches a maximum displacement and then decreases upon cooling. The difference can likely be attributed to the fact that some of the Monte Carlo simulations resulted in excessively large deflections beyond failure. Including these in the calculation of the mean response results in a mean that is much higher than the deterministic simulation.

To evaluate the reliability of the system, failure was defined by the BS 476 criteria, which limits displacement to $L/20 = 244$ mm and the rate of deformation to $L^2/9000d = 13$ mm/min. The probability of failure P_f was calculated by evaluating the total number of simulations in which the structure failed, i.e.,

$$P_f = \frac{n_f}{n}, \tag{10}$$

where n_f is the number of failed simulations and n is the total number of simulations. In this case, 947 simulations failed out of a total of 10,000 simulations, resulting in a failure

probability of 9.47 percent. The calculated failure probability can subsequently be used to evaluate the adequacy of the design based on a target level of risk, although a risk analysis was beyond the scope of the present study.

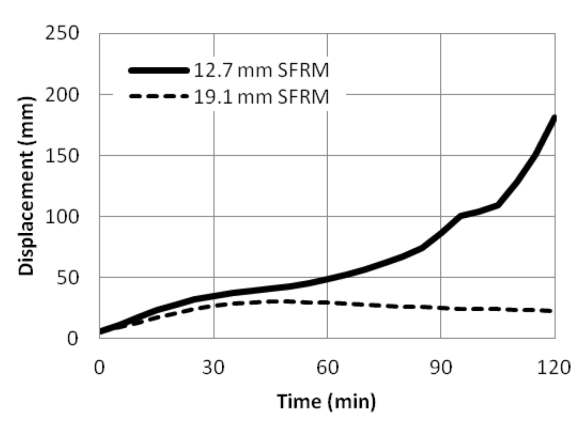

Figure 2-10 Mean deformation response due to increased SFRM thickness

The quantification of structural reliability gives the analyst the ability to rationally improve the design based on the performance criteria. For example, in the present study, it was highlighted that the structural response was highly sensitive to the thickness of the spray applied fire resistant material. Therefore, an analysis was conducted for the same system with the SFRM thickness increased by 6.4mm to provide a comparison. The mean deformation shown in Fig. 2-10 demonstrates that the displacements were considerably low using the increased SFRM thickness. It was found that increasing the SFRM thickness by 6.4mm resulted in a significant decrease in the failure probability, from 9.47 percent to 2.45 percent. Alternative fire protection measures could also be explored to reduce the expected fire load, and different structural configurations could be investigated to improve the structural resiliency while reducing the overall cost. Thus, the probabilistic analysis enables the design of integrated, robust fire safety solutions with explicit consideration for the passive resistance provided by the structure.

The study also highlights the importance of relating the limit state function(s) to the desired performance objectives. Here, failure was defined in terms of the ultimate capacity of the beam, which was correlated to the maximum deformation and rate of deformation based on the BS 476 criteria. However, more stringent deformation criteria could be imposed if, for example, the performance objectives involved minimizing the

operation downtime and expediting the occupancy of the building following a fire event with a specified severity.

2.5 Conclusions

A framework for the probabilistic evaluation of structural fire resistance has been investigated to simulate the stochastic response of structures given uncertainties in the fire load and structural resistance parameters. The methodology requires the statistical properties of the uncertain parameters to be specified, a stochastic simulation of the thermo-mechanical response of the structure, and the evaluation of the structural reliability based on a suitable performance function. For stochastic modeling of the thermo-mechanical response, sequentially coupled finite element analyses were embedded within a Monte Carlo simulation. The computational efficiency of the analysis was improved by using sensitivity analyses to reduce the dimensionality of the problem and selecting Latin hypercube sampling to decrease the total number of Monte Carlo iterations.

The methodology was demonstrated through an application in which the failure probability of a protected steel beam was evaluated given an uncertain natural fire event. In the case considered here, a 1-hour rated beam was found to resist the natural fire load with 9.47 percent probability of failure, thus indicating that the structure is likely to resist the predicted fire load. However, discussion is needed regarding what might be considered an *acceptable* level of risk in structural fire design. While the failure probability was less than ten percent, the response demonstrated a high level of variability in the temperature distribution and corresponding deformation response indicating that the failure probability may be substantially higher in other types of structural systems, depending on the details of the design and the magnitude of the fire event. The findings demonstrate that a probabilistic evaluation is necessary to ensure a consistent level of safety for fire resistant design. Furthermore, it is evident that a designer can capitalize on the enhanced understanding obtained by probabilistic analysis to make rational comparisons between alternative fire resistant designs, an additional benefit that is not afforded with current design practices.

The study has demonstrated that there is a significant need for data regarding uncertainty in parameters affecting structural fire resistance. This research also shows that additional work is needed in the definition of limit state criteria for structural systems, particularly as the failure criteria relate to various levels of performance (e.g., collapse prevention vs. expedited occupancy following a fire event). Additionally, more efficient stochastic modeling techniques should be explored for fire-structure applications because the simulation time needed to perform Monte Carlo simulation makes it impractical for industry applications.

References

AISC (2005). *Steel Construction Manual*, 13th Ed. American Institute of Steel Construction, USA.

ASTM E119 (1999). *Standard Test Methods for Fire Tests of Building Construction Materials. E119*. American Society for Testing and Materials, West Conshohocken, PA.

Bailey, C.G. (2006). "Advances in Fire Engineering Design of Steel Structures," *Proceedings of the Institution of Civil Engineers: Structures and Buildings*, 159, 21-35.

BS 476 (2008). *Fire Tests on Building Materials and Structures*, BS 476-10, 2009, British Standards Institution, London.

Buchanan, A.H. (2001). *Structural Design for Fire Safety*, John Wiley and Sons Ltd, England.

Choi, S.K., Grandhi, R.V., and Canfield, R.A. (2007). *Reliability-based Structural Design*, Springer-Verlag, London.

Culver, C.G. (1976). *Survey Results for Fire Loads and Live Loads in Office Buildings*, National Bureau of Standards, Washington, DC.

EC1 (2005). *Eurocode 1: Actions on Structures, Part 1-2: General Actions—Actions on Structures Exposed to Fire*, BSI EN 1991-1-2. British Standards Institution: London.

EC3 (2005). *Eurocode 3: Design of Steel Structures, Part 1-2: General Rules--Structural Fire Design*, BSI EN 1993-1-2, British Standards Institution, London.

Ellingwood, B.R. (2005). "Load Combination Requirements for Fire-resistant Structural design," *Journal of Fire Protection Engineering*, 15,43-61.

Fellinger, J.H.H., and Both, C.K. (2000). "Fire Resistance: Reliability vs. Time Analyses," *Proceedings of Composite Construction in Steel and Concrete IV*, Hajjar, J.F. (ed). ASCE: USA. 816-827.

Haldar, A., and Mahadevan, S. (2000). *Reliability Assessment Using Stochastic Finite Element Analysis*, John Wiley and Sons, New York.

Helton, J.C., and Davis, F.J. (2003). "Latin hypercube Sampling and the Propagation of Uncertainty in Analyses of Complex Systems," *Reliability Engineering & System Safety*, 81, 23-69.

Hietaniemi, J. (2007). "Probabilistic Simulation of Fire Endurance of a Wooden Beam," *Structural Safety*, 29, 322-336.

Huang, P.T., and Delichatsios, M.A. (2010). "Quantitative Risk Analysis for the Response of Steel Beams in Fires," *Journal of Structural Fire Engineering*, 1, 231-241.

Iqbal, S., and Harichandran, R.S. (2010). "Capacity Reduction and Fire Load Factors for Design of Steel Members Exposed to Fire," *Journal of Structural Engineering*, 136, 1554-1562.

Iqbal, S., and Harichandran, R.S. (2011). "Capacity Reduction and Fire Load Factors for LRFD of Steel Columns Exposed to Fire," *Fire Safety Journal*, 46, 234-242.

ISO (1999). *Fire resistance tests – Elements of building construction*, International Standard 834. ISO, Geneva, Switzerland.

Jeffers, A.E., and Sotelino, E.D. (2009). "Fiber Heat Transfer Element for Modeling the Thermal Response of Structures in Fire," *Journal of Structural Engineering*, 135, 1191-1200.

Jensen, E., Van Horn, J., and Eamon, C.D. (2010). "Variability of Fire and Concrete Temperatures and the Associated Uncertainty in Structural Behavior," *Proceedings of 6th International Conference on Structures in Fire*, Kodur, V.

and Franssen, J.M. (eds). DESTech Publications: USA. 959-966.

Khorasani, N.E., Garlock, M.E., and Gardoni, P. (2012). "Reliability Analysis of Steel Perimeter Columns under Fire," *Proceedings of the 7th International Conference on Structures in Fire*, Fontana, M., Frangi, A., and Knobloch, M. (eds). ETH Zurich: Zurich, 541-550.

Lange, D., Usmani, A., and Torero, J. (2008). "The Reliability of Structures in Fire," *Proceedings of the 5th International Conference on Structures in Fire*, Tan, K.H., Kodur, V.K.R., and Tan, T.H. (eds). Research Publishing Services: Singapore. 760-770.

Lennon, T., Moore, D.B., Wang, Y.C., and Bailey, C.G. (2007). *Designers' Guide to EN1991-1-2, EN1992-1-2, EN1993-1-2, and EN1994-1-2: Handbook for the Fire Design of Steel Composite, and Concrete Structures to the Eurocodes*. Thomas Telford, London.

Magnusson, S.E., and Pettersson, O. (1980/81). "Rational Design Methodology for Fire Exposed Load Bearing Structures," *Fire Safe Journal*, 3, 227-241.

MATLAB, v.7.11 (2010). MathWorks Inc, Natick, MA.

Nowak, A.S., and Collins, K.R. (2000). *Reliability of Structures*. McGraw-Hill, USA.

Puatatsananon, W., and Saouma, V.E. (2006). "Reliability Analysis in Fracture Mechanics Using the First-order Reliability Method and Monte Carlo Simulation," *Fatigue & Fracture of Engineering Materials & Structures*, 29(11), 959-975.

Ravindra, M.K., and Galambos, T.V. (1978). "Load and Resistance Factor Design for Steel," *Journal of the Structural Division*, 104, 1337-1353.

Ryder, N.L., Wolin, S.D., and Milke, J.A. (2002). "An Investigation of the Reduction in Fire Resistance of Steel Columns Caused by Loss of Spray-Applied fire

protection," *Journal of Fire Protection Engineering*, 12, 31-44.

Sakji, S., Soize, C., and Heck, J.V. (2008). "Probabilistic Uncertainty modeling for thermo-mechanical analysis of plasterboard submitted to fire load," *Journal of Structural Engineering*, 134, 1611-1618.

Singh, V.P., Jain, S.K., and Tyagi, A. (2007). *Risk and Reliability Analysis: A Handbook for Civil and Environmental Engineers*. American Society of Civil Engineers, USA.

Vaidogas, E.R., and Juocevicius, V. (2008). "Reliability of a Timber Structure Exposed to Fire: Estimation Using Fragility Function," *Mechanika*, 73, 35-42.

Van Coile, R., Annerel, E., Caspeele, R., and Taerwe, L. (2011). "Probabilistic Analysis of Concrete Beams during Fire," *Proceedings of the International Conference on Application in Structural Fire Engineering*. Wald, F., Horova, K., and Jirku, J. (eds), Prazska Technika, Prague. 127-132.

Wainman, D.E., and Kirby, B.R. (1988). *Compendium of UK Standard Fire Test Data: Unprotected Structural Steel – 1*, Rep. No. RS/RSC/S10328/1/87/B, British Steel Corporation, England.

Witteveen, J., and Twilt, L. (1981/82). "A Critical View on the Results of Standard Fire Resistance Tests on Steel Columns," *Fire Safety Journal*, 4, 259-270.

CHAPTER 3 : DIRECT DIFFERENTIATION METHOD FOR RESPONSE SENSITIVITY ANALYSIS OF STRUCTURES IN FIRE[2]

3.1 Introduction

Response sensitivity, which is defined as the influence ratio of a specified structural response with respect to the perturbation of an input variable, has been widely used in various engineering disciplines. In structural engineering, the response sensitivity plays an important role in parameter importance studies, reliability analyses, and design optimization. Two methods are available to calculate the response sensitivity: the finite difference method (FDM) and the direct differentiation method (DDM). The finite difference method uses a finite difference approximation of the response sensitivity such that the response sensitivity is approximated based on a small perturbation in the parameter (Scott et al. 2004). Although the FDM is versatile and widely applied in probabilistic analysis software such as the NESSUS (Thacker et al. 2006), it is computationally inefficient because it requires an additional simulation to evaluate the response for each perturbation in parameter. Furthermore, the accuracy of the FDM is limited by the size of the perturbation, and there is no way to determine *a priori* the size of the perturbation that is needed to achieve a converged solution. The direct differentiation method, on the other hand, involves deriving analytical expressions for the response gradients by directly differentiating the governing finite element equations. While the method requires some initial effort to formulate the analytical expressions, the response sensitivities are calculated exactly, without the need to perform additional simulations. Thus, the direct differentiation method provides an exact value for the response sensitivity with minimal computational expense.

[2] Contents of this chapter have been published as Guo, Q. and Jeffers, A.E., "Direct Differentiation Method for Response Sensitivity Analysis of Structures in Fire," *Engineering Structures*, 77, 172-180, 2014.

A number of researchers have applied the direct differentiation method to the sensitivity analysis of structures at ambient temperature. Early studies focused on response sensitivity analysis in linear systems (Prasad and Emerson 1982, Giles and Rogers 1982, Wallerstein 1984, and Choi et al. 1985). Formulations have since been developed for nonlinear systems with geometric and material parameters (Choi and Santos 1987, Choi and Choi 1990, Tsay and Arora 1990, Zhang et al. 1992, Zhang and Der Kiureghian 1993, Haukaas and Der Kiureghian 2005, and Barbato et al. 2007). In the analysis of structural frames, the DDM has been applied to a range of nonlinear displacement-based and force-based frame elements (Scott et al. 2004, Haukaas and Der Kiureghian 2005, Barbato et al. 2007, Conte et al. 2004, Haukaas 2006, and Haukaas and Scott 2006), with consideration for inelastic material behavior as well as geometric nonlinear effects. The DDM has also been applied to problems outside of structural mechanics. For example, Kleiber et al. (1997) used the DDM to formulate response sensitivities in the heat transfer analysis of structures, although no consideration was given for systems that exhibit coupling between fields, such as thermal-stress analysis in solids. Bebamzadeh and Haukaas (2009) used the DDM to formulate response sensitivities for the thermal-stress analysis of composites during manufacturing. They described the application of the DDM to a system that exhibited multidisciplinary coupling, although the focus was on a linear system in which the material properties were independent of temperature.

From a review of literature, it can be seen that considerable advances have been made in the application of the direct differentiation method for response sensitivity analysis of structures and other types of engineering systems. However, the focus has almost entirely been on systems that are not coupled to another field (e.g., thermo-structural coupling in heated structures). In cases that involved thermo-structural coupling, no known work has considered nonlinear, temperature-dependent material properties, which are critical in the analysis of structural response in fire. Due to the growing interest in performance-based fire safety engineering of structures, methods to evaluate parameter importance and structural reliability are gaining increasing attention from the fire safety community. In the pursuit of more advanced simulation techniques for structural fire engineering, it is necessary that a robust methodology exists for evaluating the response sensitivity of a structure for parameters that exist in the fire, thermal, and structural domains.

The present study therefore seeks to extend the DDM to determine the response sensitivity of a structure exposed fire, with particular consideration for the interdependencies between the fire, thermal, and structural domains. The paper describes the analytical system that is being modeled and presents the DDM formulation for nonlinear heat transfer and structural elements with temperature-dependent material properties. The response sensitivity formulations are validated by considering a simply supported steel beam exposed to natural fire conditions. Comparisons are made between the proposed DDM formulation and the traditional finite difference approximations to evaluate the accuracy and efficiency of the DDM formulation.

3.2 Analytical System for Structural Response in Fire

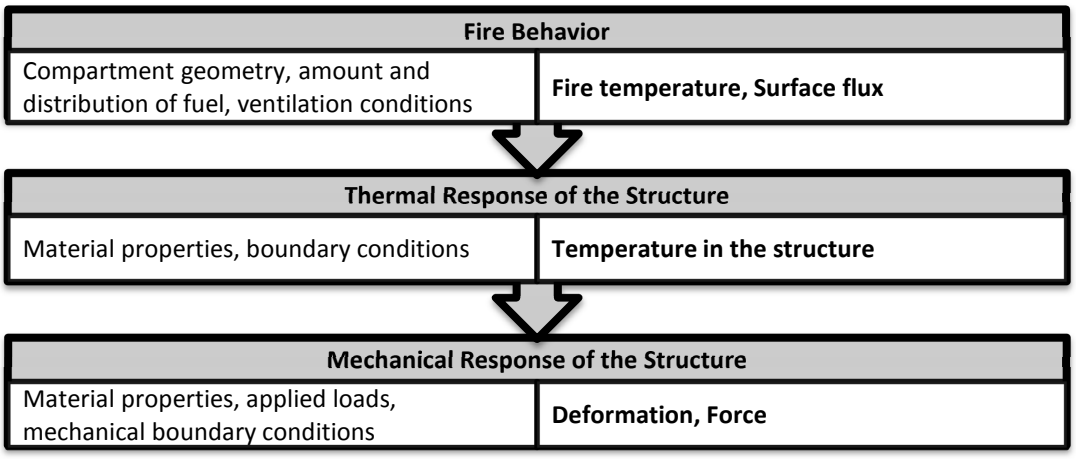

Figure 3-1 Propagation of uncertainty in the structural fire simulation (adapted from Guo et al 2013)

The analysis of a structure exposed to fire involves three sequentially coupled processes as illustrated in Fig. 3-1: the fire behavior, the thermal response of the structure, and the mechanical response of the structure (Guo et al. 2013). The behavior of a fully developed (i.e., post-flashover) compartment fire is generally expressed as a gas of uniform temperature that transmits heat to the structure by convection and radiation. The temperature of the fire can be determined by a parametric fire curve that depends on factors such as the fuel load density, the ventilation factor, the compartment geometry, and the thermal inertia of the compartment lining. Based on the thermal boundary conditions imposed by the fire, the temperatures in the structure can be more accurately evaluated by conduction heat transfer analysis using the finite element or finite difference

method. The transient temperature distributions in the structure are inputted in the structural model, and the mechanical response of the structure is subsequently evaluated by finite element analysis, taking into account the temperature-dependent material properties and thermal expansion of the heated structure. The left-hand column in Fig. 3-1 illustrates the important parameters that exist in each of the domains, and the right-hand column lists the output quantities for each simulation. It can be seen that variations in parameters that appear in the fire and thermal domains will affect the structural temperatures, hence affecting the deformation response of the structure. The details of the fire, thermal, and structural models are given in the following subsections.

3.2.1 Parametric fire curve for compartment fire exposure

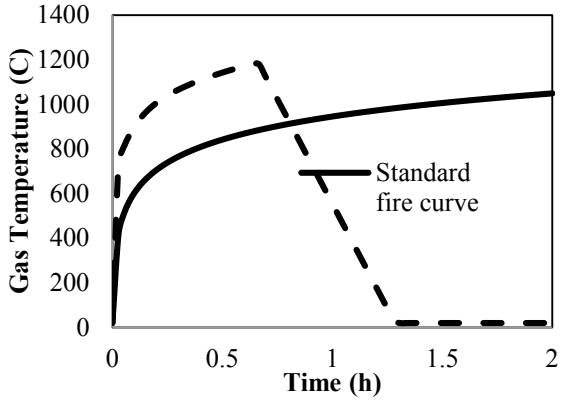

Figure 3-2 Fire temperature-time relationship

To simplify the framework, the fire behavior is modeled using the Eurocode parametric temperature-time curve as modified by Buchanan (2001). It should be noted that more complicated fire models, such as computational fluid dynamics and zone models, could also be applied to simulate the fire exposure, although the boundary conditions in the heat transfer model may hold a different form than what is given in Section 3.2.2. The parametric fire model provides an approximation of the time-temperature relationship for a post-flashover compartment fire based on the fuel load density, the ventilation factor, the compartment geometry, and the thermal inertia of the compartment lining. As shown in Fig. 3-2, the Eurocode parametric fire curve can have a higher temperature than the standard ISO-834 fire during the heating phase and also includes a cooling phase. The gas temperature T_f (°C) during the period of burning is given as

$$T_f = 1325\left(1 - 0.324e^{-0.2t^*} - 0.204e^{-1.7t^*} - 0.472e^{-19t^*}\right), \tag{1}$$

where t^* is a fictitious time given by

$$t^* = \Gamma t . \tag{2}$$

Here, t is the time (hours) and Γ is a non-dimensional coefficient given by

$$\Gamma = \frac{\left(F_v/0.04\right)^2}{\left(b/1900\right)^2} . \tag{3}$$

In Eq. (3), F_v = ventilation factor and b = thermal inertia of the surroundings, which depends on the density, conductivity, and specific heat of the walls, floor, and ceiling of the compartment. The duration t_d of the burning period is calculated as

$$t_d = 0.00013 e_t / F_v , \tag{4}$$

where the e_t = fire load. After time t_d, the gas temperature is assumed to decay linearly according to the rate defined in (Buchanan 2001).

3.2.2 Heat transfer model

The finite element equations governing transient heat transfer in solids are given as

$$\mathbf{C}\dot{\mathbf{T}} + \mathbf{K}\mathbf{T} = \mathbf{R} \tag{5}$$

where $\mathbf{C}$ = heat capacity matrix, $\mathbf{K}$ = conductivity matrix, $\dot{\mathbf{T}}$ = array containing the first derivative of the nodal temperatures with respect to time, $\mathbf{T}$ = array of nodal temperatures, $\mathbf{R}$ = array of thermal loads (Cook et al. 2001). The general equations for the conductivity matrix $\mathbf{K}$, the heat capacity matrix $\mathbf{C}$, and the thermal load vector $\mathbf{R}$ are given as

$$\mathbf{C} = \bigcup \int_V \mathbf{N}^T c\rho \mathbf{N} dV \tag{6}$$

$$\mathbf{K} = \bigcup \left(\int_V \mathbf{B}^T k \mathbf{B} dV + \int_S \mathbf{N}^T h \mathbf{N} dS + \int_S \mathbf{N}^T h_r \mathbf{N} dS \right) \tag{7}$$

$$\mathbf{R} = \bigcup \left(\int_V \mathbf{N}^T q dV + \int_S \mathbf{N}^T q_s'' dS + \int_S \mathbf{N}^T h T_f dS + \int_S \mathbf{N}^T h_r T_f dS \right) \tag{8}$$

where $\mathbf{N}$ = shape function matrix and $\mathbf{B} = \{\partial\}\mathbf{N}$; k = thermal conductivity; h = convection heat transfer coefficient; c = specific heat; ρ = mass density; q = rate of internal heat generation per unit volume; q_s'' = surface heat flux. In Eqs. (7)-(8), h_r is the linearized radiation heat transfer coefficient, which is calculated from

$$h_r = \varepsilon\sigma(T_f + T_s)(T_f^2 + T_s^2), \tag{9}$$

where ε = emissivity, σ = the Stefan-Boltzmann constant, T_f = temperature of the surroundings (i.e., the fire temperature), and T_s = temperature at the structure's surface. The integrals in Eqs. (6)-(8) are evaluated each element's volume V and surface S for which the respective boundary conditions are applied. The union symbol $\bigcup$ denotes the assembly over all elements in the computational domain.

To improve the efficiency of the heat transfer analysis and to simplify the transfer of thermal data to a structural analysis, a special-purpose code based on the fiber element model proposed by (Jeffers and Sotelino 2009, and Jeffers and Sotelino 2012) was used in the heat transfer analysis. As shown in Fig. 3-3, the fiber heat transfer element uses a fiber discretization over the length of a beam. The fibers were arranged in a rectilinear grid over the cross-section. The formulation was based on the assumption that each fiber's temperature was lumped in the transverse direction such that heat transfer over the section was approximated by a finite difference calculation. Along the element's length, temperatures could be approximated by quadratic interpolation functions to evaluate the thermal response under non-uniform heating. However, the temperature gradient along the length was ignored in this research due to the uniform fire exposure. Similar to a traditional finite difference model, the temperature of an internal fiber is dependent on the energy transferred by conduction from the adjacent fiber. For external fibers, the boundary terms are approximated by the appropriate finite differences.

The DDM formulation is presented in Section 3.3.2 for a general heat transfer finite element based on the element matrices given in Eqs. (5) - (8). The detailed equations for the special case of the fiber heat transfer element are not given here for simplicity.

3.2.3 Structural model

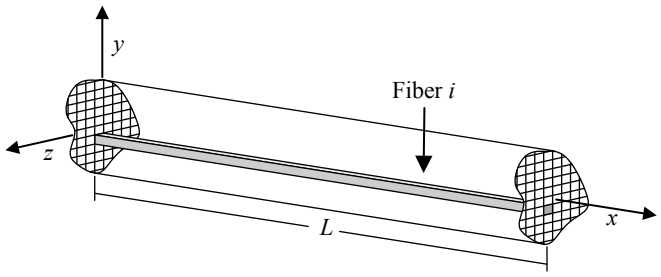

Figure 3-3 Fiber element for heat transfer and structural simulation (adapted from Jeffers and Sotelino 2012)

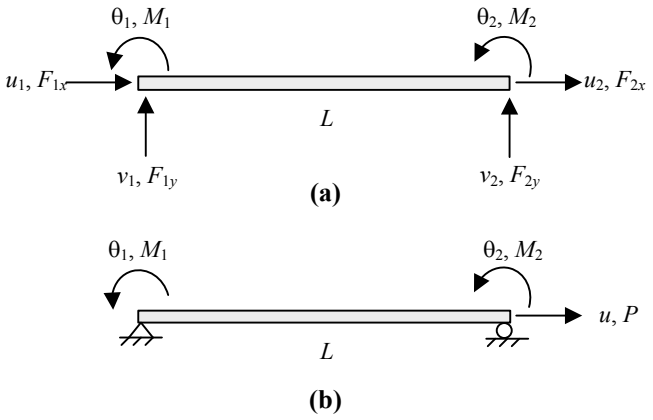

Figure 3-4 Degrees of freedom for the structural element: (a) at the full element level, and (b) at the reduced element level (adapted from Jeffers and Sotelino 2012)

A 2D displacement-based frame element is used here to carry out the structural analysis. As shown in Fig. 3-3, the structural element uses the same fiber discretization as the heat transfer element to facilitate the transfer of temperatures from the heat transfer analysis to the structural analysis. The fiber discretization also allows the element to account for the spread of plasticity during yielding as well as variations in material properties over the cross-section due to temperature dependence. A co-rotational formulation is used to derive the element stiffness matrix by considering natural deformations independent of rigid body displacement (Crisfield 1991). The element can therefore also handle geometrically nonlinear effects such as global buckling. Nodal displacements $\mathbf{u} = \left[u_1, v_1, \theta_1, u_2, v_2, \theta_2\right]^T$ and natural deformations $\mathbf{d} = \left[u, \theta_1, \theta_2\right]^T$ are illustrated in Figs. 3-4a and 3-4b, respectively.

C^1 cubic interpolation functions are used to describe the axial and transverse displacements, $u(x)$ and $v(x)$, in terms of the natural deformations $\mathbf{d}$:

$$\begin{Bmatrix} u(x) \\ v(x) \end{Bmatrix} = \begin{bmatrix} \frac{x}{L} & 0 & 0 \\ 0 & x - \frac{2x^2}{L} + \frac{x^3}{L^2} & -\frac{x^2}{L} + \frac{x^3}{L^2} \end{bmatrix} \begin{Bmatrix} u \\ \theta_1 \\ \theta_2 \end{Bmatrix} \tag{10}$$

where L = element length.

The strain ε_i in fiber i is calculated by applying Euler-Bernoulli beam theory, assuming that deformations are small and plane sections remain plane. In particular,

$$\varepsilon_i = \frac{du}{dx} - y_i \frac{\partial^2 v}{\partial x^2} - \varepsilon_{th} \tag{11}$$

where y_i = position of fiber i with respect to the neutral axis and ε_{th} = thermal strain in fiber i.

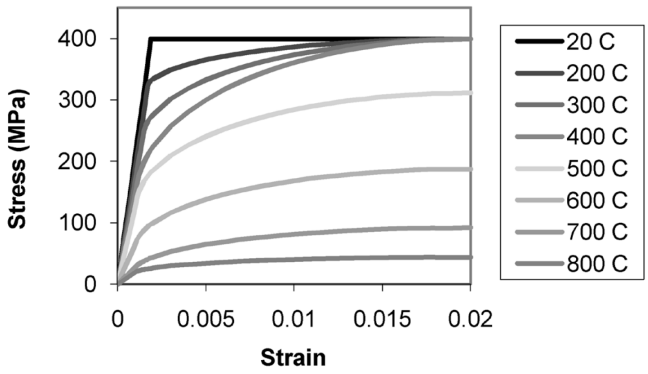

Figure 3-5 Temperature-dependent stress-strain relationship for steel (EC3 2005)

Based on the mechanical strain ε_i and temperature T_i, the tangent modulus E_i and the fiber stress σ_i can be determined from the constitutive law for the material. The strain-stress relationship of steel at elevated temperature is shown in Fig. 3-5 (EC3 2005).

The reduced element stiffness matrix $\mathbf{k}_r$ is given as

$$\mathbf{k}_r = \sum_{i=1}^{n_{fib}} \left(\int_L \mathbf{B}_i^T E_i A_i \mathbf{B}_i dx \right) \tag{12}$$

where n_{fib} = number of fibers in the cross section, E_i = tangent modulus of fiber i, A_i = area of fiber i, and $\mathbf{B}_i$ = strain-displacement matrix for fiber i, which is given by

$$\mathbf{B}_i = \left[\frac{1}{L} \quad -y_i \left(-\frac{4}{L} + \frac{6x}{L^2} \right) \quad -y_i \left(-\frac{4}{L} + \frac{6x^2}{L^2} \right) \right]. \tag{13}$$

The full element stiffness matrix is obtained by expanding the element degrees of freedom to include rigid body modes through a geometric transformation, as described by (Crisfield 1991). The structural stiffness matrix $\mathbf{K}$ is then obtained by assembling the element matrices over the domain.

For determining the force unbalance in the nonlinear analysis of structures, the internal force vector is calculated from the internal stress as

$$\mathbf{p}^{\text{int}} = \sum_{i=1}^{n_{fib}} \left(\int_L \mathbf{B}_i^{\mathbf{T}} \sigma_i A_i dx \right), \tag{14}$$

where σ_i = stress in fiber i.

Note that the force in Eq. (14) must also be transformed into the full element degrees of freedom by a geometric transformation, as described by (Crisfield 1991). The internal force vector $\mathbf{P}^{\text{int}}$ for the structure is obtained by assembling the internal force vectors for all elements, i.e.,

$$\mathbf{P}^{\text{int}} = \bigcup \left(\mathbf{p}^{\text{int}} \right) \tag{15}$$

Substituting Eq. (14) gives

$$\mathbf{P}^{\text{int}} = \bigcup \sum_{i=1}^{n_{fib}} \left(\int_L \mathbf{B}_i^T \sigma_i A_i dx \right) \tag{16}$$

3.3 Response Sensitivity Analysis by the Direct Differentiation Method

The goal of a response sensitivity analysis is to measure the sensitivity of the structural response (e.g., the structural displacement u) with respect to parameter X (i.e., $\partial \mathbf{u} / \partial X$).

This can be accomplished by directly differentiating of the governing finite element equations given in Section 3-2. The following formulation extends the DDM to the analysis of structures in fire by accounting for temperature-dependence in the structural model. To account for parameters that appear in the fire and thermal domains, partial derivatives with temperature response sensitivities must be passed into the structural model from the heat transfer model. These issues are described in the following subsections.

3.3.1 Response sensitivity analysis in the structural model

In the nonlinear analysis of structures, an incremental iterative solution is obtained by enforcing equilibrium at the nodes such that

$$\mathbf{P}_n^{\text{int}} = \mathbf{P}_n^{\text{ext}}, \tag{17}$$

where $\mathbf{P}_n^{\text{int}}$ = vector of the internal forces, and $\mathbf{P}_n^{\text{ext}}$ = vector of the external forces. Equation (17) should be satisfied at every time step n. As the internal forces $\mathbf{P}_n^{\text{int}}$ depends on parameter X both explicitly and implicitly through the displacement response, differentiating Eq. (17) directly by parameter X gives (Haukaas 2006)

$$\mathbf{K}_n \frac{\partial \mathbf{u}_n}{\partial X} = \frac{\partial \mathbf{P}_n^{\text{ext}}}{\partial X} - \frac{\partial \mathbf{P}_n^{\text{int}}}{\partial X} \tag{18}$$

where $\mathbf{K}_n = \frac{\partial \mathbf{P}_n^{\text{int}}}{\partial \mathbf{u}_n}$ is the algorithmically consistent stiffness matrix and $\mathbf{u}_n$ = the vector of nodal displacements. $\frac{\partial \mathbf{u}_n}{\partial X}$ is the displacement sensitivity vector, which is the quantity of interest in the response sensitivity analysis. $\frac{\partial \mathbf{P}_n^{\text{ext}}}{\partial X}$ can readily be evaluated because the external force acting on a structure is in most cases an explicit function of parameter X. The challenge therefore is in deriving expressions for the sensitivity $\frac{\partial \mathbf{P}_n^{\text{int}}}{\partial X}$ of the internal force vector.

The expression for the derivative of the internal force vector with respect to parameter X in a general structural element is (Haukaas and Der Kiureghian 2005)

$$\frac{\partial \mathbf{P}_n^{\text{int}}}{\partial X} = \bigcup \left(\int_V \left(\frac{\partial \mathbf{B}^T}{\partial X} \boldsymbol{\sigma}_n + \mathbf{B}^T \mathbf{E} \frac{\partial \boldsymbol{\varepsilon}_n}{\partial X} + \mathbf{B}^T \frac{\partial \boldsymbol{\sigma}_n}{\partial X} \right) dV \right), \tag{19}$$

where ε_n = strain tensor, E = constitutive matrix, and σ_n = stress tensor. In the analysis of structures in fire, however, $\boldsymbol{\varepsilon}_n$ and $\boldsymbol{\sigma}_n$ are dependent on temperature. Using the chain rule to account for parameters X that exist in the thermal domain, the general expression becomes

$$\frac{\partial \mathbf{P}_n^{\text{int}}}{\partial X} = \bigcup \left(\int_v \left(\frac{\partial \mathbf{B}^T}{\partial X} \boldsymbol{\sigma}_n + \mathbf{B}^T \mathbf{E} \frac{\partial \boldsymbol{\varepsilon}_n}{\partial X} + \mathbf{B}^T \mathbf{E} \frac{\partial \boldsymbol{\varepsilon}_n}{\partial \mathbf{T}_n} \frac{\partial \mathbf{T}_n}{\partial X} + \mathbf{B}^T \frac{\partial \boldsymbol{\sigma}_n}{\partial X} + \mathbf{B}^T \frac{\partial \boldsymbol{\sigma}_n}{\partial \mathbf{T}_n} \frac{\partial \mathbf{T}_n}{\partial X} \right) dV \right) \tag{20}$$

where the $\mathbf{T}_n$ = vector of nodal temperatures at time step n, which must be passed in from the thermal modal. Note that thermal response sensitivities $\frac{\partial \mathbf{T}_n}{\partial X}$ must be computed in the heat transfer model. Expressions for $\frac{\partial \mathbf{T}_n}{\partial X}$ are derived in section 3.3.2.

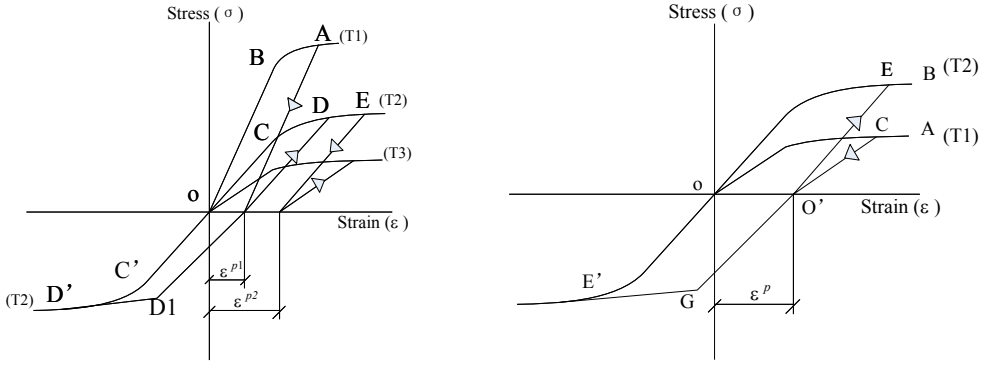

(a) (b)

Figure 3-6 Development of plastic deformation: (a) heating phase, (b) cooling phase (adapted from El-Rimawi et al. 1996)

Equation (20) must be modified during the cooling phase of fire development. El-Rimawi et al. (El-Rimawi et al. 1996) provided an approach to calculate the load reversal in structural members during the cooling phase of a fire. The main procedure is shown in Fig. 3-6. During heating (Fig. 3-6a), the structure incurs plastic strain (e.g., ε^{p1} and ε^{p2}) as the strength of the system declines with increasing temperature and the structure is stressed beyond the elastic limit. During cooling (Fig. 3-6b), it is assumed that the residual plastic strain accrued during heating stays constant, while the strength and

stiffness of the system is recovered with decreasing temperature. For example, at temperature T_1 in Fig. 3-6b, the structure has been stressed beyond the elastic limit (point *C*) with a corresponding residual plastic strain of ε^p. As temperature decreases from T_1 to T_2, the material is assumed to unload by the path *CO′* and reload by the path *O′EB*, where the curve *EOE′* is the temperature-dependent stress-strain relationship given in the Eurocode (EC3 2005) at temperature T_2, i.e., $\sigma_{T_2}(\varepsilon)$. Thus, during cooling from temperature T_{n-1} to T_n, the stress σ_n at step *n* is calculated from the strain ε_n as

$$\sigma_n = \min[E^0(\varepsilon_n - \varepsilon_n^p), \sigma_{T_n}] \tag{21}$$

where ε_n^p is the residual plastic strain at step *n*, E^0 is the initial tangent modulus at temperature T_n, and σ_{T_n} is the temperature-dependent stress-strain relationship from (EC3 2005) evaluated at temperature T_n and strain ε_n. For the case when $E^0(\varepsilon_n - \varepsilon_n^p)$ is smaller than σ_{T_n}, the tangent stiffness E in Eq. (20) is replaced by the initial tangent stiffness E^0 and stress σ_n is replaced by $E^0(\varepsilon_n - \varepsilon_n^p)$. Partial derivatives of the plastic strain ε_n^p (i.e., $\frac{\partial \varepsilon_n^p}{\partial X}$ and $\frac{\partial \varepsilon_n^p}{\partial T}\frac{\partial T}{\partial X}$) are calculated in the previous $(n-1)$ step based on the fact that $\varepsilon_n^p = \varepsilon_{n-1} - \frac{\sigma_{n-1}}{E_0}$.

For the fiber-based frame element, the internal force vector is calculated according to Eq. (16). Differentiating Eq. (16) with respect to parameter *X* gives

$$\frac{\partial \mathbf{P}^{\text{int}}}{\partial X} = \bigcup_{i=1}^{nfib} A_i \cdot \int_L \left(\frac{\partial \mathbf{B}_i^T}{\partial X}\sigma_i + \mathbf{B}_i^T E_i \frac{\partial \varepsilon_i}{\partial X} + \mathbf{B}_i^T E_i \frac{\partial \varepsilon_i}{\partial T_i}\frac{\partial T_i}{\partial X} + \mathbf{B}_i^T \frac{\partial \sigma_i}{\partial X} + \mathbf{B}_i^T \frac{\partial \sigma_i}{\partial T_i}\frac{\partial T_i}{\partial X} \right) dx \tag{22.a}$$

if $\sigma_i = \sigma_{T_n}$; otherwise,

$$\frac{\partial \mathbf{P}^{\text{int}}}{\partial X} = \bigcup \sum_{i=1}^{nfib} A_i \cdot \int_L \left(\frac{\partial \mathbf{B}_i^T}{\partial X} \sigma_i + \mathbf{B}_i^T E_i^0 \frac{\partial \varepsilon_i}{\partial X} + \mathbf{B}_i^T E_i^0 \frac{\partial \varepsilon_i}{\partial T_i} \frac{\partial T_i}{\partial X} - \mathbf{B}_i^T E_i^0 \frac{\partial \varepsilon_i^p}{\partial X} - \mathbf{B}_i^T E_i^0 \frac{\partial \varepsilon_i^p}{\partial T_i} \frac{\partial T_i}{\partial X} \right) dx \qquad (22.b)$$

The time step notation *n* has been omitted in the Eq. (22). All parameters are evaluated at the current time step *n* except for $\frac{\partial \varepsilon_i^p}{\partial X}$ and $\frac{\partial \varepsilon_i^p}{\partial T_i} \frac{\partial T_i}{\partial X}$, which are evaluated at time step *n* – 1.

To conduct the response sensitivity analysis, Eq. (22) is substituted into Eq. (18). $\partial T_i / \partial X$ is passed from the heat transfer analysis, and analytical expressions can be derived for the remaining terms in Eq. (22). As a result, the response sensitivity $\frac{\partial \mathbf{u}_n}{\partial X}$ is the only unknown quantity in Eq. (18).

3.3.2 Response sensitivity analysis in the heat transfer model

To obtain the thermal response sensitivities $\frac{\partial \mathbf{T}_n}{\partial X}$ that are needed in the structural analysis, the DDM must be applied to the heat transfer model. Temporal discretization of Eq. (5) can be achieved by a backward difference technique, in which the temperature states $\mathbf{T}_n$ and $\mathbf{T}_{n-1}$, which are separated by time increment Δt, are related according to (Jeffers and Sotelino 2012)

$$\mathbf{T}_n = \mathbf{T}_{n-1} + \Delta t \cdot \dot{\mathbf{T}}_{n-1} \qquad (23)$$

Substituting Eq. (23) into Eq. (5) gives

$$\left(\frac{1}{\Delta t} \mathbf{C}_n + \mathbf{K}_n \right) \mathbf{T}_n = \frac{1}{\Delta t} \cdot \mathbf{C}_n \cdot \mathbf{T}_{n-1} + \mathbf{R}_n \qquad (24)$$

Differentiating Eq. (24) with respect to parameter X and rearranging terms yields

$$\mathbf{\Psi} \frac{\partial \mathbf{T}_n}{\partial X} = \mathbf{\Omega} \qquad (25)$$

where

$$\boldsymbol{\Psi} = \frac{1}{\Delta t}\mathbf{C}_n + \mathbf{K}_n + \frac{1}{\Delta t}\frac{\partial \mathbf{C}_n}{\partial \mathbf{T}_n}(\mathbf{T}_n - \mathbf{T}_{n-1}) + \frac{\partial \mathbf{K}_n}{\partial \mathbf{T}_n}\mathbf{T}_n - \frac{\partial \mathbf{R}_n}{\partial \mathbf{T}_n} \tag{26}$$

$$\boldsymbol{\Omega} = -\frac{\partial \mathbf{K}_n}{\partial X}\mathbf{T}_n - \frac{\partial \mathbf{K}_n}{\partial T_f}\frac{\partial T_f}{\partial X} - \frac{1}{\Delta t}\frac{\partial \mathbf{C}_n}{\partial X}(\mathbf{T}_n - \mathbf{T}_{n-1}) + \frac{1}{\Delta t}\mathbf{C}_n\frac{\partial \mathbf{T}_{n-1}}{\partial X} + \frac{\partial \mathbf{R}_n}{\partial X} + \frac{\partial \mathbf{R}_n}{\partial T_f}\frac{\partial T_f}{\partial X} \tag{27}$$

The terms in Eqs. (26) - (27) are obtained by differentiation Eqs. (6) - (8) with respect to parameter X for parameters that appear in the heat transfer model and with respect to gas temperature T_f for parameters that appear in the fire model, resulting in

$$\frac{\partial \mathbf{C}_n}{\partial X} = \bigcup\left(\int_V \mathbf{N}^T \frac{\partial \rho c}{\partial X}\mathbf{N}dV + \int_V\left(\frac{\partial \mathbf{N}^T}{\partial X}\rho c\mathbf{N} + \mathbf{N}^T\rho c\frac{\partial \mathbf{N}}{\partial X}\right)dV\right) \tag{28}$$

$$\frac{\partial \mathbf{K}_n}{\partial X} = \bigcup\left(\begin{array}{l}\int_V \mathbf{B}^T\frac{\partial k}{\partial X}\mathbf{B}dV + \int_V \frac{\partial \mathbf{B}^T}{\partial X}k\mathbf{B}dV + \int_V \mathbf{B}^T k\frac{\partial \mathbf{B}}{\partial X}dV + \int_S \mathbf{N}^T\frac{\partial\left(h+h_r\right)}{\partial X}\mathbf{N}dS \\ +\int_S \frac{\partial \mathbf{N}^T}{\partial X}\left(h+h_r\right)\mathbf{N}dS + \int_S \mathbf{N}^T\left(h+h_r\right)\frac{\partial \mathbf{N}}{\partial X}dS\end{array}\right) \tag{29}$$

$$\frac{\partial \mathbf{R}_n}{\partial X} = \bigcup\left(\begin{array}{l}\int_V \mathbf{N}^T\frac{\partial q}{\partial X}dV + \int_V \frac{\partial \mathbf{N}^T}{\partial X}qdV + \int_S \mathbf{N}^T\frac{\partial q_s''}{\partial X}dS + \int_S \mathbf{N}^T\frac{\partial\left(hT_f\right)}{\partial X}dS \\ +\int_S \mathbf{N}^T\frac{\partial\left(h_rT_f\right)}{\partial X}dS + \int_S \frac{\partial \mathbf{N}^T}{\partial X}\left(q_s'' + hT_f + h_rT_f\right)dS\end{array}\right) \tag{30}$$

$$\frac{\partial \mathbf{K}_n}{\partial T_f} = \bigcup\left(\int_S \mathbf{N}^T\frac{\partial h_r}{\partial T_f}\mathbf{N}dS\right) \tag{31}$$

$$\frac{\partial \mathbf{R}_n}{\partial T_f} = \bigcup\left(\int_S \mathbf{N}^T h dS + \int_S \mathbf{N}^T\left(h_r + \frac{\partial h_r}{\partial T_f}T_f\right)dS\right) \tag{32}$$

3.4 Procedure of Analysis

Figure 3-7 illustrates the procedure for performing the response sensitivity analysis of structures exposed to fire. First, the gas temperature T_f is calculated according to Eq. (1). To get the sensitivity $\partial T_f / \partial X$, Eq. (1) is differentiated with respect to parameter X. The structural temperatures T_n are then calculated using the finite element method. At each time step n, the thermal response sensitivity $\frac{\partial \mathbf{T}_n}{\partial X}$ is calculated based on the converged structural temperatures T_n according Eq. (26). After completion of the heat

transfer analysis, the structural analysis is conducted using the finite element method to determine the structural displacements u_n. At each time step n, the displacement response sensitivity $\frac{\partial \mathbf{u}_n}{\partial X}$ is calculated according to Eq. (18) based on the converged structural model.

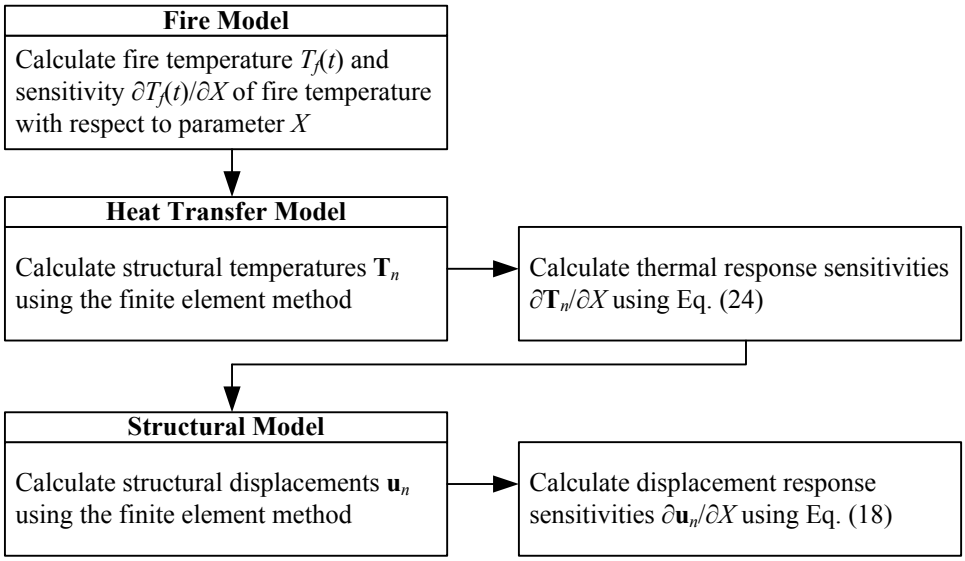

Figure 3-7 Calculation procedure for response sensitivity analysis in a sequentially coupled fire-structural model

3.5 Analysis of a Protected Steel Beam Exposed to Natural Fire

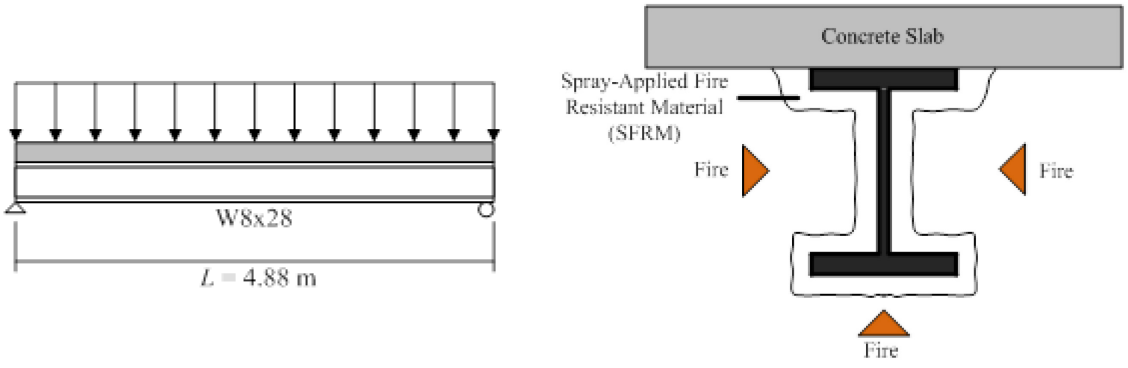

(a) (b)

Figure 3-8 Protected steel beam exposed to fire: (a) loading, and (b) cross-section (adapted from Guo et al. 2013)

To verify the formulation, an analysis was conducted for a protected steel beam exposed to natural fire. Response sensitivities were calculated using the DDM formulation and

compared to response sensitivities obtained using the FDM. In the FDM, a perturbation ΔX was applied to the parameter and the change in response (i.e., ΔT or Δu) was evaluated. Response sensitivities were then approximated as

$$\frac{\partial T}{\partial X} \approx \frac{\Delta T}{\Delta X}, \qquad \frac{\partial u}{\partial X} \approx \frac{\Delta u}{\Delta X} \ . \tag{33}$$

A convergence study was conducted and it was determined that a perturbation of 0.01% was sufficiently accurate for all parameters considered here.

Table 3-1 Parameter values

Parameter, *X*		**Value**
Room Characteristics	Ventilation Factor	0.04 $m^{1/2}$
	Fuel Load	564 MJ/m^2
	Thermal Initial	423.5 $Ws^{1/2}/m^2K$
Boundary Conditions	Convection	35 W/m^2K
	Emissivity	0.80
Properties of SFRM	Thickness	12.7 mm
	Conductivity	0.120 W/m-K
	Specific Heat	1200 J/kg-K
	Density	300 kg/m^3
Properties of Steel	Conductivity	EC3 [25]
	Specific Heat	EC3 [25]
	Density	EC3 [25]
	Yield (at Ambient)	345 MPa
Load	Dead load	5410 N/m
	Live Load	880 N/m

The system, which is shown in Fig. 3-8, is a simply supported beam subjected to a uniformly distributed load. The beam was assigned a $W8\times28$ cross-section based on the AISC steel design specification (AISC 2005) and the ANSI/UL 263 requirements for prescriptive fire resistant design in the U.S. A cementitious spray-applied fire resistant material (SFRM) shown in Fig. 3-8b was selected to provide a one-hour fire resistance rating. The beam supported a non-composite concrete slab. Due to the non-composite action, it was assumed that the slab did not affect the mechanical resistance provided by

the structure. For simplicity, it was also assumed that the concrete acted as an insulated boundary condition at the top surface of the steel beam. This assumption led to temperatures in the upper flange that were somewhat higher than would be expected in reality. Values for the model parameters were based on the analysis by Guo et al. (Guo et al. 2013) and are reproduced in Table 3-1 for clarity.

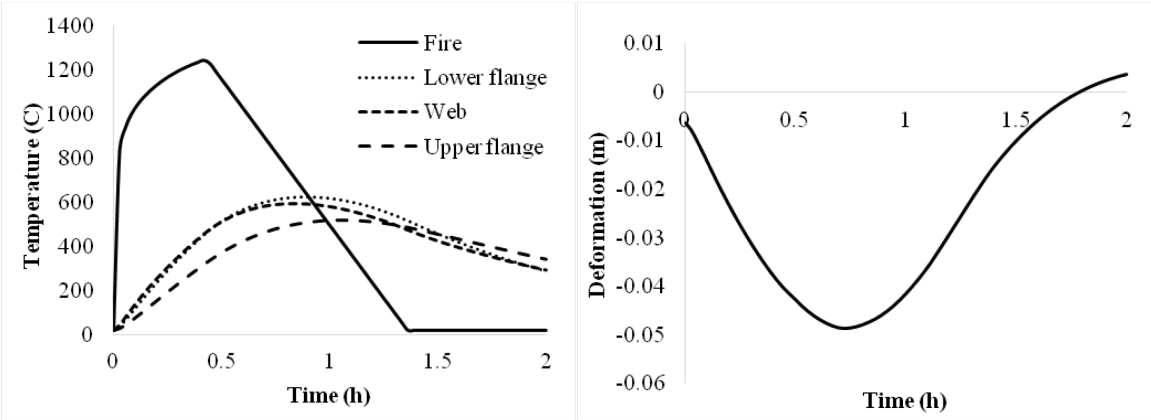

(a) (b)

Figure 3-9 Thermal-structural response of the protected beam exposed to natural fire: (a) gas and steel temperatures, and (b) mid-span displacement

Results from the thermo-structural analysis are shown in Fig. 3-9. The gas temperature in Fig. 3-9a was generated based on the natural compartment fire exposure described in Section 3.2.1, which exhibits periods of growth, burning, and decay. Under the calculated fire exposure, the temperatures in the steel increase to a maximum value of approximately 620 ^{o}C and then decrease as the fire decays. A small temperature gradient develops over the beam section due to the non-uniform heating applied over the cross-section. Under the heating and applied load, the steel beam deflects downward due to loss of mechanical integrity in the steel, with a maximum deflection of approximately 50 mm after 45 min of fire exposure. During cooling, the beam recovers some of this deformation due to thermal contraction. Because of the assumed insulated boundary condition at the interface between the steel and concrete, the temperature gradient reverses directions during cooling, resulting in a spurious upward deflection towards the end of the analysis.

Based on the response sensitivity and the expected variability in each parameter (Guo et al. 2013), the following parameters were selected for inclusion in the response sensitivity

analysis using the DDM: the fuel load density, the thermal inertia of the compartment, the ventilation factor, the thickness and thermal conductivity of the SFRM, and the dead and live loads. Results from the sensitivity analysis are presented in Fig. 3-10 – Fig. 3-12. Note that response sensitivity results presented in Fig. 3-10 – Fig. 3-12 are normalized in terms of the parameter value *X*.

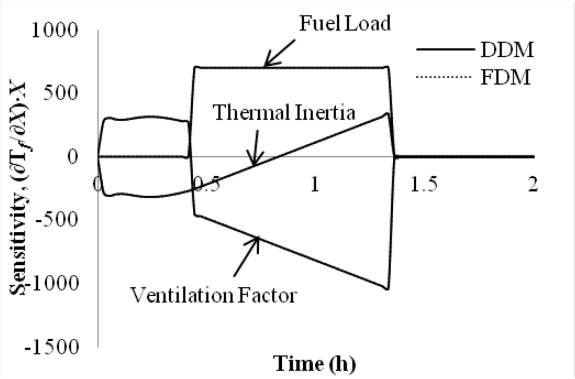

Figure 3-10 Response sensitivity in fire model

Response sensitivity values in the fire model are shown in Fig. 3-10. It can be seen that the gas temperature described in Section 3.2.1 is sensitive to the ventilation factor F_v and thermal inertia b during the period of heating based on the relationships given in Eqs. (1) - (3). From Eq. (4), the fuel load only affects the duration of burning, resulting in a null sensitivity coefficient until the cooling phased is reached. The variation of the sensitivity coefficients with time can be seen in Fig. 3-10. For example, an increase in the ventilation factor will cause the fire to burn at higher temperatures during the burning phase. However, the increase in ventilation also causes the fuel to expend more rapidly, thus decreasing the gas temperature during the cooling phase.

Thermal response sensitivity values that were obtained in the heat transfer model are illustrated in Fig. 3-11. Note that the thermal response sensitivity shown in Fig. 3-11 was calculated based on the temperature at a single point in the bottom flange of the beam. The thermal response sensitivity is shown in Fig. 3-11a for parameters that appear in the fire domain and in Fig. 3-11b for parameters that appear in the heat transfer domain. It should be noted that parameters that appear in the fire model do not directly affect the structural temperature. However, their influence on the gas temperature T_f will affect the internal temperatures that develop in the structure by changing the boundary conditions to

which the structure is subjected. As shown in Fig. 3-11, the comparisons between the DDM and FDM analyses illustrate very good agreement between the two methods.

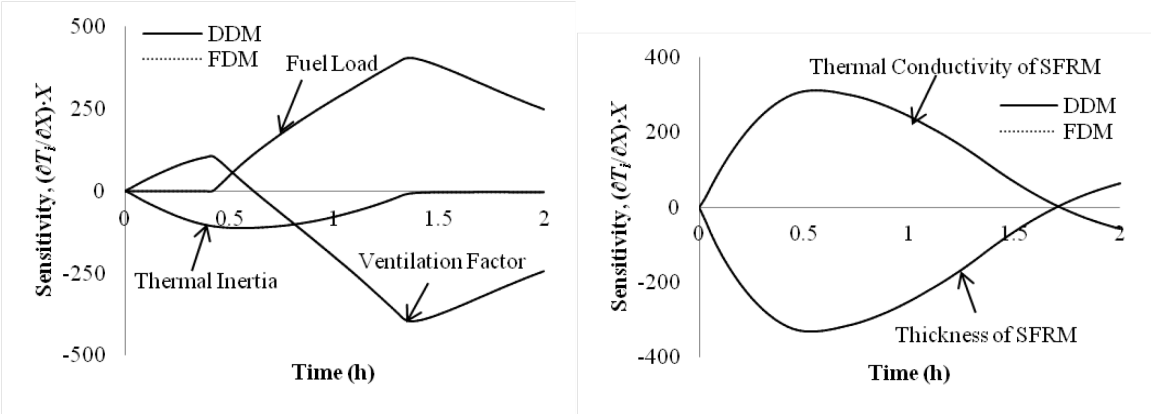

(a) (b)

Figure 3-11 Response sensitivity in the heat transfer model for temperature T_i in a fiber in lower flange: (a) for parameters in fire model, (b) for parameters in heat transfer model

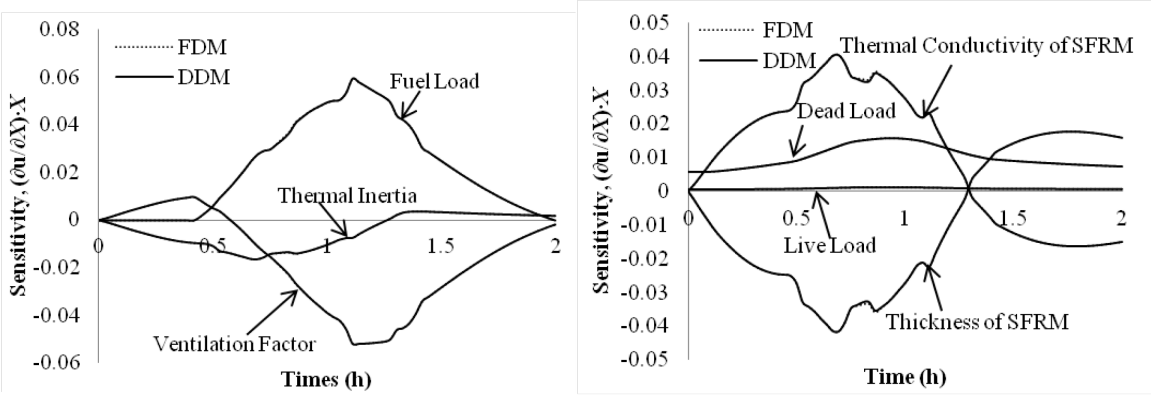

(a) (b)

Figure 3-12 Response sensitivity in the structural model: (a) for parameters in fire model; (b) for parameters in thermal and structural models

The displacement response sensitivity calculated based on the mid-span deflection is shown in Fig. 3-12. Figure 3-12a illustrates the sensitivity with respect to parameters in the fire domain, and Fig. 3-12b illustrates the sensitivity with respect to parameters in the thermal and structural domains. From Fig. 3-12, it can be seen that the DDM and FDM show good agreement. While the sensitivity coefficient may be needed as a function of time for reliability or optimization calculations, the response sensitivity at the point of maximum displacement is generally most useful for design purposes. Table 3-2 provides

a comparison of the response sensitivity values at the point of maximum displacement, as calculated using the DDM and FDM. The absolute error is also shown. In all cases, the relative error is less than 0.02%, demonstrating a high level of accuracy.

Table 3-2 Response sensitivity at the point of maximum deflection in the beam

Parameter, X	Calculated Sensitivity Coefficient		Absolute Error	Relative Error
	FDM	DDM		
Ventilation factor	-0.013335979	-0.013336393	4.13×10^{-7}	0.0031%
Thermal inertia	0.029059525	0.029058587	9.38×10^{-7}	0.0032%
Fire load	-0.015721863	-0.015722195	3.32×10^{-7}	0.0021%
Thickness of SFRM	-0.039136022	-0.03914279	6.77×10^{-6}	0.0173%
Conductivity of SFRM	0.038188896	0.038186279	2.62×10^{-6}	0.0069%
Dead load	0.014016662	0.014016574	8.80×10^{-8}	0.0000%
Live load	0.000945409	0.000945408	4.01×10^{-10}	0.0000%

The purpose of exploring the use of the DDM for response sensitivity analysis is to establish a more efficient means for evaluating the response sensitivity in structures exposed to fire. Therefore, the simulation times have also been recorded. For the analysis presented here, the DDM required 10.2s, where as the FDM required 164.6s computing time. The magnitude of cost savings would be amplified in the consideration of larger structural systems and with the inclusion of additional model parameters in the sensitivity analysis. In addition, optimization and reliability algorithms generally involve iterations to evaluate the response and response gradients under changing parameters, thus requiring the response sensitivity to be evaluated several times. The cost savings associated with the use of DDM make the use of these methods for structural fire engineering applications much more attractive.

3.6 Conclusions

This paper considered the extension of the direct differentiation method (DDM) to the analysis of structures in fire, which is a problem that involves multidisciplinary coupling

between the fire, thermal and structural domains. The paper focused on a sequentially coupled model for evaluating structural response in fire. The approach involved formulating the governing finite element equations for the nonlinear heat transfer and structural analyses and differentiating the equations with respect to parameter X. Chain rule differentiation enabled the interdependencies between the fire, thermal, and structural domains to be appropriately modeled in the response sensitivity analysis.

The proposed model was verified by considering the response sensitivity of a protected steel beam exposed to a natural compartment fire. The system involved nonlinear and temperature-dependent material properties in both the thermal and structural domains. Comparisons between the DDM and the finite difference method (FDM) illustrated that the DDM offers excellent accuracy. In addition, it was found that the DDM resulted in considerable cost savings in comparison to the FDM because additional simulations were not required to evaluate the response under a perturbed parameter value.

The improved accuracy, efficiency, and numerical stability of the direct differentiation method make the method an attractive means for evaluating the response sensitivity of structures exposed to fire. The sensitivity coefficients, such as those shown in Table 3-2, can be used to identify important parameters that affect the response, allowing the engineer to optimize the design. Furthermore, the response sensitivity is a necessary parameter in reliability analysis and design optimization problems. Thus, the DDM formulations are important in the movement towards performance-based design methodologies that seek to account for uncertainty and to achieve optimal structural designs.

References

AISC (2005). *Steel construction manual*, 13th ed., American Institute of Steel Construction, Chicago, IL, United States.

Barbato, M., Zona, A., and Conte, J.P. (2007). "Finite Element Response Sensitivity Analysis Using Three-field Mixed Formulation: General Theory and Application to Frame Structures," *International Journal for Numerical Methods in Engineering*, 69, 114-61.

Bebamzadeh, A., Haukaas, T., Vaziri, R., Poursartip, A., and Fernlund, G. (2009). "Response Sensitivity and Parameter Importance in Composites Manufacturing," *Journal of Composite Materials*, 43, 621-59.

Buchanan, A.H. (2001). *Structural Design for Fire Safety*, Wiley, Chichester, England.

Choi, J.H., Choi, K.K. (1990). "Direct Differentiation Method for Shape Design Sensitivity Analysis Using Boundary Integral Formulation," *Computers & Structures*, 34, 499-508.

Choi, K.K., Santos, J.L.T. (1987). "Design Sensitivity Analysis of Non-linear Structural Systems Part I: Theory," *International Journal for Numerical Methods in Engineering*, 24, 2039-55.

Choi, K.K., Santos, J.L.T., and Frederick, M.C. (1985). "Implementation of Design Sensitivity Analysis with Existing Finite Element Codes," *Proceedings of ASME Design Engineering Conference and Exhibition on Mechanical Vibration and Noise*, Cincinnati, OH, United States, 10-13 Sept.

Conte, J.P., Barbato, M., and Spacone, E. (2004). "Finite Element Response Sensitivity Analysis Using Force-based Frame Models," *International Journal for Numerical Methods in Engineering*, 59, 1781-820.

Cook, R.D., Malkus, D.S., Plesha, M.E., and Witt, R.J. (2001). *Concepts and*

Applications of Finite Element Analysis, 4th ed., Wiley, New York, NY.

Crisfield, M.A. (1991). *Non-linear Finite Element Analysis of Solids and Structures*, Vol. 1, Wiley, New York, NY.

EC3 (2005). *Eurocode 3: Design of Steel Structures, Part 1-2: General Rules - Structural Fire Design. BSI EN 1993-1-2*, British Standards Institution, London.

El-Rimawi, J.A., Burgess, I.W., and Plank, R.J. (1996). "The Treatment of Strain Reversal in Structural Members During the Cooling Phase of a Fire," *Journal of Constructional Steel Research*, 37, 115-135.

Giles, G.L. and Rogers, Jr. J.L. (1982). "Implementation of Structural Response Sensitivity Calculations in a Large-scale Finite Element Analysis System," *Proceedings of 23rd Structures, Structural Dynamics and Materials Conference*, New Orleans, LA, United States; 10-12 May, 348-359.

Guo, Q., Shi, K., Jia, Z., and Jeffers, A.E. (2013). "Probabilistic Evaluation of Structural Fire Resistance," *Fire technology*, 49(3), 793-811.

Haukaas, T. (2006). "Efficient Computation of Response Sensitivities for Inelastic Structures," *Journal of Structural Engineering*, 132, 260-6.

Haukaas, T. and Der Kiureghian, A. (2005). "Parameter Sensitivity and Importance Measures in Nonlinear Finite Element Reliability Analysis," *Journal of Engineering Mechanics*, 131, 1013-26.

Haukaas, T. and Scott, M.H. (2006). "Shape Sensitivities in the Reliability Analysis of Nonlinear Frame Structures," *Computers & Structures*, 84, 964-77.

Jeffers, A.E. and Sotelino, E.D. (2009). "Fiber Heat Transfer Element for Modeling the Thermal Response of Structures in Fire," *Journal of Structural Engineering*, 135, 1191-200.

Jeffers, A.E. and Sotelino, E.D. (2012). "An Efficient Fiber Element Approach for the

Thermo-structural Simulation of Non-uniformly Heated Frames," *Fire Safety Journal*, 51, 18-26.

Kleiber, M., Antunez, H., Hien, T., and Kowalczyk, P. (1997). *Parameter Sensitivity in Nonlinear Mechanics*, 1st Ed., John Wiley and Sons Ltd, West Sussex, UK.

Prasad, B., and Emerson, J.F. (1982). "A General Capability of Design Sensitivity for Finite Element System," *Proceedings of the 23rd Structures, Structural Dynamics and Materials Conference*, New Orleans, LA, United States, 10-12 May, 175-186.

Scott, M.H., Franchin, P., Fenves, G.L., and Filippou, F.C. (2004). "Response Sensitivity for Nonlinear Beam-column Elements," *Journal of Structural Engineering*, 130, 1281-8.

Thacker, B.H., Riha, D.S., Fitch, S.H.K., Huyse, L.J., and Pleming, J.B. (2006). "Probabilistic Engineering Analysis Using the NESSUS Software," *Structural Safety*, 28, 83-107.

Tsay, J.J. and Arora, J.S. (1990). "Nonlinear Structural Design Sensivitity Analysis for Path Dependent Problems Part 1: General Theory," *Computer Methods in Applied Mechanics and Engineering*, 81, 183-208.

Wallerstein, D.V. (1984). "Design Enhancement Tools in MSC/NASTRAN," *NASA Langley Research Center Recent Experiences in Multidisciplinary Analysis and Optimization*, 505-526.

Zhang, Q., Mukherjee, S., and Chandra, A. (1992). "Shape Design Sensitivity Analysis for Geometrically and Materially Nonlinear Problems by the Boundary Element Method," *International Journal of Solids and Structures*, 29, 2503-25.

Zhang, Y. and Der Kiureghian, A. (1993). "Dynamic-response Sensitivity of Inelastic Structures," *Computer Methods in Applied Mechanics and Engineering*, 108, 23-36.

CHAPTER 4 : APPLICATION OF ANALYTICAL RELIABILITY METHODS TO THE ANALYSIS OF STRUCTURES IN FIRE[3]

4.1 Introduction

The performance-based design method, which has been widely used in the earthquake and wind resistant design of structures, gives engineers the flexibility to design an optimal solution given existing constraints. Reliability evaluation is an important component of performance-based design, and a lot of research has been conducted to evaluate structural reliability in support of performance-based methods (Wen 2001).

The core difficulty in reliability analysis is the integration of the multi-dimensional probability density function in the failure field. Theories to simplify this integration have been developed. Analytical reliability methods (i.e., the First- and Second-Order Reliability Methods, or FORM/SORM), idealize the limit state function as linear or quadratic and estimate the reliability at the most probable point of failure, i.e., the point on the limit state function with the shortest distance to the origin in standard normal space (Der Kiureghian 2005). In this manner, the reliability analysis is transformed into an optimization problem. A significant amount of research has focused on refining the optimization algorithm for linear and nonlinear stochastic finite elements (Hasofer and Lind 1974, Rackwitz and Fiessler 1978, Hohenbichler and Rackwitz 1988, Der Kiureghian and De Stefano 1991, and Haukaas and Der Kiureghian 2006). Analytical reliability methods are able to estimate the reliability rapidly and with reasonable accuracy but are often inaccurate for problems with large numbers of random variables and irregular response surfaces (Rackwitz 2001). Simulation-based techniques (e.g., classical and advanced Monte Carlo simulation or MCS) are more versatile, particularly

[3] Contents of this chapter have been published as Guo, Q. and Jeffers, A.E., "Finite Element Reliability Analysis of Structures Subjected to Fire," *Journal of Structural Engineering*, doi: 10.1061/(ASCE)ST.1943-541X.0001082, 2014.

for problems involving large numbers of parameters and spanning multiple physical domains (Zio 2013). However, MCS (even with importance sampling) is overwhelmingly expensive for calculating failure probabilities that are relatively small (Madsen et al. 2006), and therefore MCS tends to be less attractive to researchers.

The performance-based design philosophy has only recently been considered for the fire resistant design of structures. As a part of the performance evaluation, some researchers have considered extending reliability analyses and safety assessment to structures subjected to fire hazards. For example, progress on the reliability evaluation of steel structures in fire has been published by Beck (1985), Shetty et al. (1998), Fellinger and Both (2000), Teixeira and Guedes Soares (2006), Khorasani et al. (2012), and Guo et al. (2012). Most of the research to date has focused on using MCS to quantify structural reliability, although a few researchers have considered using FORM/SORM (Shetty et al. 1998) and constructing fragility curves (Vaidogas and Juocevicius 2008) for structural fire engineering applications.

The review of literature illustrates that, although a lot of progress has been made in the evaluation of structural reliability under fire, previous work is predominantly limited to Monte Carlo simulation. On the other hand, analytical reliability methods are well established for structural evaluation at room temperature and their extension to structures threatened by fire hazards will promote the performance-based fire resistant design methodology due to the simplicity and low computational cost of the methods. Shetty et al. (1998) presented a reliability-based framework that was based on FORM/SORM; however, the authors did not present any numerical results or perform a systematic assessment of the suitability of FORM/SORM algorithms for structures in fire. Therefore, it is presently unknown whether the coupling of multiple fields (i.e., fire, heat transfer, and structural models) and the large number of uncertain parameters that are involved will result in convergence problems or poor accuracy in the reliability analysis. To address this need, the FORM/SORM algorithms are extended in the present paper to the analysis of structural members exposed to fire. Results from the FORM/SORM analyses are evaluated based on comparison to MCS. The paper considers an application of a

protected steel column subjected to the Eurocode parametric fire (EC1 2005) that is frequently used in performance-based structural fire engineering.

4.2 Methodology

The evaluation of structural performance in fire involves three sequentially coupled processes: (1) a fire simulation to determine thermal boundary conditions at the structural surface, (2) a heat transfer analysis to calculate temperatures within structure elements under the specified boundary conditions, and (3) a structural analysis to determine the force-deformation response of the structure. In reliability analysis, it is necessary to consider uncertain parameters that exist in each stage of the analysis, which are expressed as a random vector $\mathbf{X} = \left(X_1, X_2, \ldots X_n \right)$. Due to the coupling between the fire, thermal, and structural domains, there is a propagation of uncertainty that must be accounted for in the reliability analysis of structures in fire.

In reliability analysis, the limit state function $G(\mathbf{X}) = 0$ is defined as a function of the random vector. The failure probability P_f can then be calculated as

$$P_f = \int_{G(\mathbf{X})<0} f_{\mathbf{X}}(\mathbf{X}) d\mathbf{X}, \tag{1}$$

where $f_{\mathbf{X}}(\mathbf{X})$ is the joint probability density function, which is integrated over the failure region, $G(\mathbf{X}) < 0$. In most practical cases, $G\left(\mathbf{X}\right)$ is not an explicit expression of $\mathbf{X}$ and so it is not possible to evaluate the integral in Eq. (1) analytically. Therefore, the failure probability can be solved numerically using various techniques, including FORM/SORM, MCS, and the response surface method (Nowak and Collins 2000, Huang and Delichatsio 2010, Puatatsananon and Saouma 2006, Singh et al. 2007). This paper considers the extension of FORM/SORM to structures in fire, which involves the sequential coupling of fire, thermal, and structural models. The performance function $G(\mathbf{X})$ is evaluated by finite element analysis, and uncertain parameters X_i appear in all three domains. Details about the extended FORM/SORM analysis are given in the following section. MCS is also included for comparison.

4.2.1 First- and second-order reliability methods

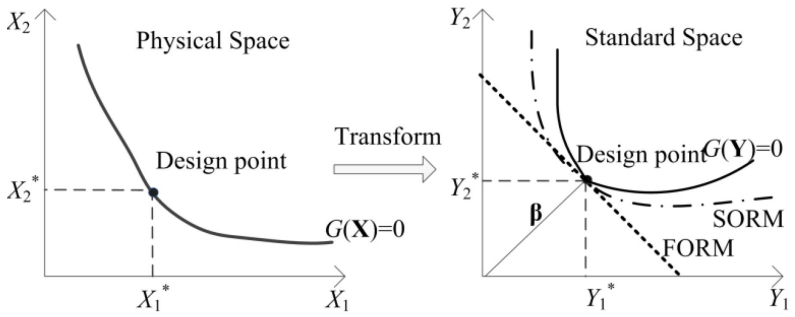

Figure 4-1 Calculation of failure probability using FORM/SORM (Haldar and Mahedevan, 2000)

The First-Order and Second-Order Reliability Methods (FORM/SORM) are the most frequently used analytical methods for evaluating structural reliability. These methods simplify the limit state function by a first- or second-order Taylor series expansion of the limit state function about the design point (Haldar and Mahadevan 2000). As shown in Fig. 4-1, the design point is defined as the point on the limit state curve that has the shortest distance to the origin in standard normal space. In standard normal space, the transformed parameters Y_i have zero mean and unit standard deviation. The distribution of parameters in standard normal space is obtained by the transformation

$$F_Y(y) = F_X(x), \tag{2}$$

where F_Y is the cumulative distribution function of the standard normal distribution, and the F_X is the original cumulative distribution function of the parameter (Der Kiureghian 2005). It should be noted that Eq. (2) only applies for independent, non-normal random parameters, and the Jacobian of the transformation is a diagonal matrix having the elements

$$J_{ii} = \frac{f_X(x_i)}{f_Y(y_i)}. \tag{3}$$

where the f_Y is the probability density function of the standard normal distribution, and the f_X is the original probability density function.

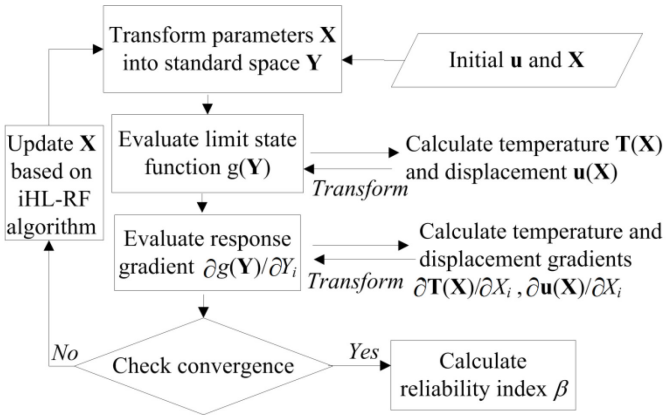

Figure 4-2 iHL-RF algorithm applied to structural response in fire

Because the performance function $G(\mathbf{X})$ is an implicit function in terms of the random vector $\mathbf{X}$, it is necessary to apply an iterative solution algorithm to find the design point on the limit state surface. Prior research has shown that the improved Hasofer-Lind-Rackwitz-Fiessler (iHL-RF) exhibits rapid convergence and numerical stability for problems with normal and non-normal distributed variables (Zhang and Der Kiureghian 1995). As shown in Fig. 4-2, it is easy to determine whether the point is an extreme value on the limit state function once all of the parameters have been transformed to standard normal space, and the performance function $G(\mathbf{X})$ and its derivative(s) have been calculated at the trial point. Note that Fig. 4-2 illustrates the iHL-RF algorithm for the first-order reliability analysis, although the basic technique is the same for the second-order reliability analysis.

To adapt the FORM/SORM methodology to the analysis of structures in fire, the iHL-RF algorithm must be extended to include the fire, thermal, and structural models in the evaluation of the performance function $G(\mathbf{X})$ and the response gradients (e.g., $\partial G(\mathbf{X})/\partial X_i$ in the first-order analysis). In the present study, performance is expressed in terms of a limiting displacement, and so the performance function is a function of the limiting structural displacement $u(\mathbf{X})$. To obtain the vector of structural displacements $\mathbf{u}(\mathbf{X})$, the fire temperature $T_f(t)$ is calculated and applied as a mixed radiation and convection boundary condition in the heat transfer model. A heat transfer analysis is subsequently conducted to evaluate the nodal temperatures $\mathbf{T}(\mathbf{X})$ in the structure. The

nodal temperatures $\mathbf{T}(\mathbf{X})$ are used in the structural model to calculate thermal strains associated with thermal expansion and to account for temperature dependence in the constitutive model. Thus, $\mathbf{u}(\mathbf{X})$ is an implicit function of the fire temperature $T_f(t)$ and the nodal temperatures $\mathbf{T}$. To obtain the response gradients (e.g., $\partial G(\mathbf{X})/\partial X_i$ in the first-order analysis), chain rule differentiation must be used, i.e.,

$$\frac{\partial G(\mathbf{X})}{\partial X_i} = \frac{\partial G(\mathbf{X})}{\partial u(\mathbf{X})} \frac{\partial u(\mathbf{X})}{\partial X_i}. \tag{4}$$

Thus, the response sensitivity $\partial u(\mathbf{X})/\partial X_i$ is needed.

The response sensitivity can be calculated by finite difference or direct differentiation methods. The finite difference method (FDM) uses a finite difference approximation for the response sensitivity such that

$$\frac{\partial u(\mathbf{X})}{\partial X_i} \approx \frac{\Delta u(\mathbf{X})}{\Delta X_i}. \tag{5}$$

As a result, the response sensitivity is approximated by perturbing parameter X_i about its current value by ΔX_i and calculating the perturbation in the response, $\Delta u(\mathbf{X})$. The direct differentiation method (DDM) is an alternative approach in which analytical expressions for the response sensitivities are derived by directly differentiating the governing finite element equations.

Once the iHL-RF algorithm has converged, the probability of failure evaluated by the FORM or SORM is calculated by integrating the joint probability density functions on one side of the limit state function. As all parameters have been transformed to standard normal space as independent, normally distribution parameters, the integral can be simplified in the FORM calculation as

$$P_{f\_FORM} = 1 - \Phi(\beta), \tag{6}$$

where Φ is the cumulative density function for a standard normal distribution and β is the distance from the origin to the design point. A simple expression to compute the probability of failure using the second-order approximation was given by Breitung (1984)

using the theory of asymptotic approximations. Thus, the failure probability is calculated in the SORM as

$$P_{f\_SORM} = \Phi(-\beta)\prod_{i=1}^{n-1}\frac{1}{\sqrt{1+\psi(\beta)\kappa_i}}, \tag{7}$$

where κ_i is the principle curvature, and $\psi(\beta)$ is given as

$$\psi(\beta) = \frac{\varphi(\beta)}{\Phi(-\beta)}. \tag{8}$$

Here, φ is the probability density function of the standard normal distribution.

4.2.2 Monte Carlo simulation and Latin Hypercube sampling

The adequacy of the FORM/SORM methods is evaluated by comparison to Monte Carlo simulation (MCS), which is described as follows. Instead of integrating probability function of the random vector in the failure domain (i.e., Eq. (1)), random samples of each uncertain parameter are generated in MCS based on the probabilistic characteristics of the parameter. A series of deterministic analyses are subsequently conducted based on each possible combination of random parameters. For a sufficiently large sample size, the probabilistic response of the system can be deduced from the large number of deterministic simulations.

For reliability analysis, the probability of failure from the MCS is estimated as

$$P_f = \frac{N_f}{N}, \tag{9}$$

where N_f is the number of simulations for which the system has failed according to the assumed limit state function, and N is the total number of simulations. If the system has a small failure probability, a large sampling space is required, resulting in excessive computational costs. In this study, Latin hypercube sampling (LHS) was applied to improve the efficiency of the MCS (Zio 2013). In particular, LHS enforces a dense stratification over the entire range of the uncertain variable with a relatively small sample size and avoids the iterated internal ranking among random parameters. Some research has shown that the Latin Hypercube sampling only provides a small improvement over

the standard MCS for estimating small failure probabilities (Pebesma and Heuvelink 1999). However, LHS was found to be effective at improving computational efficiency in the illustrative example that follows.

4.3 Analysis of a Protected Steel Column Exposed to Natural Fire

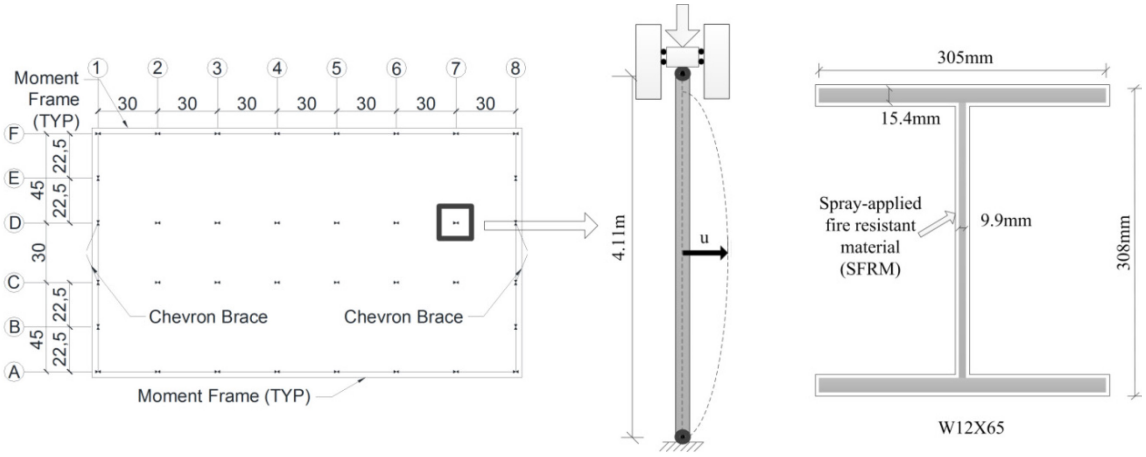

Figure 4-3 A protected and ideally pinned steel column

Numerical simulations were conducted to assess the application of FORM/SORM to evaluate structural reliability under fire. The analysis considers the reliability analysis of a protected steel column exposed to natural fire. As shown in Fig. 4-3, the column is an interior column (D7) in the second floor of a four-story building, as given in a design example by AISC (2011). According to the design requirements, a $W12\times65$ section was chosen for strength. The geometric properties of the section are shown in Fig. 4-3. The slenderness ratio of the column is 53.6, which corresponds to an intermediate length column for buckling resistance. The column was assumed to fail by global buckling, and the local stability of the cross section was verified during the ambient temperature design (i.e., based on slenderness ratios $b_f / 2t_f$ and $h / 2t_w$). It was assumed that the column was protected by a cementitious spray-applied fire resistant material (SFRM). The SFRM thickness of 28.6mm (9/8 in.) was selected from the UL fire resistance directory to provide a 2h fire resistance rating. The density of the SFRM was assumed to be 300 kg/m^3, and the thermal conductivity and specific heat were assumed to be 0.12 W/(m·K) and 1200 J/(kg·K), respectively (Iqbal and Harichandran 2010). The temperature-

dependent thermal and mechanical material properties for steel were assumed to follow the Eurocode (EC3 2005).

The dead load and live load calculated from the design were 1226 kN and 605 kN, respectively. Under natural fire exposure, there is a low probability that the maximum live load and fire accident will occur at the same time (Ellingwood 2005) so arbitrary-point-in-time dead and live loads were used to simulate the actual load that might be acting on the structure in the rare event of fire. The arbitrary-point-in-time dead load P_{DL} and live load P_{LL} are equal to the design dead load and live load multiplied by factors of 1.05 and 0.24, respectively (Iqbal and Harichandran 2010). In the probabilistic analysis, the axial load P was calculated as

$$P = E(AP_{DL} + BP_{LL}), \tag{10}$$

where A, B, and E are stochastic parameters that account for variability in the loads (Ravindra and Galambos 1978). The nominal yield strength for steel was 345 MPa. Based on the fact that the actual yield strength tends to exceed the nominal strength that is assumed in design, a factor of 1.04 was multiplied on the nominal value.

Natural fire exposure was modeled using the Eurocode parametric fire (EC1 2005). During the heating phase, the fire temperature is given as

$$T_f = 20 + 1325(1 - 0.324e^{-0.2t^*} - 0.204e^{-1.7t^*} - 0.472e^{-19t^*}), \tag{11}$$

where t^* is fictitious time, which is related to the opening factor O and the thermal inertia of the surrounding compartment. The duration of the burning (in hours) is defined as $t_d = \max\left(0.2\times10^{-3}\cdot\frac{q_{t,d}}{O}, t_{\lim}\right)$, where the $q_{t,d}$ is the fuel load per total surface area and the limiting time $t_{\lim}$ is taken as 20 min, assuming a medium growth fire. The fire temperature during the decay phase is defined as

$$T_f = \begin{cases} T_{\max} - 625(t^* - t^*_{\max}) & \text{for } t^*_{\max} \le 0.5 \\ T_{\max} - 250(3 - t^*_{\max})(t^* - t^*_{\max}) & \text{for } t^*_{\max} \le 2 \\ T_{\max} - 250(t^* - t^*_{\max}) & \text{for } t^*_{\max} > 2 \end{cases}, \quad (12)$$

The column was located in a compartment with floor dimensions of 4.75×6.70 m (15×22 ft) and a height of 3.04 m (10 ft). The mean fuel load per floor area was taken as 564 MJ/m^2 according to the survey by Culver (1976), resulting in a fuel load per total surface area of 132.9 MJ/m^2. The wall and ceiling were assumed to be lined gypsum board, which has a mean thermal inertia b of 423.5 Ws$^{1/2}$/m^{2}K (Iqbal and Harichandran 2010). The column was assumed to be heated uniformly on all sides by convection and radiation from the fire. The convection heat transfer coefficient and the emissivity were taken as 35 W/(m$^2 \cdot$K) and 0.80, respectively, based on the definition for natural fire exposure in Eurocode (EC1 2005).

It should be noted that only the statistical uncertainty has been considered, and the model uncertainty has been ignored in this study. The exclusion of model uncertainty results in a higher reliability level than if model uncertainty had been considered.

4.3.1 Validation of the thermo-structural model

The thermo-structural analysis of the column was conducted in a finite element code that was programmed in Matlab. Fiber-based heat transfer elements (Jeffers and Sotelino 2009) were used to calculate the temperature of the column under fire. The structural response was modeled using 2D displacement-based distributed plasticity (i.e., fiber-based) frame elements. A corotational frame formulation (Yaw et al. 2009) was used to include the large displacements and large rotations in the structural analysis. Residual stresses were modeled assuming a bilinear distribution across the flanges and web (Chan and Chan 2001), and initial out of straightness was modeled as a half sine wave with an amplitude of 1/1000 of the length of the column (Ziemian 2010).

The structural model was validated against steel column tests by Wainman and Kirby (1988) and numerical simulations by Jeffers and Sotelino (2012). The tests by Wainman and Kirby involved steel columns with blocked-in webs subjected to the ISO 834 standard fire. The columns failed by global buckling in the experimental tests and

therefore can be used to evaluate the accuracy of the current structural model. The blocks placed around the webs of the columns were intended to protect the columns against fire exposure and therefore did not contribute to the structural response of the columns. In the model, the temperature in the steel was based on the reported average web and flange temperatures measured during the test. The results for one column test are shown in Fig. 4-4. The axial deformation calculated by our structural model is compared with the experimental result, Jeffers and Sotelino's result, and an Abaqus model in Fig. 4-4a. It can be seen that the current model agrees well with previous experimental and numerical results, both in terms of the predicted deformation as well as the temperature at failure. As the lateral deformation in the mid-height was not reported in the Wainman and Kirby (1988) and Jeffers and Sotelino (2012), a comparison is made between the Abaqus model and our structural model in Fig. 4-4b. Note that Fig. 4-4 shows the column deformation as a function of the average flange temperature in the steel rather than the furnace temperature.

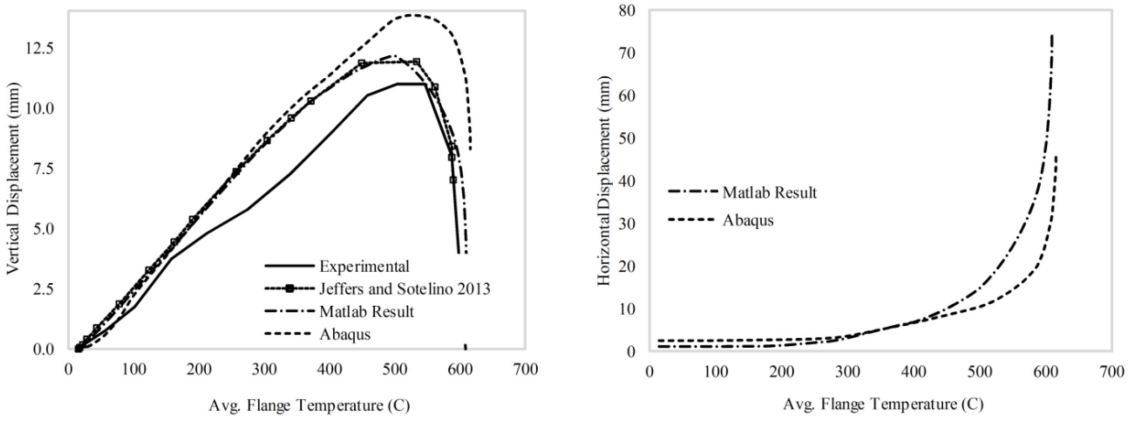

(a) (b)

Figure 4-4 Displacement of the column: a) axial displacement at the top of the column, b) horizontal displacement in the mid-height of the column

4.3.2 Sensitivity analysis to determine parameter importance

There are a large number of uncertain parameters in the numerical model. In particular, the Eurocode parametric fire curve (i.e., Eqs. (11) - (12)) is dependent on the fuel load density, the thermal inertia, and the opening factor. The temperature of the column is

dependent on the convection heat coefficient, the surface emissivity, the thickness of the spray-applied fire resistant material (SFRM), and the density, thermal conductivity, and specific heat for the SFRM and the steel, as well as the fire temperature. The structural model depends on the mechanical properties of the steel, the magnitude of the applied load, and the initial imperfection, as well as the structural temperatures. Table 4-1 lists the model parameters as well as their statistical properties (if reported in the literature). It was assumed that all parameters were uncorrelated for simplicity. Note that the yield strength and elastic modulus in Table 4-1 are given at ambient temperature, although these parameters also exhibit variability with increasing temperature.

Table 4-1 Statistical properties and response sensitivity for uncertain parameters

Parameter		Distribution	Mean Value	COV	Sensitivity	References
Room Properties	Fuel Load	Extreme I	564 MJ/m^2	0.62	0.0185	Culver (1976), Iqbal and Harichandran (2010)
	Thermal Inertia	Normal	423.5 Ws$^{0.5}$/m^{2}K	0.09	-0.1180	
Properties of the SFRM	Thickness	Lognormal	Nominal + 1.6mm	0.2	-3.0688	Iqbal and Harichandran (2010)
	Density	Normal	300 Kg/m3	0.29	-0.3455	
	Conductivity	Lognormal	0.120 W/mK	0.24	2.8536	
	Specific heat	--	1200J/kg-K	--	-0.3455	
Properties of the steel	Density	--	EC3	--	-0.5705	
	Conductivity	--	EC3	--	-0.5705	
	Specific heat	--	EC3	--	-1.9653	
	Yield Stress	Normal	Nominal x 1.04	0.08	-2.6557	
	Elastic Modulus	--	200 GPa	--	-1.2547	
Heat Transfer	Convection	--	35 W/m^{2}K	--	0.0030	
	Emissivity	--	0.8	--	0.0248	
Load	Dead Load	Normal	1.05 x Nominal	0.1	3.0019	Ellingwood (2005), Iqbal and Harichandran (2010), Ravindra and Galambos (1978)
	Live Load	Gamma	0.24 x Nominal	0.6	0.3387	
	A Factor	Normal	1	0.04	3.0019	
	B Factor	Normal	1	0.2	0.3387	
	E Factor	Normal	1	0.05	3.3406	
Geometry	Imperfection	--	L/1000	--	0.3717	

A sensitivity analysis was conducted to identify the importance of the various parameters. During the sensitivity analysis, the simulation was conducted using mean values for all parameters. As all parameters were assumed to be independent, the response gradient was calculated by perturbing each parameter about its mean value and approximating the gradient as a first order finite difference (i.e., Eq. (5)). A convergence test demonstrated that a perturbation of 0.1 percent in each parameter provided a converged first-order

derivative. The response sensitivity was calculated for the mid-height displacement $u_{\max}$ (shown in Fig. 4-3) and was non-dimensionalized based on the mean value of each parameter X_i, i.e., $(\partial u_{\max} / u_{\max}) / (\partial X_i / X_i)$. A positive sensitivity coefficient indicates that an increasing of parameter X_i increases the mid-height deflection (i.e., worsens the structural performance), while a negative value means that an increasing of parameter X_i decreases the mid-height deflection (i.e., improves the structural performance).

The response sensitivity coefficients are shown in Table 4-1. In the fire model, the fuel load density and thermal inertia were treated as random parameters due to their large variances, despite their small sensitivity coefficients. In the heat transfer model, the thickness and conductivity of the SFRM were selected as random parameters due their large sensitivity coefficients and variances. Thermal properties for steel were treated as deterministic due to relatively low variances despite having large sensitivity coefficients. Based on the sensitivity analysis, the load parameters were all treated as probabilistic, whereas the geometric imperfection was not.

4.3.3 Reliability analysis

As described in the methodology section, the reliability was evaluated using FORM, SORM, and LHS. Prior reliability analyses for columns in fire have focused on evaluating failure in terms of a critical load or critical stress in the section (Khorasani et al. 2011, Tan et al. 2006). This type of failure criterion is impractical for non-uniformly heated structures because the temperature gradient over the cross-section naturally leads to variable material properties throughout column due to the constitutive model's dependence on temperature. Here, failure was defined in terms of a limiting deformation rather than a critical load. This definition provides a more convenient way to estimate the structural response because the deflection is the typical output from a finite element simulation. A limiting displacement tends to be conservatively defined as a point prior to the column losing all of its strength (i.e., incipient collapse). However, there is little information regarding the maximum deflection that a column can tolerate before the structure loses stability at elevated temperature. Given the limited guidance on the subject, story drift limits in ASCE 7 (2005) for lateral loads due to seismic and wind effects were

deemed reasonable limits for lateral column deflections. In particular, the drift is limited to L/400 under 10-year wind condition and 0.025L (inter-story drift) for seismic risk occupancy category II based on ASCE 7. For fire hazard, the limiting mid-height deflection was taken as L/200, which is between the story drift limits imposed on buildings for lateral loads at ambient temperature.

In the FORM and SORM analyses, the iHL-RF algorithm was used to identify the design point on the limit state function, as discussed in methodology section. A convergence study was conducted to ensure that the algorithm converged (within an acceptable tolerance) to the same design point with different starting values for parameter X_i. For example, with the problem reduced to two uncertain parameters (i.e., the fuel load density and thickness of SFRM), different starting values were chosen for the fuel load density and SFRM thickness. The limit state function obtained by LHS for 1.5 h of fire exposure is shown in Fig. 4-5 along with two search paths from the FORM analysis using the iHL-RF algorithm. It can be seen that the iHL-RF algorithm converged in less than 10 iterations to the same design point on the limit state surface (within a tolerance of 0.1). Similar robustness of the iHL-RF algorithm was observed for cases involving larger numbers of uncertain parameters.

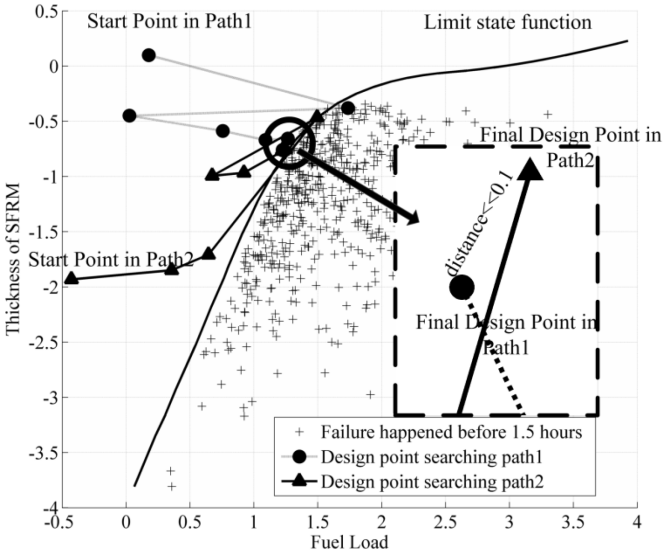

Figure 4-5 Path for searching the design point

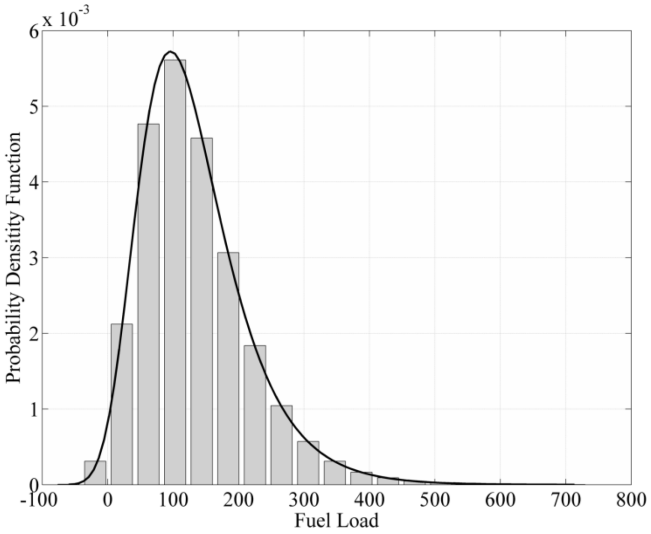

Figure 4-6 Sampling result of the fuel load

LHS was performed for comparison with the FORM/SORM analyses. For a system with a theoretical failure probability of 0.01, a classical Monte Carlo simulation with a sample size of 10,000 would result in a calculated failure probability of 0.01 ± 0.002 (Haldar and Mahadevan 2000), and LHS provides a similar level of accuracy. A preliminary analysis indicated that the failure probability was likely to be greater than 0.01 in the present study, indicating that 10,000 sample values would allow the failure probability to be calculated within a reasonable level of accuracy. Therefore, a Latin hypercube sample of 10,000 was generated. The sampled result for each parameter was verified with its theoretical distribution, as shown in Fig. 4-6. The 10,000 deterministic simulations were separated into 40 batches, and each batch was submitted to an individual node on the NYX cluster at the Center for Advanced Computing at University of Michigan.

4.3.4 Results from the reliability analysis

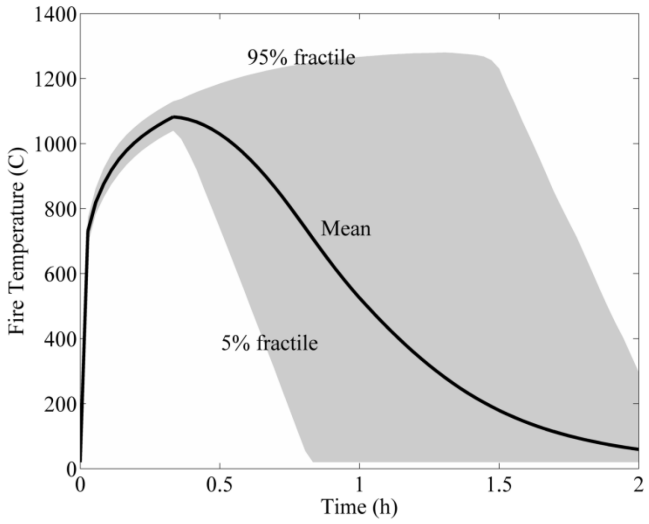

Figure 4-7 Fire temperatures obtained by LHS

Based on the statistical distributions of the fire parameters introduced in previous section, 10,000 natural fire curves were obtained in the LHS. As shown in Fig. 4-7, the mean fire temperature is illustrated along with the 0.05 and 0.95 fractiles. The fire curves have similar heating phases based on Eq. (11), but the duration of burning varies considerably between 20 min to 2 h due to the variance of the fuel load density. The maximum fire temperature exceeded 1300 C in several instances.

The fire curves obtained from the LHS were combined with the random values for the thickness and conductivity of the spray-applied fire resisitant materials (SFRM) in the 2D heat transfer model for the column. The mean flange temperatures are shown in Fig. 4-8 along with the 0.05 and 0.95 fractiles. With the help of the SFRM, the maximum temperature in the column is less than 500 C in most cases (88.08%). However, the other 11.92% cases in which the steel temperature exceeded the critical temperature for prescriptive fire rating of columns indicating that there may be a significant chance of failure.

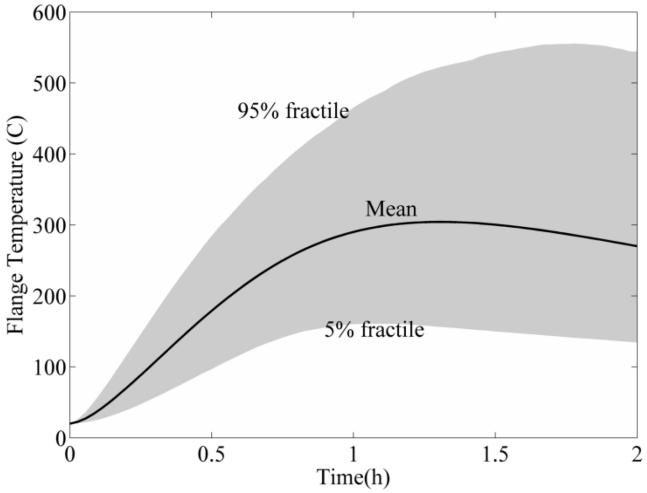

Figure 4-8 Temperature in the column flange

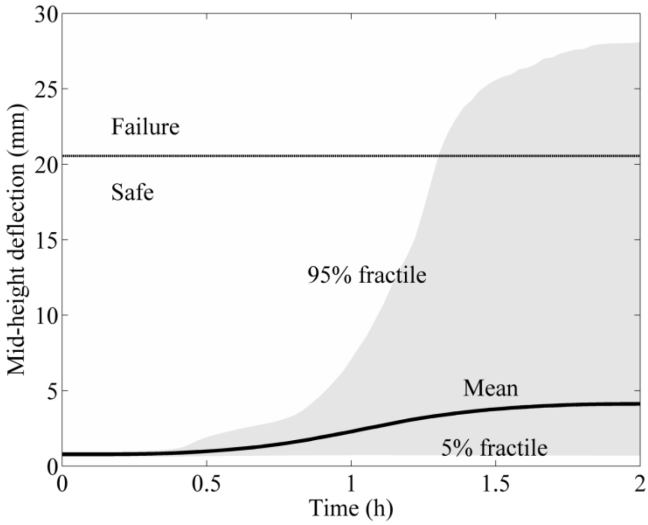

Figure 4-9 Mid-height deflection of column

The temperatures from the heat transfer LHS were entered into the structural model along with the random values for the applied load, load factors, and yield stress. The mean mid-height deflection is plotted in Fig. 4-9 along with the 0.05 and 0.95 fractiles. The column generally recovers some of the lateral displacement during cooling. However, the mean deflection shown in Fig. 4-9 continues to increase in time. This behavior arises from the fact that the mean deflection is skewed by the disproportionately large displacements in the columns that have failed.

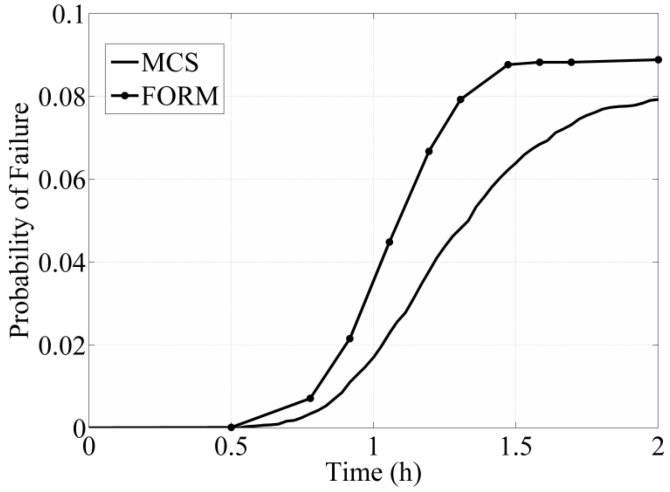

Figure 4-10 Probability of failure with time

The column reliability was based on the limiting deflection of $L/200 = 20.6$ mm, which is shown in Fig. 4-9. Based on the results of the LHS, the failure probability was calculated as a function of time by observing the number of simulations that had failed at the given time, i.e., Eq. (9). The problem was also evaluated using FORM and SORM. The evolution of the failure probability in time is shown in Fig. 4-10 for the LHS and FORM analyses. It can be seen that the FORM results in noticeable errors, particularly at earlier times. The total failure probability after two hours of fire exposure was calculated as 7.92% by LHS, 8.8% by FORM, and 7.37% by SORM. According to this evaluation, the reliability index at the ambient temperature is 7.4, which is significantly higher than 3, the value specified by AISC. The high level of reliability may be caused by the conservatism of the design, an incomplete selection of random variables, or consideration for a single failure criterion. The reliability index decreases to 1.4 after 2 hours fire exposure. The comparison between LHS and FORM illustrates that these two methods give fairly good agreement. The response surface is studied in detail in the following section to give a better understanding of the source of error.

The total computing time for LHS is calculated by summing up the CPU time in the 40 computing nodes that were used in parallel, which was 173.7 hours. To calculate the total failure probability, the FORM and SORM required 0.4 hours and 3.8 hours, respectively. This result shows that the FORM and SORM are much more efficient than the LHS.

4.4 Discussion

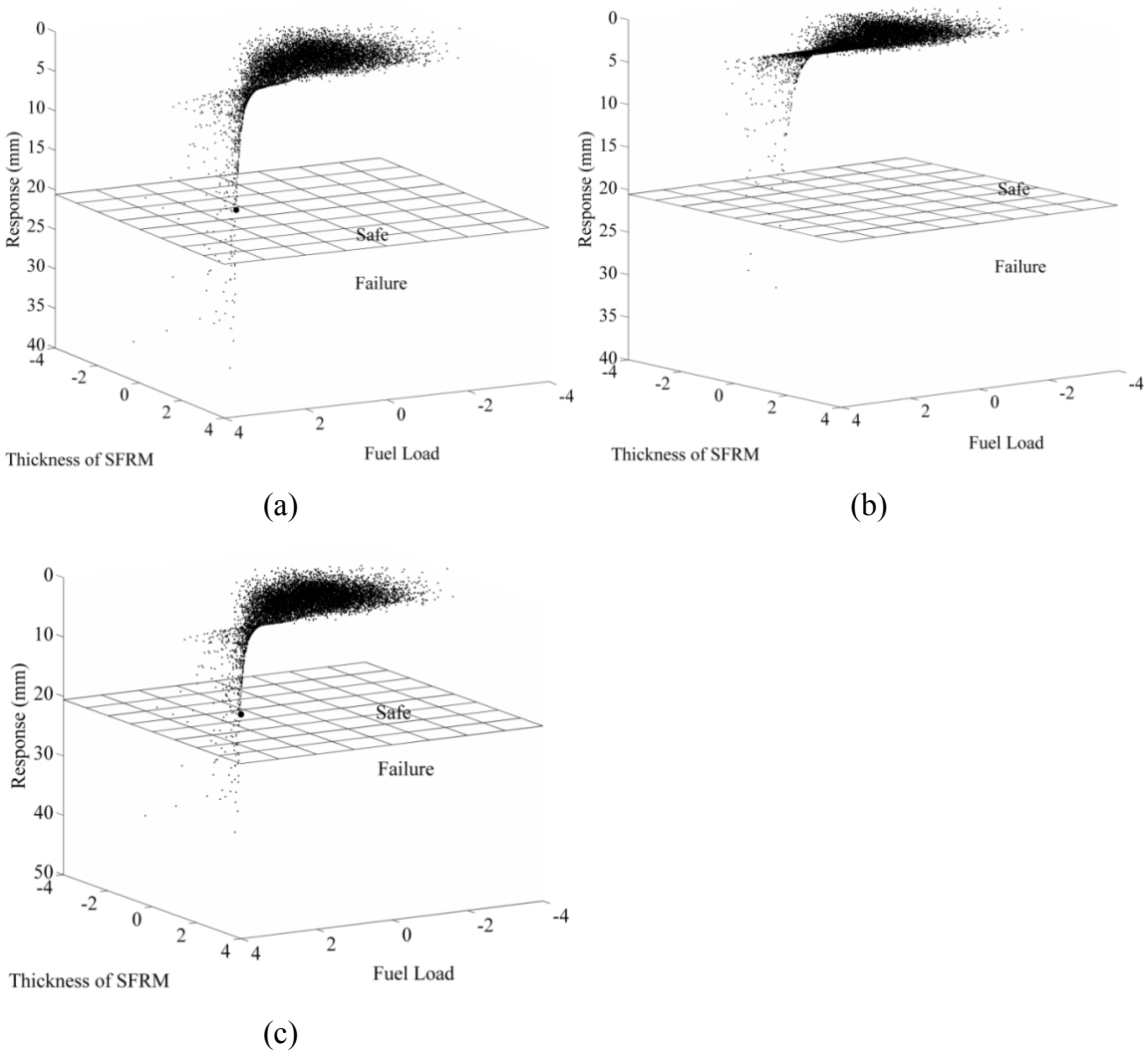

Figure 4-11 Structural response by the LHS: a) at 1 h, b) at 1.5 h, c) at 2 h

An in-depth study of the response surface was conducted to better understand the source of the discrepancies between the FORM and LHS results. To better illustrate the results, the problem was reduced to two random parameters, namely, the fuel load density and the thickness of the SFRM. All other parameters were treated as deterministic and their values equal to their mean values.

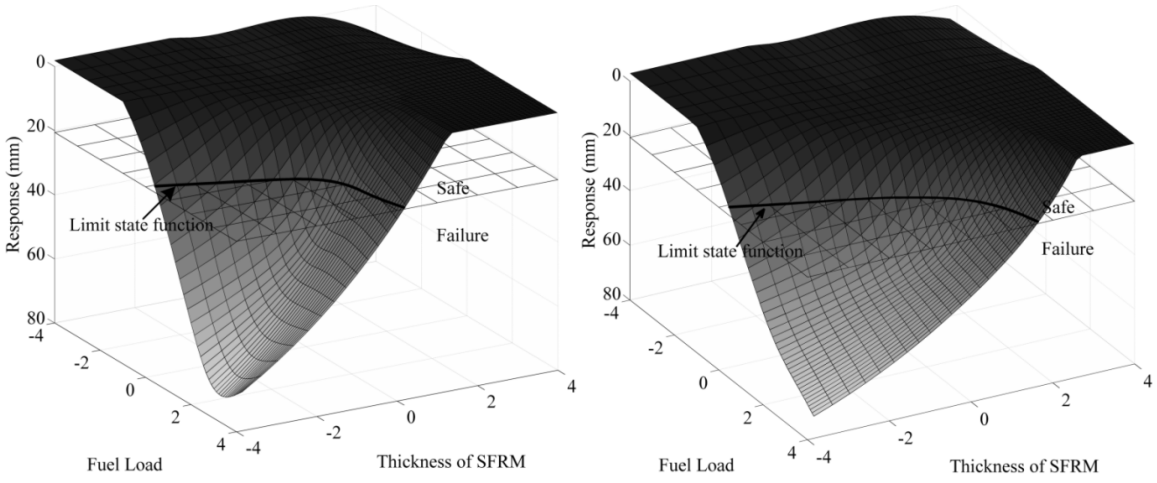

Figure 4-12 Response surface: a) at 1 h, and b) at 2 h

The response (i.e., the mid-height displacement of the column) calculated by LHS is illustrated in Fig. 4-11 at various times for two random parameters. It can be seen that the number of cases that exceeded the failure criterion increased significantly after 1 h of fire exposure, as indicated by the increasing number of points lying below the failure surface in Figs. 4-11(b) and (c). The FORM performs the calculation along the limit state function, which is the intersection between the response surface and the failure surface. To better understand the shape of the response surface (and hence the suitability of a first-order approximation), a curve fitting technique (D'Errico 2006) was applied to plot the response surface at different time steps based on the LHS results. The response surfaces at 1.5 h and 2 h are plotted in Fig. 4-12. The response surface at 1 h is not shown due to the lack of data points around the failure area, which resulted in a poor approximation by the curve fitting function.

As shown in Fig. 4-12a, the response surface exhibits a nonlinearity that resembles a kink, resulting in a limit state function that is practically bilinear. As time increases, the response surface becomes smoother but remains nonlinear. These effects are more noticeable in the 2D plot shown in Fig. 4-13. In particular, the failure points from the LHS (which indicate the shape of the limit state function) are plotted in Fig. 4-13 at 1 h, 1.5 h, and 2 h. The design point (i.e., the most probable point of failure) according to the FORM is also shown for various times along with the corresponding reliability index β. The FORM represents the limit state surface as a linear function based on the slope of the

response surface at the design point. Therefore, it can be seen that the FORM gives a poor estimate of the response at 1 h but gives improved accuracy at 2 h as the response surface becomes smoother.

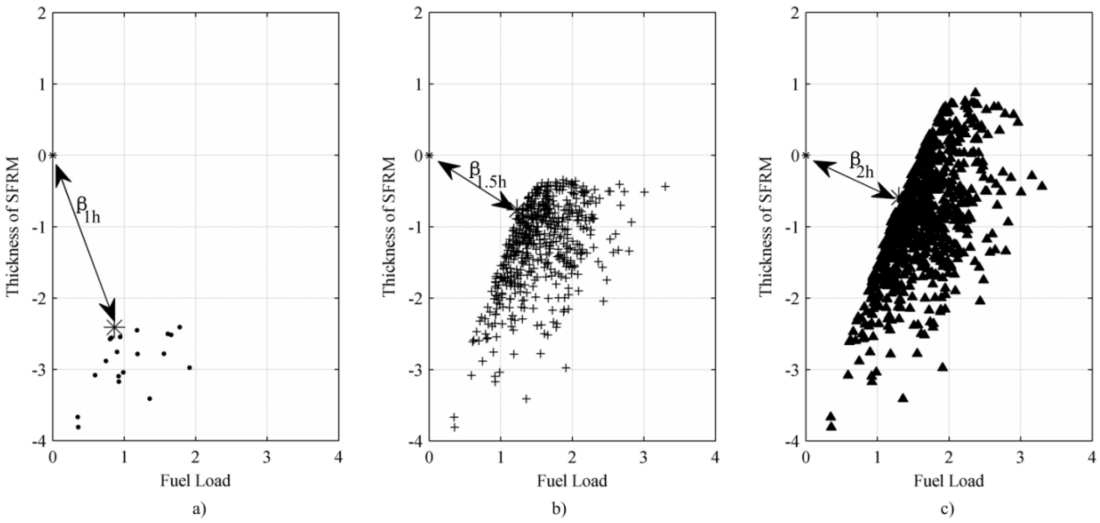

Figure 4-13 Limit state function and design point at different times: a) 1 hour; b) 1.5 hours; c) 2 hours

In Fig. 4-14, the actual limit state function is close to bilinear at 1.5 h, although the FORM assumes that the response surface is linear about the design point (i.e., the limit state function is assumed to be a straight line that is perpendicular to reliability index). The limit state function assumed in the SORM is a parabolic curve based on the curvature around the design point. It can be seen that the SORM fails to give improved accuracy due to the variable curvature of the limit state function. The limit state functions used in FORM and SORM include many points that are not actually on the failure surface, resulting in an overestimation of the failure probability at 1.5 h. This error can be seen in the plot of the failure probability shown in Fig. 4-15 for the two-parameter problem. In particular, the calculated failure probability is 5.25% by LHS, 7.43% by FORM, and 6.93% by SORM at 1.5 h. Note that the actual limit state function shown in Fig. 4-14 is the curve-fitted result from the LHS.

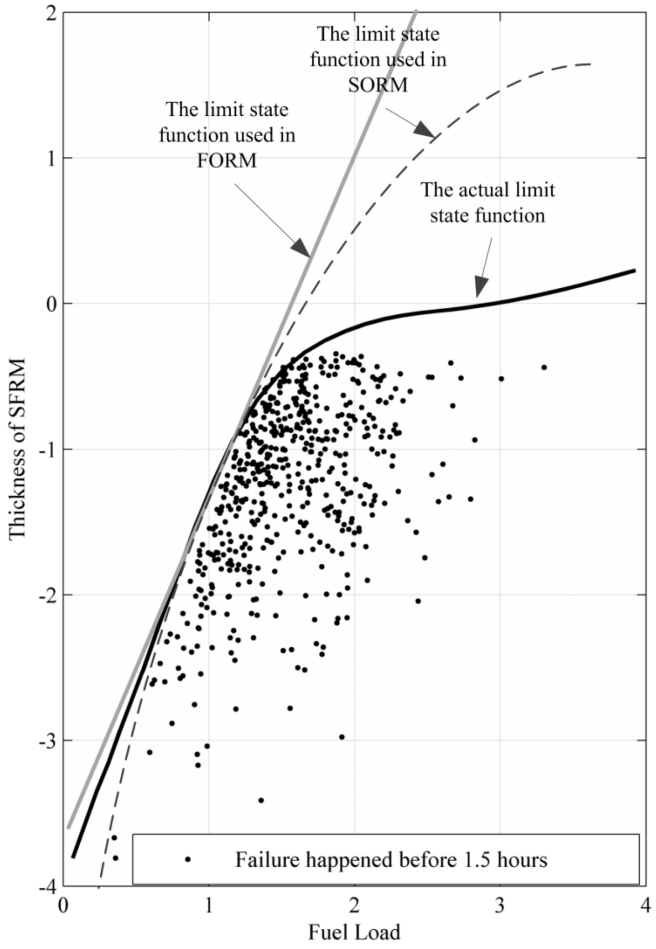

Figure 4-14 Limit state function in FORM and SORM at 1.5 h

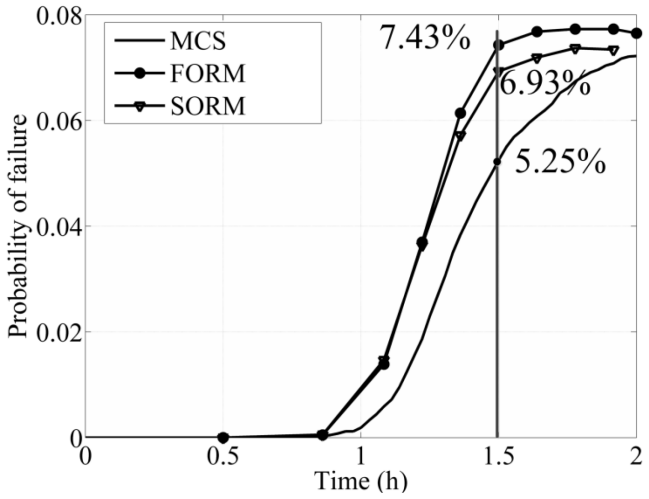

Figure 4-15 Probability of failure with two random variables

The source of the bilinear nature of the response surface stemmed from the fact that the fire temperature from the parametric fire curve was not sensitive to the fuel load during the heating phase (i.e., the fuel load only affects the duration of heating in the Eurocode parametric fire). The bilinear behavior of the response surface does not appear when a different fire model is used, i.e., one in which the fire temperature depends on the fuel load during both heating and cooling phases. Examples of such fire models include the zone models and Ma and Makelainen's model (2000). The use of a different fire model can remove the kink in the response surface, but the response surface is still nonlinear, hence introducing errors in the first- and second-order reliability methods.

4.5 Summary and Conclusions

The analytical reliability methods (i.e., FORM/SORM) have been extended to evaluate the structural reliability under fire. The reliability analysis requires statistical properties for the uncertain parameters and the definition of a suitable failure criterion. Failure was defined in terms of a limiting deformation for generality and ease of implementation in the finite element reliability analysis. The dimensionality of the model was reduced by taking into consideration the sensitivity of the model as well as the variances of the input parameters. Three sequentially coupled analyses were performed to determine the fire temperature, the temperatures in the structure, and the force-deformation response of the structure in the reliability analysis. As the analytical reliability method requires the response and response gradients to be calculated several times during the analysis, the direct differentiation method was used to improve the accuracy and efficiency of the FORM/SORM analyses.

The suitability of the analytical reliability methods was determined by considering an application of a protected steel column under natural fire. The 2-hour rated column was found to have a failure probability of approximately 8% (reliability index of 1.4) under natural fire exposure, which indicates that the structure is likely to survive. However, discussion is needed amongst the fire safety engineering community regarding what constitutes an acceptable level of safety in the fire resistant design of structures. The FORM/SORM analysis was compared to LHS, and it was found that the methods yielded similar results. The iHL-RF algorithm converged without problems despite the existence

of parameters in multiple domains. A comprehensive assessment of the response surface indicated that the problem is nonlinear, resulting in some error between the FORM and LHS results. For the application considered here, the FORM provided conservative results, whereas the SORM provided minimal improvement in accuracy over the FORM and resulted in a prediction that was not always conservative. The additional computational expense of performing a second-order analysis (i.e., using SORM) is not justified. This conclusion is supported by evidence that the response surface does not resemble a quadratic function.

In summary, it is believed that the FORM can provide a rapid estimation of the failure probability of structural elements subjected to natural fire. The FORM allows the reliability to be calculated in a matter of minutes on a single processor, whereas MCS and Latin Hypercube sampling require excessive computational cost and therefore are prohibitive for most researchers. However, it should also be noted that the error from FORM cannot be determined unless a careful error analysis has been conducted. The sampling methods are still recommended for most applications at the current stage. Additional work is needed to extend the reliability analysis to structural systems, which involve interactions between structural members and exhibit more complex failure behaviors. It is also recommended that future research focuses on more efficient simulation techniques that yield improved accuracy over FORM while providing improved computational efficiency over standard MCS.

References

AISC (2011). *Steel Construction Manual Design Example v14.0*, URL: http://www.aisc.org/WorkArea/showcontent.aspx?id=29596, American Institute of Steel Construction.

ASCE 7 (2005). *Minimum Design Loads for Buildings and Other Structures*, American Society of Civil Engineers, Reston, VA.

Beck, V.R. (1985). "The Prediction of Probability of Failure of Structural Steel Elements under Fire Conditions," *Transactions of the Institution of Engineers, Australia: Civil Engineering*, 27, 111-118.

Breitung, K. (1984). "Asymptotic Approximation for Multi-normal Integrals," *Journal of Engineering Mechanics*, 110(3), 357–366.

Chan, S.L., and Chan, B.H.M. (2001). "Refined Plastic Hinge Analysis of Steel Frames under Fire," *Steel and Composite Structures*, 1, 111-130.

D'Errico, J.R. (2006), "Understanding Gridfit," Matlab File Exchange, URL: http://www.mathworks.com/matlabcentral/fileexchange/8998-surface-fitting-using-gridfit

Der Kiureghian, A. (2005). "First- and Second-order Reliability Methods," Chapter 14 in *Engineering Design Reliability Handbook*, Nikolaidis E. et al. (Eds), CRC Press, Boca Raton.

Der Kiureghian, A., and De Stefano, M. (1991). "Efficient Algorithm for Second-order Reliability Analysis," *Journal of Engineering Mechanics*, 117(12), 2904-23.

EC1 (2005). *Eurocode 1: Actions on Structures, Part 1–2: General Actions—Actions on Structures Exposed to Fire*, BSI EN 1991–1-2. British Standards Institution, London.

EC3 (2005). *Eurocode 3: Design of Steel Structures, Part 1-2: General Rules--Structural Fire Design*, BSI EN 1993-1-2, British Standards Institution, London.

Ellingwood, B.R. (2005). "Load Combination Requirements for Fire-resistant Structural Design," *Journal of Fire Protection Engineering*, 15, 43-61.

Fellinger, J.H.H., and Both, C.K. (2000). "Fire Resistance: Reliability vs. Time Analyses," *Proceedings of Composite Construction in Steel and Concrete IV*, Hajjar, J.F. (Ed.), ASCE, USA, 816-827.

Guo, Q., and Jeffers, A.E. (2013). "Stochastic Finite Element Methods for the Reliability-Based Fire-Resistant Design of Structures," *Proceedings of the 3rd International Conference on Applications in Structural Fire Engineering*, Prague, Czech Republic, April. 19-20.

Guo, Q., Shi, K., Jia, Z., and Jeffers, A.E. (2012). "Probabilistic Evaluation of Structural Fire Resistance," *Fire Technology*, 49, 793-811.

Haldar, A., and Mahadevan, S. (2000). *Reliability Assessment Using Stochastic Finite Element Analysis,* John Wiley and Sons, New York.

Hasofer, A.M., and Lind, N.C. (1974). "Exact and Invariant Second-moment Code Format," *Journal of the Engineering Mechanics Division*, ASCE, 100(1), 111-121.

Haukaas, T., and Der Kiureghian, A. (2006). "Strategies for Finding the Design Point in Nonlinear Finite Element Reliability Analysis," *Probabilistic Engineering Mechanics*, 21(2), 133-147.

Iqbal, S., and Harichandran, R.S. (2010). "Capacity Reduction and Fire Load Factors for Design of Steel Members Exposed to Fire," *Journal of Structural Engineering*, 136, 1554-1562.

Jeffers, A.E., and Sotelino, E.D. (2009). "Fiber Heat Transfer Element for Modeling the Thermal Response of Structures in Fire," *Journal of Structural Engineering*, 135,

1191-1200.

Jeffers, A.E., and Sotelino, E.D. (2012). "Analysis of Steel Structures in Fire with Force-based Frame Elements," *Journal of Structural Fire Engineering*, 3, 287-300.

Khorasani, N.E., Garlock, M.E., and Gardoni, P. (2012). "Reliability Analysis of Steel Perimeter Columns under Fire," *Proceedings of the 7th International Conference on Structures in Fire*, Fontana et al. (Eds.), ETH Zurich, Zurich, 541-550.

Madsen, H.O., Krenk, S., and Lind, N.C. (2006), *Methods of Structural Safety*, Dover Publications, New York, USA.

Nowak, A.S., and Collins, K.R. (2000). *Reliability of Structures*, McGraw-Hill, Boston, USA.

Pebesma, E.J., and Heuvelink, G.B.M. (1999). "Latin Hypercube Sampling of Gaussian Random Fields," *Technometrics*, 41(4), 203-212.

Puatatsananon, W., and Saouma, V.E. (2006). "Reliability Analysis in Fracture Mechanics Using the First-order Reliability Method and Monte Carlo Simulation," *Fatigue & Fracture of Engineering Materials & Structures*, 12, 323-335.

Rackwitz, R. and Fiessler, B. (1978). "Structural Reliability under Combined Load Sequences," *Computers & Structures*, 9, 489-494.

Rackwitz, R. (2001). "Reliability Analysis - A Review and Some Perspectives," *Structural Safety*, 23, 365-395.

Shetty, N.K., Guedes Soares, C., Thoft-Christensen, P., and Jensen, F.M. (1998). "Fire Safety Assessment and Optimal Design of Passive Fire Protection for Offshore Structures," *Reliability Engineering and System Safety*, 61, 139-149.

Singh, V.P., Jain, S.K., and Tyagi, A. (2007). *Risk and Reliability Analysis: A Handbook for Civil and Environmental Engineers*, American Society of Civil

Engineers, Reston, VA.

Tan, K.H., Toh, W.S., Huang, Z.F., and Phng G.H. (2007). "Structural Responses of Restrained Steel Columns at Elevated Temperatures. Part 1: Experiments." *Engineering Structures*, 29(8), 1641-1652.

Wen, Y.K. (2001), "Reliability and Performance-based Design." *Structural Safety*, 23, 407-428.

Zhang, Y., and Der Kiureghian, A. (1995). "Two Improved Algorithms for Reliability Analysis in Reliability and Optimization of Structural Systems." Rackwitz R., Augusti G, and Borri A., editors. *Proceedings of the 6th IFIPWG 7.5 Working Conference on Reliability and Optimization of Structural Systems and Computer Methods in Applied Mechanics and Engineering*, 297-304.

Zio, E. (2013). *The Monte Carlo Simulation Method for System Reliability and Risk Analysis,* Springer Series in Reliability Engineering, Springer-Verlag, London.

CHAPTER 5 : EVALUATING THE RELIABILITY OF STRUCTURAL SYSTEMS IN FIRE USING SUBSET SIMULATION[4]

5.1 Introduction

Some progress has been made in recent years to apply probabilistic methods to the analysis of structures in fire. Iqbal and Harichandran (2010) derived probability-based load and resistance factors for structural design. Van Coile et al. (2014) proposed a method to objectively compare structural safety with design alternatives based on reliability evaluation. Jensen et al. (2010) used probabilistic methods to account for uncertainty associated with fire resistance tests of concrete structures, and reliability analyses were conducted by Eamon and Jensen (2012, 2013) for reinforced concrete and prestressed concrete beams. Lange et al. (2014) established a performance-based design methodology for structures in fire based on the performance based earthquake engineering methodology developed in the Pacific Earthquake Engineering Research (PEER) Center. A probabilistic plastic limit analysis using Monte Carlo simulation was performed by Nigro et al. (2014) for fire-risk analysis. Guo et al. (2013) and Guo and Jeffers (2014) investigated the reliability of isolated structural members using the Latin Hypercube simulation and the first/second-order reliability methods, respectively. Prior research has focused on the reliability of structural components rather than structural systems, and limited attention was given to computational efficiency, which is a necessary consideration when studying the response of large-scale structural systems. Additionally, probabilistic fire models were limited to standard and parametric fire curves which did not account for the potential for fire spread.

This study seeks to improve the reliability framework for structural fire engineering in three ways: (1) introducing subset simulation to the fire-structure analysis, (2) including a

[4] The contents of this chapter will be submitted for publication in the *Fire Safety Journal*. Co-author Jason Martinez produced the structural model of the composite floor system and validated the model against the Cardington fire test.

more comprehensive probabilistic fire model, and (3) considering the structural system behavior. A protected steel column is analyzed first to present the procedure of subset simulation as applied to structures in fire and to compare the accuracy and efficiency between subset simulation and Latin Hypercube simulation. A model of a steel-concrete composite floor system is then produced and probabilistic simulations are carried out for a residential building using a zone fire model. The zone fire model is able to provide a more realistic simulation of the fire growth and spread in a building with multiple rooms, and it allows a more realistic treatment of the random parameters. The 3D model for the composite floor system is created in Abaqus to simulate the structural system response under different fire exposures. Because a system-level analysis is performed, multiple failure criteria can be considered.

5.2 Methodology

The analysis of most structures in fire involves three sequentially coupled processes: a fire analysis to determine the thermal boundary conditions at the fire-structure interface, a heat transfer analysis to determine the temperature distributions in structural members, and a structural analysis to determine the load-displacement response of the structure. For the fire analysis, parametric fire curves (e.g., EC1 2005) are most commonly applied. However, more realistic fire growth and spread can be accounted for using a zone model. The zone model divides a compartment into several uniform zones (typically a hot upper layer and a cool lower layer) and the temperature in each zone is assumed to be uniform. Conservation of mass and energy is satisfied in the zone model, taking into account the geometry of the room, the location of the fire source, the heat release rate of the fuel, and the geometry and orientation of the vents. Fire spread from object to object and from room to room can be simulated in a zone model. The temperature distributions of structural members are determined through the heat transfer analysis using analytical (e.g., EC3 2005) or numerical (e.g., finite element) methods. The structural analysis is most commonly carried out using nonlinear finite element analysis, taking into account thermal expansion due to heating and degradation of the material properties with temperature. Complex system-level structural responses, such as tensile membrane action in composite floor systems, can be simulated using finite element analysis.

The reliability analysis of systems can be performed using analytical (e.g., first-order reliability method) or statistical methods (e.g., Monte Carlo simulaition). Monte Carlo simulation (MCS) has been widely applied in various fields because of its great versatility. However, classical MCS needs an extremely large sample size to conduct an accurate reliability evaluation, especially when the failure probability is small. Advanced Monte Carlo methods use improved sampling to reduce the total number of simulations. The Latin Hypercube method is an improved sampling method that was originally developed by McKey et al. (1979). In statistical sampling, a Latin square is a square grid containing sample positions for which there is only one sample in each row and each column. The Latin Hypercube is based on this concept that each sample is the only one in each axis-aligned hyperplane that contains the sample (Zio 2013). Because of the structured alignment, the Latin hypercube sampling method ensures that the sampling is distributed over the range of each uncertain variable while preserving the desirable parameters' probability distributions. Additional research has been conducted to control the correlated parameters (Olsson et al. 2003) and to adapt the method to sequentially coupled complex systems (Breeding et al. 1992; Helton and Davis 2003).

The subset simulation was developed by Au and Beck (2001) for efficiently computing small failure probabilities. The concept of a "subset" is to generate several intermediate failure events which have higher conditional failure probabilities than the targeted failure probability. The methodology transfers the rare event to a sequence of simulations of more frequent events that require smaller sample sizes. For example, if the targeted failure event is F, and intermediate events $F_1 \supset ... \supset F_n = F$ are sequentially constructed, the failure probability $P(F)$ can be described as

$$P(F) = P(F_1)\prod_{i=1}^{n-1} P\left(F_{i+1} \middle| F_i\right). \quad (1)$$

Thus, even if the target failure probability $P(F)$ is extremely small, the conditional failure probability $P\left(F_{i+1} \middle| F_i\right)$ could be much larger (Zio 2013). The Markov chain Monte Carlo simulation may be used to sample parameters within the conditional failure region. As it is difficult to choose appropriate intermediate failure events, the common strategy is

to set a constant conditional failure probability for $P\left(F_{i+1}\middle|F_i\right)=p$ so that the intermediate failure event F_i is inversely determined. According to Au and Beck (2001), $p=0.1\sim0.2$ yields a good result.

The initial step of the subset simulation is the same as the standard Monte Carlo simulation, but the sample size is much smaller (e.g., 500). The first intermediate failure region is chosen to cause a failure probability that equals p, which means there are $(p\times N)$ cases located within the intermediate failure region. These cases are treated as the seeds for the Markov Chain in the next sampling to generate more cases within the intermediate failure region. The modified Metropolis algorithm in the Markov Chain Monte Carlo simulation is given as follows:

> "For every $j=1,...,n$, let $p_j^*(\xi|\theta)$, called the 'proposal PDF', be a one-dimensional PDF for θ with the symmetry property $p_j^*(\xi|\theta) = p_j^*(\theta|\xi)$. Generate a sequence of samples $\{\boldsymbol{\theta}_1,\boldsymbol{\theta}_2,...\}$ from a given sample $\boldsymbol{\theta}_1$ by computing $\boldsymbol{\theta}_{k+1}$ from $\boldsymbol{\theta}_k=\left[\boldsymbol{\theta}_k(1),...,\boldsymbol{\theta}_k(n)\right]$, $k=1,2,...$, as follows:
>
> 1. *Generate a 'candidate' state* $\tilde{\boldsymbol{\theta}}$ *:* For each component $j=1,...,n$, simulate ξ_j from $p_j^*(\cdot|\boldsymbol{\theta}_k(j))$. Compute the ratio $r_j=q_j(\xi_j)/q_j(\boldsymbol{\theta}_k(j))$. Set $\tilde{\boldsymbol{\theta}}(j)=\boldsymbol{\theta}_k(j)$ with the remaining probability $1-\min\{1,r_j\}$.
>
> 2. *Accept/reject* $\tilde{\boldsymbol{\theta}}$: Check the location of $\tilde{\boldsymbol{\theta}}$. If $\tilde{\boldsymbol{\theta}}\in F_i$, accept it as the next sample, i.e. $\boldsymbol{\theta}_{k+1}=\tilde{\boldsymbol{\theta}}$; otherwise reject it and take the current sample as the next sample, i.e $\boldsymbol{\theta}_{k+1}=\boldsymbol{\theta}_k$." (Au and Beck 2001)

In this study, the "proposal PDF" is taken as the uniform distribution with the mean value equal to the current value and the standard deviation equal to the original standard deviation of each the parameter.

A large number of uncertainties exist in the problem of fire-structure interaction, and many parameters significantly affect the structural performance under fire. The sources of

uncertainty include the fire location, the fuel load density, the ventilation conditions, the thermal and mechanical properties of all building materials, the level of protection (for protected members), and the applied load as well as the modelling error and the limits in the supporting databases. The modeling error and limits in the supporting databases are classified as the epistemic uncertainty or systematic uncertainty, which arise from the lack of knowledge and can be reduced by improving models and extending databases. The rest of the uncertainties are referred to as the aleatoric uncertainty or statistical uncertainty, which cannot be eliminated with the development of simulation technologies and improved knowledge (Phan et al. 2010). In this study, only the aleatoric uncertainties are included in the reliability evaluation.

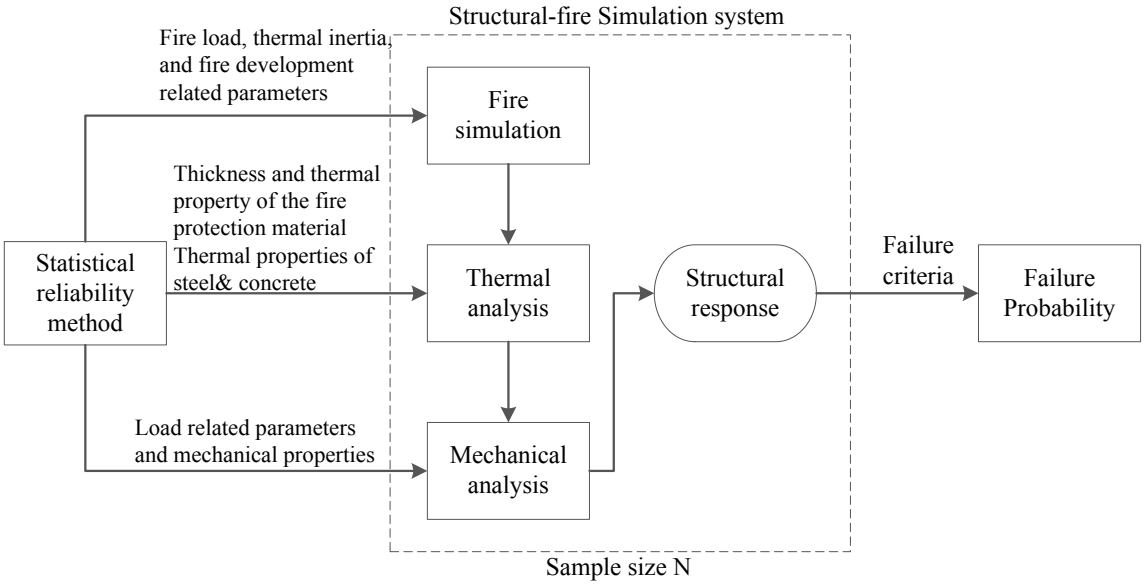

Figure 5-1 Framework for the structural reliability evaluation under fire

A framework for the reliability-based structural analysis under fire is shown in Fig. 5-1 based on the previous discussion about the modeling and reliability methods. In reliability assessment, it is always a challenge to find the balance between accuracy and efficiency. The statistical reliability methods require hundreds or even thousands simulations. If the average simulation time for a single fire-thermal-structural analysis is several minutes, the total computing time for even a relatively small sample size can be several days. More efficient techniques may be applied but can reduce the accuracy of the

simulation. The engineer needs to determine the optimum approach by considering the possible error level and the current computational capability.

5.3 Case 1. Protected Steel Column

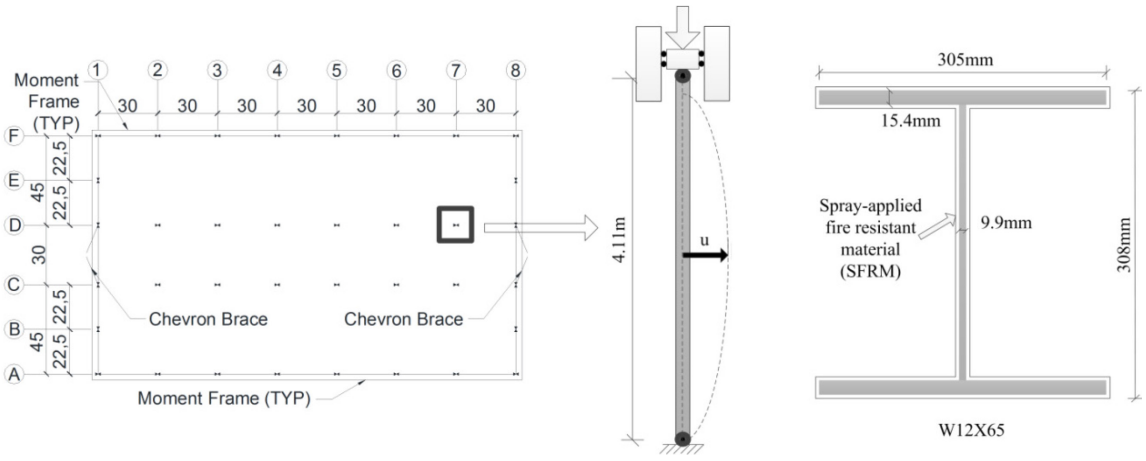

Figure 5-2 Protected and ideally pinned steel column (Guo and Jeffers 2014)

The first analysis considers the reliability of a protected steel column in the second floor of a four-story building given by AISC (2011). In a previous study by Guo and Jeffers (2014), the reliability of the same column was assessed by the Latin Hypercube simulation, first-order reliability method, and second order reliability method. Although the first-order and second-order reliability methods are able to provide a rapid estimation of the failure probability of structural elements subjected to natural fire, the accuracy cannot be determined without a detailed failure surface analysis. To explore a more efficient and robust reliability method, the subset simulation is applied here to evaluate the structural reliability under fire load.

Based on the design by AISC (2011), the column has a W12×65 section, and it is assumed to be protected by a cementitious spray-applied fire resistant material (SFRM) with a thickness of 28.6 mm. The calculated dead load and live load are 1226 and 605 kN, respectively. The arbitrary-point-in-time dead load and live load are equal to the design dead load and live load multiplied by factors of 1.05 and 0.24, respectively (Iqbal and Harichandran 2010). The total axial load P was calculated as

$$P = E(AP_{DL} + BP_{LL}) \quad (2)$$

where A, B, and E are the stochastic parameters that account for variability in the loads (Ravindra and Galambos 1978). The parametric fire curve in the Eurocode (EC1 2005) was selected to model the natural fire exposure of the column. The thermo-structural analysis of the column was conducted in a finite-element code programmed in Matlab using a fiber-based heat transfer element (Jeffers and Sotelino 2009) and a 2D displacement-based distributed-plasticity frame element. The uncertain parameters are listed in Table 5-1. More details of this model can be found in (Guo and Jeffers 2014).

Table 5-1 Statistical properties for uncertain parameters (Guo and Jeffers 2014)

Parameter		Distribution	Mean Value	COV	References
Room Properties	Fuel Load	Extreme I	564 MJ/m^2	0.62	Culver (1976), Iqbal and Harichandran (2010)
	Thermal Inertia	Normal	423.5 Ws$^{0.5}$/m^{2}K	0.09	
Properties of the SFRM	Thickness	Lognormal	Nominal + 1.6mm	0.2	Iqbal and Harichandran (2010)
	Density	Normal	300 Kg/m3	0.29	
	Conductivity	Lognormal	0.120 W/mK	0.24	
	Specific heat	--	1200J/kg-K	--	
Properties of the steel	Density	--	EC3	--	
	Conductivity	--	EC3	--	
	Specific heat	--	EC3	--	
	Yield Stress	Normal	Nominal x 1.04	0.08	
	Elastic Modulus	--	200 GPa	--	
Heat Transfer	Convection	--	35 W/m^{2}K	--	
	Emissivity	--	0.8	--	
Load	Dead Load	Normal	1.05 x Nominal	0.1	Ellingwood (2005), Iqbal and Harichandran (2010), Ravindra and Galambos (1978)
	Live Load	Gamma	0.24 x Nominal	0.6	
	A Factor	Normal	1	0.04	
	B Factor	Normal	1	0.2	
	E Factor	Normal	1	0.05	
Geometry	Imperfection	--	L/1000	--	

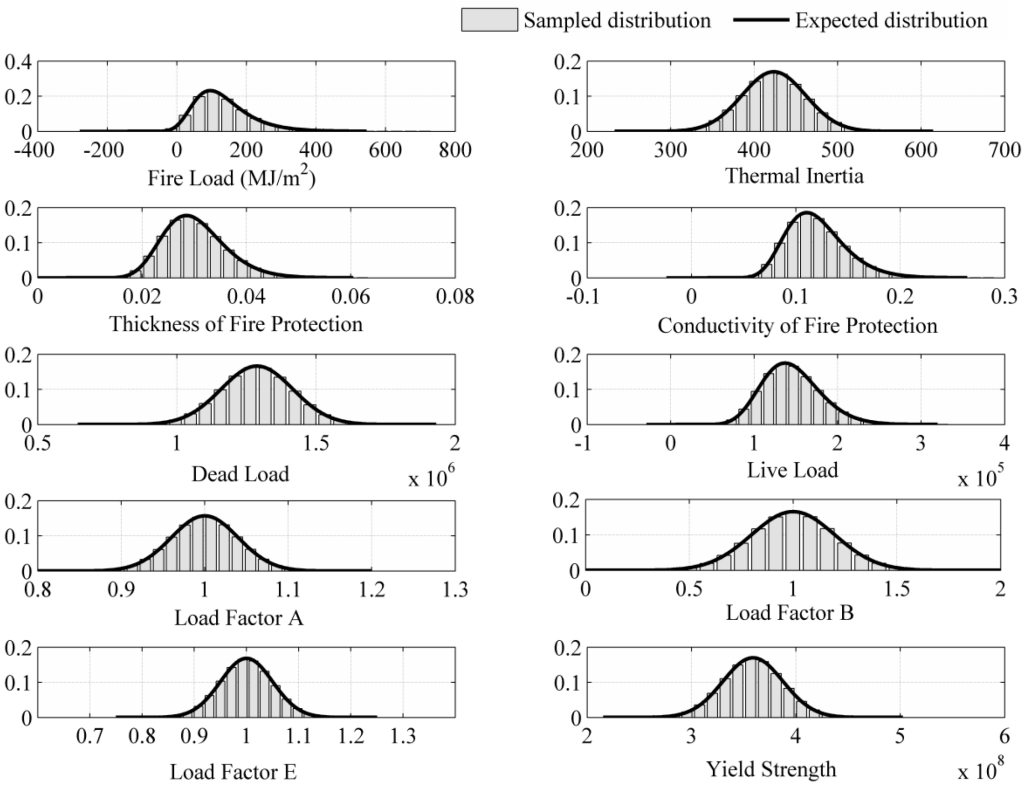

Figure 5-3 Parameter distributions

As shown in Fig. 5-3, 10,000 cases with desirable parameter distributions are generated for the Latin Hypercube simulation. The failure criteria for the column is set as a limiting lateral deflection of L/100=41.1mm (Guo and Jeffers 2014). The predicted deflection results of all sampled cases are shown in Fig. 5-4 for various fuel loads, and the failure probability calculated by Latin Hypercube simulation is 3.59%, which is equal to a safety index of 1.8.

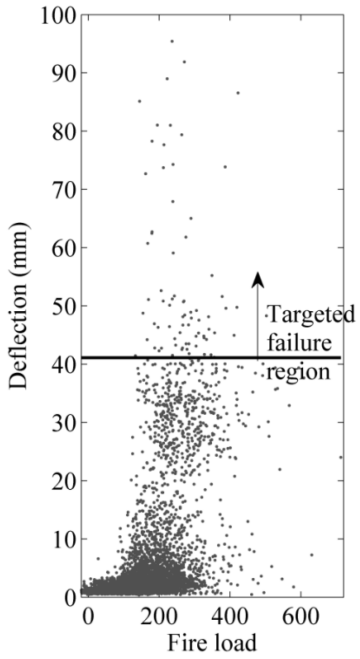

Figure 5-4 Structural responses

In the subset simulation, the first step is the same as the standard Monte Carlo Simulation, but a small sample size of 500 is used in this study. As shown Fig. 5-5a, the threshold value $p = 0.2$ described in Section 5.2 is used to define the intermediate failure region, which means that there are 100 cases in the first 500 sampling cases located in the first failure region. The other 400 cases can be sequentially generated within the first failure region by using the Markov Chain Monte Carlo simulation. The process repeats until the new intermediate failure region is located within the targeted failure region. In this case study, only two intermediate failure regions are needed before getting close enough to the targeted failure region as shown in Fig. 5-5c.The failure probability calculated by the subset simulation is 3.58%, which is very close to 3.59% from the Latin Hypercube method. It should be noted that the result from the subset simulation will change each time the simulation is run because the generated random samples will be different. The estimated failure probability by subset simulation is actually within a range that is defined by the coefficient of variation (COV), which is connected to the sample size and failure probability value. According to Au and Beck (2001), the estimated COV for the subset simulation with a sample size of 500 and failure probability around $10^{-2} \sim 10^{-1}$ is around 0.25, which means that there is 95% confidence that actual failure probability will

located between 1.82% and 5.33%. The upper limit of 5.33% could be used for decision making and potential risk analysis as a conservative estimate.

In actual design practice, it is difficult to decide the limiting deflection that corresponds to failure associated with loss of stability. In Fig. 5-6, the relationship between probability of failure and the limiting deflection is illustrated. In this study, the failure probability stops reducing after the horizontal deflection is larger than 0.05m, which means that the columns loss its stability after the horizontal deflection is larger than 0.05m in all cases. It can also be seen that the Latin hypercube simulation and subset simulation results match very well in Fig. 5-6 even though the total number of simulations for the subset simulation is 1300, which is significantly less than the sampling size of 10,000 in the Latin hypercube simulation.

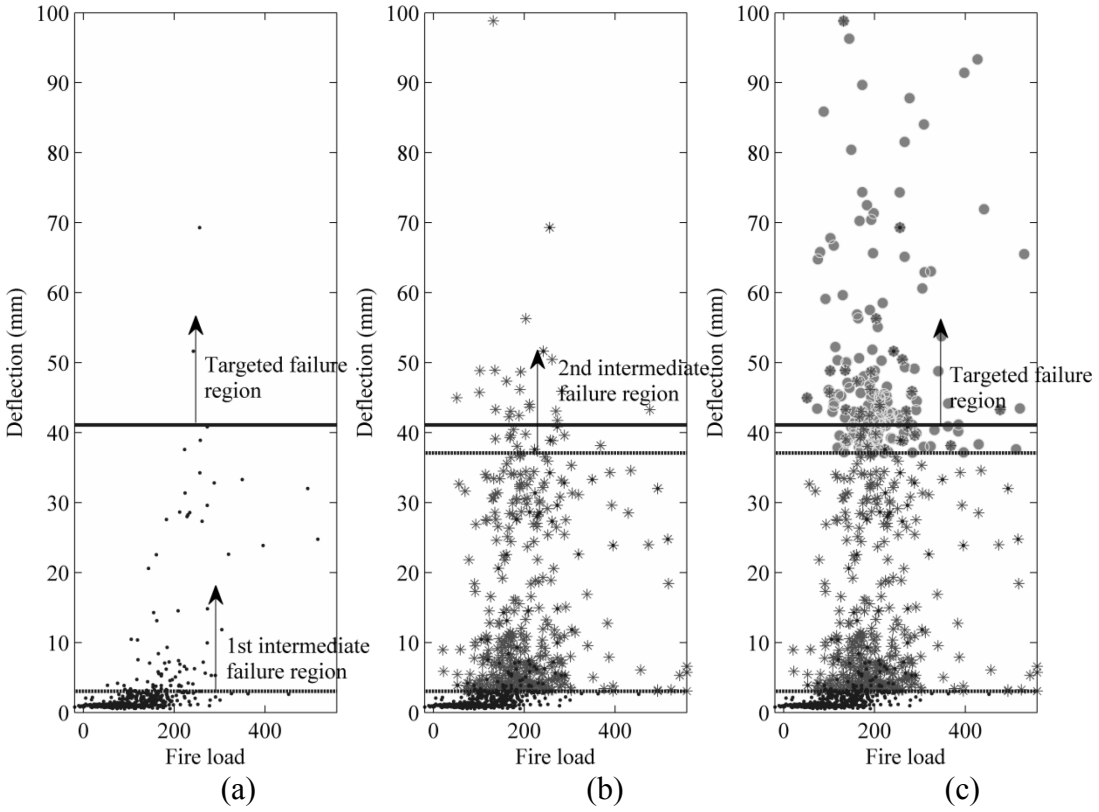

Figure 5-5 Subset simulation (a) first iteration, (b) second iteration, (c) third iteration

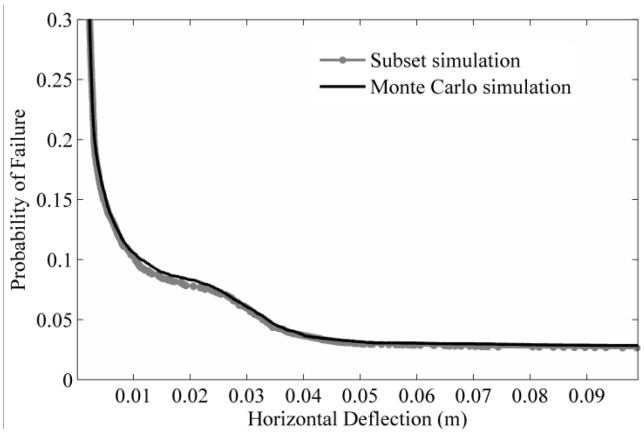

Figure 5-6 Probability of failure under different limiting values of deflection

The histograms of the conditional sampling of four selected parameters at different stages of the subset simulation are shown in Fig. 5-7. It should be noted that the solid lines represent the original distribution. The conditional distribution at different conditional levels should be different than the original distribution after the first sampling because the sampling in following iterations is under the condition that the case will be located in the intermediate failure region. The sensitivity of the response to individual uncertain parameters can be evaluated by examining the change between the conditional distribution and the original distribution. The parameters with the largest changes from the original distributions are shown in Fig. 5-7. The greater sensitivity of the response to these four parameters is in agreement with the general experience that the column would be more vulnerable under larger fire loads, with SFRM that is thinner and has higher conductivity, and for steel with lower yield strength.

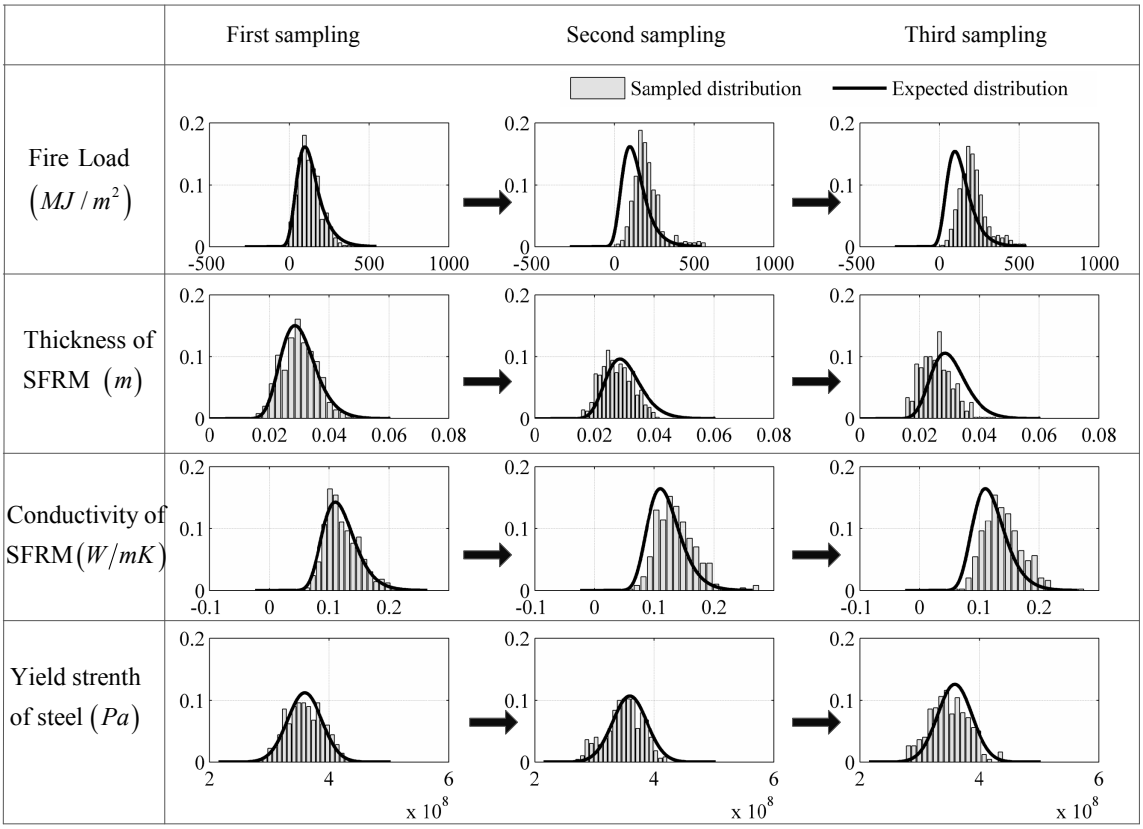

Figure 5-7 Histogram of conditional samples at different 'subset' stages

5.4 Case 2. Composite Steel-Framed Building

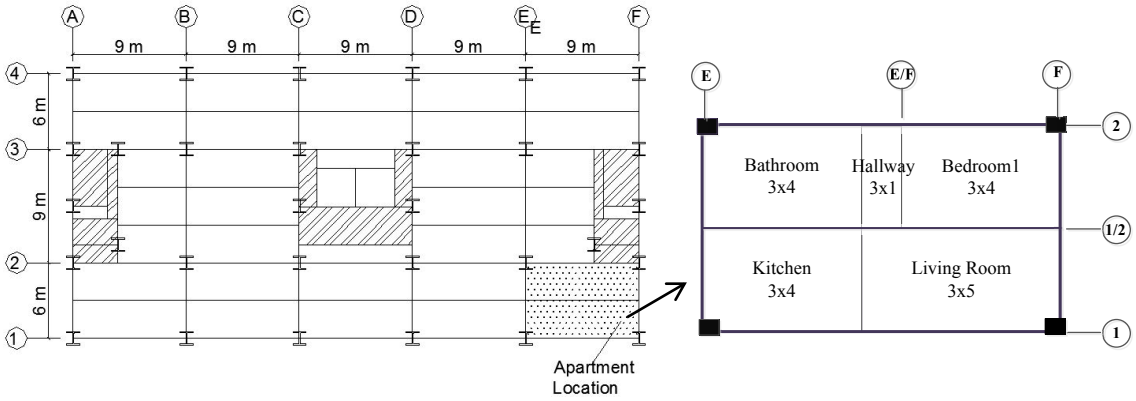

Figure 5-8 Floor plan of the composite steel-framed building: (a) structural configuration, (b) room layout

With the subset simulation adapted to the simulation of structures in fire, the analysis of a more comprehensive system is carried out. As shown in Fig. 5-8a, the detailing of the

structural system follows that of the composite steel-framed building that was tested in the Cardington fire tests. Note that the secondary floor beams were unprotected so as to develop tensile membrane action in the floor system. A one-bedroom apartment shown in Fig. 5-8b is superimposed in the corner of the building, and the fire development and spread within the apartment is considered.

5.4.1 Fire simulation

In this study, instead of using the simplified parametric fire curve, the fire behavior is simulated by the two-zone model in CFAST (Peacock et al. 2000). The one bedroom apartment shown in Fig. 5-8b has 4 major rooms: a living room, a kitchen, a bedroom, and a bathroom. The fire behavior is first validated against the Dalmarnock fire test (Rein et al. 2007). The predicted upper layer temperature in the CFAST model matches very well with the experimental result shown in Fig. 5-9, illustrating that CFAST is able to accurately predict the fire temperature in an apartment fire. Note that the multiple items of furniture were treated as a single object with a heat release rate equal to the equivalent heat release rate of all objects burning in the room. It should also be noted that the estimated heat release rate of the fire object that was used in the simulation of the Dalmarnock test was estimated from the actual oxygen consumption measured at the living room window (Koo et al. 2008).

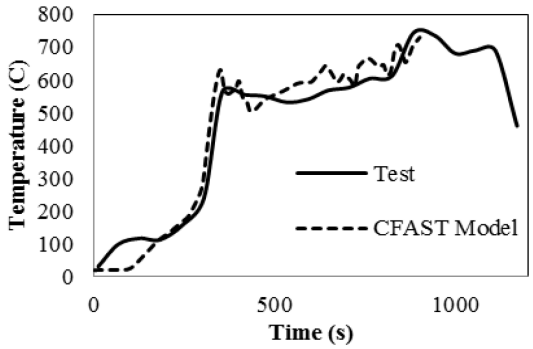

Figure 5-9 Comarison of upper layer temperature in the Dalmarnock test

In CFAST, fire spread from object to object can be simulated as (1) a time of ignition, (2) a critical temperature, or (3) a critical heat flux. Fire spread criteria based on critical temperature or critical heat flux require specification of the type of fuel that is burning in

the room, which is not always know. Several stochastic fire spread models were considered in previous studies (Elms and Buchanan 1981; Ramachandran 1990); however, they cannot be conveniently adapted into this probabilistic study nor can they utilize the latest survey data. In the present study, a concise fire growth and spread model is established that combines the latest fire incident data on the location of ignition, fuel load density, and fire spread from room to room.

In CFAST, it is possible to define multiple items (fire objects) in a compartment. However, it is generally not possible to have prior knowledge of all combustible items and their locations within a room. Thus for the fire growth inside of a room, a single burning item is used to represent the fuel load in the entire room. Koo et al. (2008) found that the differences between representing a fire as a single object and as two objects were not significant. Therefore, in our study, the fire load in a compartment is represented as a single burning object located at the center of the compartment for simplicity. Kumar and Rao (1995) investigated thirty-five residential buildings, and the statistical results of fire load in each room are shown in Table 5-2.

Table 5-2 Fire model in residential buildings (Kumar and Rao 1995; Ahrens 2013)

Room functions	Fire load (MJ/m^2)		First ignited	Spread beyond the room
	Mean	STD		
Living Room	427.6	86.9	6.7%	45%
Bedroom	495.7	170.1	11.7%	42%
Kitchen	673.0	206.9	69.9%	6%
Bathroom	382.5	124.1	-	-

The heat release rate of the single burning object is assumed to follow the t-squared fire curve, which includes a growth stage, a steady burning stage, and a decay stage. When the fire object is ignited, the heat release rate follows a parabolic relationship with time until the peak heat release rate is achieved (DiNenno 2008). The equation for heat release rate Q during the growth period is given as

$$\mathrm{Q} = (t / t_{1000})^2 , \tag{3}$$

where t_{1000} is time to reach a heat release rate of 1000 kW. The value for t_{1000} is given as 600, 300, 150, or 75 for the growth rate as slow, medium, fast, or ultrafast, respectively. In our probabilistic model, the fire is assumed to have an equal chance of developing at each of the four growth rates. Once the item reaches its peak heat release rate, the item burns under the constant heat release rate until the remaining fuel is less than 30% after which the heat release rate decreases linearly. The peak heat release rate considers both ventilation-controlled burning and fuel-controlled burning. In ventilation-controlled burning, Kawagoe (1958) summarized that the burning rate of wood fuel can be approximated by

$$\dot{\mathrm{m}} = 0.092 A_v \sqrt{H_v} , \tag{4}$$

where A_v is the area of the window opening and H_v is the height of the window opening (Buchanan 2001). The corresponding ventilation-controlled heat release rate is

$$Q_{\max} = \dot{m} \Delta H_c , \tag{5}$$

where ΔH_c is the heat of combustion of the fuel (the value of $17.5\,\mathrm{MJ/kg}$ is used in this study). In fuel controlled burning, the heat release rate can be estimated by

$$Q_{\max} = E / 1200 , \tag{6}$$

where E is the total fuel load.

The fire spread beyond a room was based on the U.S. home structure report of 2007-2011 by the National Fire Protection Association (NFPA) (Ahrens 2013). The report is based on the national fire incident reporting system (NFIR 5.0) developed by NFPA. Within the report, the ratio of the first ignited room and the subsequent probability of spread beyond the first ignited room are given as shown in Table 5-2. If the fire spread occurs, it is assumed that the room which is closest to the first ignited room begins burning, and the spread time is assumed to be any time point before the fire becomes extinct in the first ignited room. In this study, the fire spread beyond the single apartment has not been considered.

The source of uncertainty considered in the fire simulation includes the fire load, the peak heat release rate, the fire growth rate, an index to determine whether fire spread will occur or not, the time to fire spread, and the thermal inertia of the surroundings in each room.

5.4.2 Heat transfer analysis

For computational efficiency, analytical methods were used to calculate temperatures in the steel members and the finite element method was used to determine temperature in the concrete slab. The Eurocode (EC3 2005) provides an analytical approach to calculate the thermal response of unprotected and protected steel members, in which the temperature is uniformly distributed over the entire member. For unprotected beams, the increase of temperature ΔT is given by

$$\Delta T_{a,t} = k_{sh} \frac{A_m/V}{c_a \rho_a} \dot{h}_{net,d} \Delta t \qquad for\ \Delta t \le 5\text{s}, \tag{7}$$

where ρ_a is the unit mass of steel (kg/m^3), A_m/V is the section factor for the steel members (m^{-1}), c_a is the specific heat of steel (J/kgK), k_{sh} is the correction factor for the shadow effect, and $\dot{h}_{net,d}$ is the net heat flux per unit area.

The increase of temperature for protected steel members is given by

$$\Delta T_{a,t} = \frac{\lambda_p A_p/V}{d_p c_a \rho_a} \frac{\left(\theta_{g,t} - \theta_{a,t}\right)}{\left(1+\phi/3\right)} \Delta t - \left(e^{\phi/10} - 1\right) \Delta T_{g,t} \quad \text{but } \Delta T_{a,t} \ge 0 \text{ if } \Delta T_{g,t} > 0 \tag{8}$$

where T, c, and ρ are the temperature, specific heat, and unit mass and the subscript a and p refer to the steel and fire protection material, respectively. More details of the analytical approach can be found in EC3 (2005).

The Eurocode only provides a simple calculation method for slabs subjected to the standard fire exposure. Therefore, a 2D heat transfer model was generated in Abaqus to calculate the temperature gradient through the depth of the concrete slab in each room. The temperature-dependent thermal properties (i.e., thermal conductivity, density, and specific heat) of the steel and the concrete are based on the Eurocode (EC2 2005).

The uncertainty considered in the heat transfer model includes the thickness of ceramic fiber blanket for columns and the thermal conductivity of the concrete.

5.4.3 Structural model

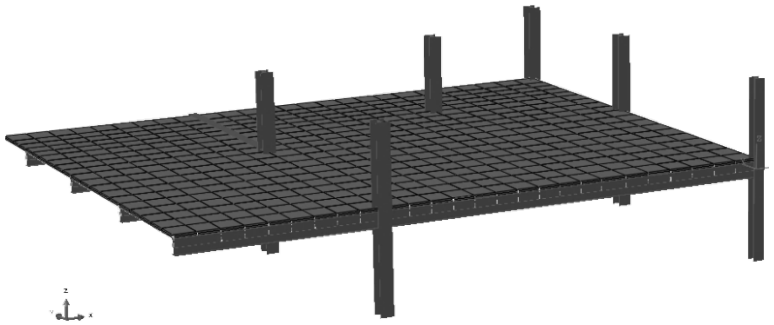

Figure 5-10 Structural model of the composite steel-framed floor system

The structural model shown in Fig. 5-10 is based on the Cardington test building. The apartment modeled in the fire simulation is assumed to be located in a corner of the first floor, which is in the similar location of Test 3 of the Cardington fire test series. Thus the model accuracy could be conveniently validated against the actual test results. With the global response of the composite floor system being of interest, a 3D macro-model of the floor system was generated using Abaqus. In this approach, the composite floor system was modeled as an assembly of beam, shell, and connector elements, to represent the steel beams, reinforced concrete slab, and shear studs, respectively. Although a continuum model has the potential to capture local failures, shell elements have additional benefits of efficiently modelling bending and membrane behavior over solid elements especially under elevated temperatures (Wang et al. 2013).

To accurately model the composite floor systems under fire, the temperature-dependent constitutive properties of steel and concrete, appropriate connection behavior, and thermal expansion have been accounted for. The Concrete Damaged-Plasticity model available in Abaqus was used to represent the inelastic behavior of plain concrete. As shown in Fig. 5-11a, the temperature dependent compressive behavior of the light-weight concrete is based on the uniaxial non-linear compressive stress-strain model defined in Eurocode (EC2 2005). The uniaxial tensile stress-strain behavior of plain concrete is

described by a bilinear curve shown in Fig. 5-11b. The tensile strength at ambient temperature was assumed to be one tenth of compressive strength at ambient temperature, and reduction factors in Eurocode (EC2 2005) were used to obtain the tensile strength at elevated temperatures. The smeared rebar layer was used to model the steel reinforcement in the concrete slab; however, this approach omits the concrete-rebar interaction, which significantly affects the tension stiffness of the reinforced concrete. In this study, the interaction was considered by decreasing the slope of the linear tensile softening branch of the post-cracking stress-strain curve (Nayal and Rasheed 2006). The uniaxial constitutive model for steel at elevated temperature also followed the Eurocode (EC3 2005) as shown in Fig. 5-12 without considering strain hardening. The thermal expansion coefficient of concrete and steel both followed the Eurocode (EC2 2005 and EC3 2005). In the Cardington test, flexible end plates and fin plates (i.e., shear tabs) were used for beam-to-column connections and beam-to-beam connections, respectively. Pinned connections were conservatively used in this study for both beam-to-beam and beam-to-column connections.

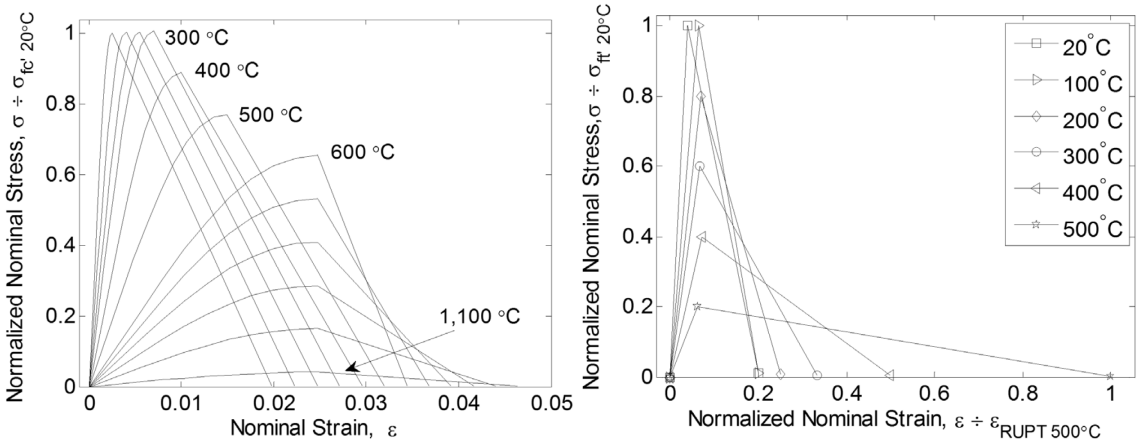

(a) (b)

Figure 5-11 Concrete strain-stress relationship at elevated temperature: (a) compression, (b) tension

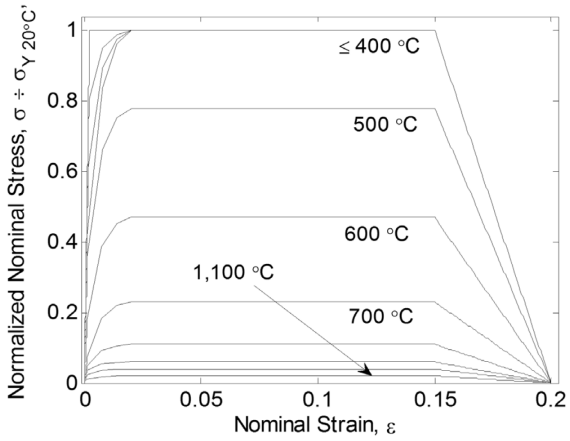

Figure 5-12 Steel strain-stress relationship at elevated temperature

The model only considered the floor system (i.e., beams, columns, and slab) of the second floor, and only one quarter of the floor system was modeled here to increase the computational efficiency of the structural analysis. The steel-concrete composite floor slab was cast onto profiled steel decking that was ribbed. The ribs have an impact on the stiffness of the floor slab in the direction parallel to the ribs, but this orthotropic property was ignored in this model for simplicity and only the top (i.e., 70mm) continuous portion of the slab was modeled. Full composite action was assumed by rigidly coupling the slab and beams together.

In the validation of the model, temperature data measured in the Cardington corner test was directly used to define the structural member temperatures in lieu of performing a heat transfer analysis. The comparison between the test result and the simulation result at the mid-span of the steel beam and center the slab is shown in Fig. 5-13. The mid-span of the beam was also the location with the largest deflection among the whole floor area during the test. The good agreement between the model and test result demonstrates that the finite element model is capable of predicting the maximum deflection of the structure at elevated temperature.

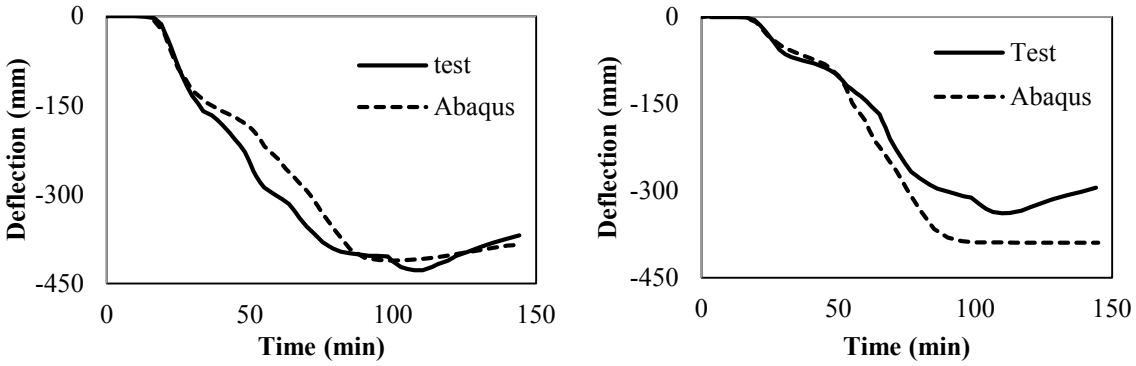

(a) (b)

Figure 5-13 Deflection of structural members: (a) mid-span of beam ½, (b) center of the slab

The uncertainty considered in the structural model includes the dead load, live load, load factors, and yield stress of steel. All uncertainties among the fire-thermal-structural modeling system are summarized in Table 5-3.

Table 5-3 Statistical properties for uncertain parameters

Uncertainties		Units	Distribution	Mean	COV	Reference
Fire Model	MaxHRR_LivingRM	KW	Normal	4744	0.1	Buchanan (2001)
	MaxHRR_Kitchen	KW	Normal	4038	0.1	
	MaxHRR_Bedroom	KW	Normal	4038	0.1	
	MaxHRR_Bathroom	KW	Normal	2381	0.1	
	FuelEnergy_LivingRM	KJ	Gumbel	6.4E6	0.20	Kumar and Rao (1995)
	FuelEnergy_Kitchen	KJ	Gumbel	8.1E6	0.34	
	FuelEnergy_Bedroom	KJ	Gumbel	5.9E6	0.31	
	FuelEnergy_Bathroom	KJ	Gumbel	4.6E6	0.32	
	Fire spread index	-	Discrete	0.5	-	Ahrens (2013)
	Spread time to closest room1	-	Discrete	0.5	-	-
	Spread time to closest room2	-	Discrete	0.5	-	-

	Fire growth rate in LivingRM	-	Discrete	0.5	-	-
	Fire growth rate in Kitchen	-	Discrete	0.5	-	-
	Fire growth rate in Bedroom	-	Discrete	0.5	-	-
	Fire growth rate in Bathroom	-	Discrete	0.5	-	-
	Thermal intertia of concrete	$J/m^2 s^{1/2} K$	Normal	1830	0.094	Iqbal and Harichandran 2010
	First ignited room	-	Discrete	0.5	-	Ahrens 2013
Heat Transfer	Thickness of column fire protection material	m	Normal	0.025	0.05	Iqbal and Harichandran 2010
	Thermal conductivity of the concrete	W/mK	Normal	EC2	0.1	
Structural model	Dead load	KN/m^2	Normal	4.32	0.1	Ellingwood (2005), Iqbal and Harichandran (2010), Ravindra and Galambos (1978)
	Live load	KN/m^2	Gamma	0.46	0.6	
	Yield of steel 50	Pa	Normal	3.7E8	0.08	
	Yield of steel 43	Pa	Normal	2.9E8	0.08	
	Load Factor A	1	Normal	1	0.04	
	Load Factor B	1	Normal	1	0.2	
	Load Factor E	1	Normal	1	0.05	

5.4.4 Latin Hypercube simulation

Latin Hypercube simulation with a sample size of 5,000 was conducted by considering the statistical properties of all random parameters listed in Table 5-3. The sampled distributions match very well with the expected distribution as shown in Fig. 5-14. The fire model, thermal analysis, and mechanical analysis were controlled by a MATLAB code, in which the structural member temperatures were seamlessly transferred to the structural model. Due to the large computational demand, simulations were run on the Flux system housed at the University of Michigan. All simulations were distributed to 8

nodes to run the jobs, and the total simulation time on each node was around 50 hours.

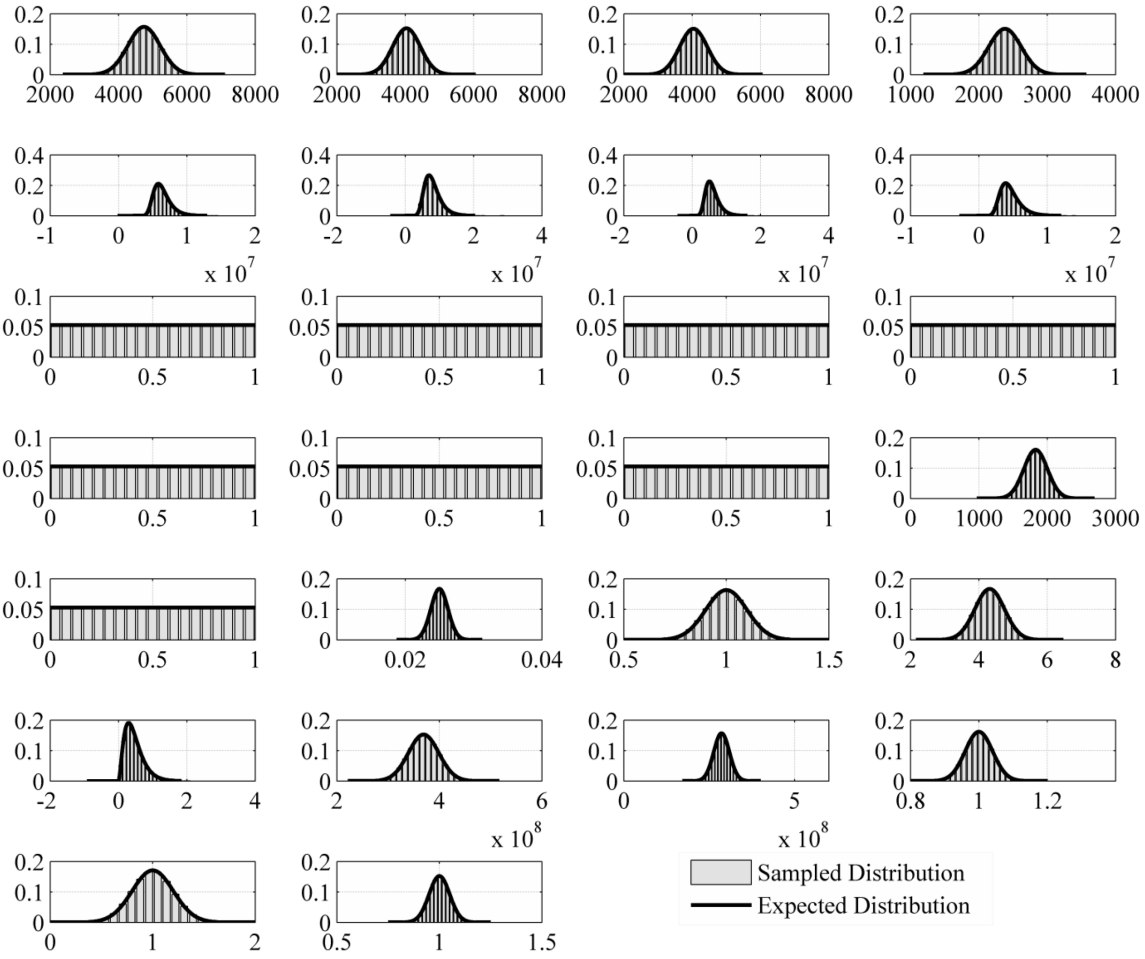

Figure 5-14 Parameter distributions

Based on the statistical characteristics of all uncertain parameters considered in the fire simulation model, a series of fire scenarios with different ignition rooms, ignition times, fire growth rates, and fire loads were obtained. The mean fire temperatures in different rooms are shown in Fig. 5-15 along with the 0.05 and 0.95 fractiles. A wide range of fires was obtained, as illustrated. The maximum fire temperature was close to 1000C while in some cases the temperature remained at ambient temperature. Because some rooms did not ignite in all fire scenarios, the mean temperature appears to be considerably lower than the maximum temperature in Fig. 5-15.

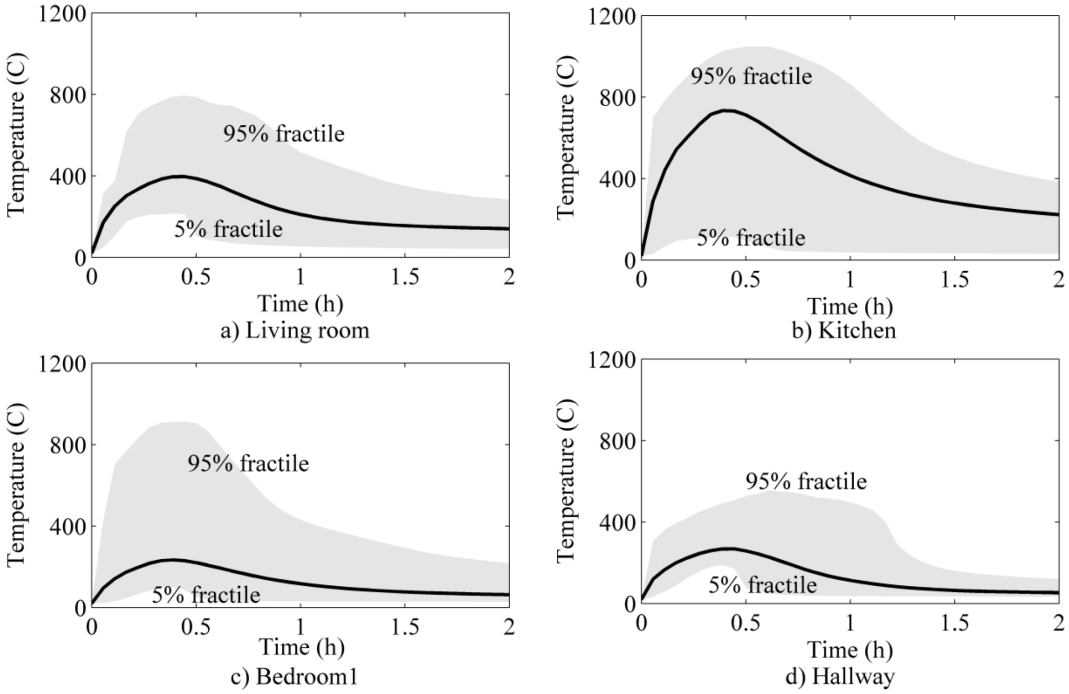

Figure 5-15 Room temperature: (a) living room, (b) kitchen, (c) bedroom, and (d) hallway

The thermal boundary conditions from these fire scenarios were passed into the heat transfer analysis described in Section 5.4.2 to obtain the temperatures of the beams, columns, and slabs. Because the kitchen has the highest probability of first ignition (as shown in Table 5-2) and the kitchen also has the highest fire temperature, the mean and 0.05 and 0.95 fractiles for the structural members around the kitchen are plotted in Fig. 5-16. The unprotected beam had temperatures that were very close to the fire temperatures. The columns were protected by the insulation, and the highest temperature of the column in the kitchen was under 250C in all fire scenarios. This signifies that there was almost no material degradation in the column, meaning that failure was not likely to occur in the column unless the fire protection had prior damage. The lower layer temperature of the slab reached as high as 1000 C, and the highest temperature at the middle layer of the slab was around 500 C. The temperature at the unexposed surface of the slab is not shown in Fig. 5-16(d) because the temperatures were lower than 200 C. According to the heat transfer analysis, the structural members in some fire scenarios have a possibility of failure as their temperatures exceeded 800 C.

The temperature of each structural member was transferred to the structural model along with the random values related to the mechanical properties of the structural materials and the load related parameters. The mean and 0.05 and 0.95 fractiles of mid-span deformations of the structural members around kitchen are shown in Figure 5-17. The maximum deflection of these structural members primarily occurred at the secondary beam and in the slab between the secondary beams and the primary beams. The mean deformation increased significantly in the first 30 minutes to one hour, and then kept increasing slowly in most cases.

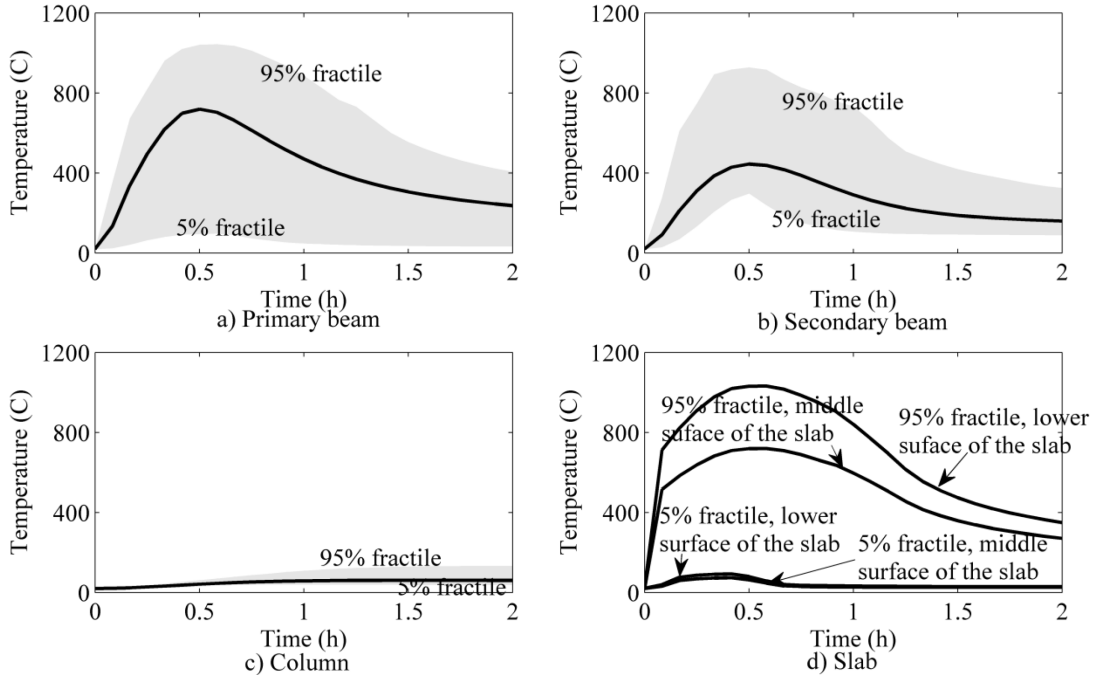

Figure 5-16 Temperature of structural members around the kitchen: (a) primary beam, (b) secondary beam, (c) column, (d) slab

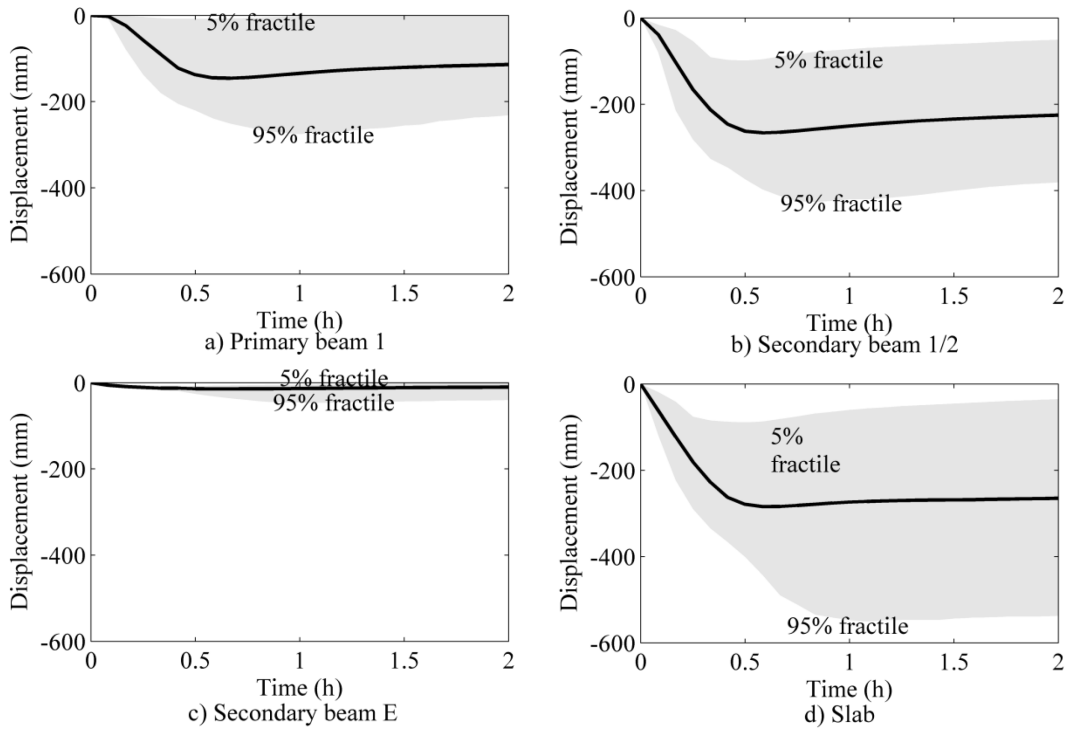

Figure 5-17 Structural response: (a) primary beam 1, (b) secondary beam ½, (c) secondary beam E, (d) slab

In the cases in which a fire spread occurred, there was more than one peak in the deformation curve, with the last peak points tending to cause the largest displacement. In order to see how the fire spread to adjacent compartments affected the structural response, one single case of the 5,000 simulations is plotted in Fig. 5-18. In this case, the fire ignited in the kitchen with a medium fire growth rate, and after 40 minutes the fire spread to the living room, as shown in Fig. 5-18(a). The slab deformation in the kitchen increased to 0.4m after the fire first ignited in the kitchen, and kept increasing another 10% after the fire spread to the living room even though the temperature in the living room was lower than the initial peak temperature. This result illustrates that a building with several rooms could have a different failure pattern than a single large compartment, and the fire spread between rooms could cause a more severe situation than a single compartment fire.

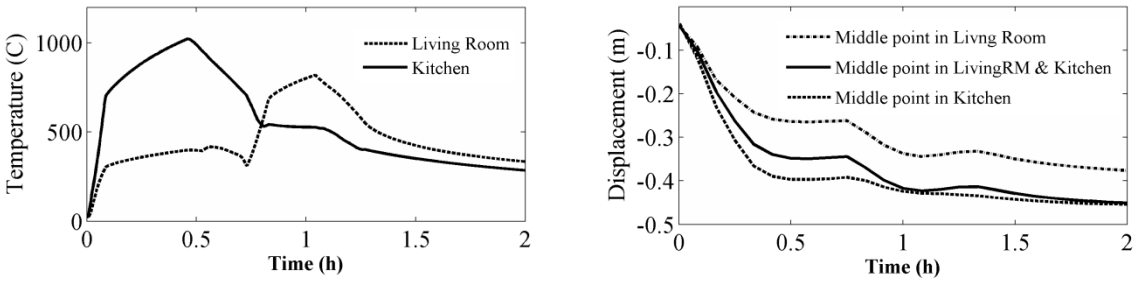

(a) Room temperature (b) Slab deformation

Figure 5-18 Single case involving fire spread from the kitchen to the living room: (a) gas temperature, (b) slab deformation

For the reliability analysis, failure was defined by the limiting displacement of L/15 for each beam and slab. The probability of failure P_f was calculated by evaluating the ratio of the failed cases to all sampled cases. There were 246 simulations that failed out of a total of 5,000 simulations, resulting in a failure probability of 4.92%.

5.4.5 Subset simulation

Multiple failure criteria exist in this application because the limiting deflection must be applied to all beams as well as the slab. To transfer the multiple failure criteria problem to a single failure criterion problem, a "critical demand to capacity ratio" is introduced as (Au and Beck 2001)

$$Y(\boldsymbol{\theta}) = \max_{j=1,\ldots,L} \min_{k=1,\ldots,L_j} \frac{D_{jk}(\boldsymbol{\theta})}{C_{jk}(\boldsymbol{\theta})} \tag{10}$$

where $D_{jk}(\boldsymbol{\theta})$, $C_{jk}(\boldsymbol{\theta})$ refer to the demand and capacity variables of the (j, k) component of a system. Thus the failure region becomes

$$F = \{Y(\boldsymbol{\theta}) > 1\} \tag{11}$$

In this problem, there is only one failure criterion for each structural member, so the critical demand to capacity ratio is

$$Y(\boldsymbol{\theta}) = \max_{j=1,\ldots,L} \frac{D_j(\boldsymbol{\theta})}{C_j(\boldsymbol{\theta})}, \tag{12}$$

where $D_j(\boldsymbol{\theta})$ is maximum deflection of the structural member and $C_j(\boldsymbol{\theta})$ equals to one fifteenth of the total span.

In the subset simulation, the first step is the same as the standard Monte Carlo simulation with a sample size of 500. The threshold value $p = 0.2$ is used to define the intermediate failure region. As shown in Fig. 5-19 there are 26 of 500 cases located in the target failure region after the first sampling. The first intermediate failure region is generated based on this result. The Markov Chain Monte Carlo simulation then generates another 400 cases within the first intermediate failure region. After the second sampling, there are 115 of 500 cases located in the target failure region, which is larger than the threshold value 0.2, so subset simulation is stopped here. The total failure probability is 4.6%, which is very close to the LHS result of 4.92%. The probability of failure is plotted against limiting deflection in Fig. 5-20 for the LHS and subset simulation and it is show that the two simulations match very well.

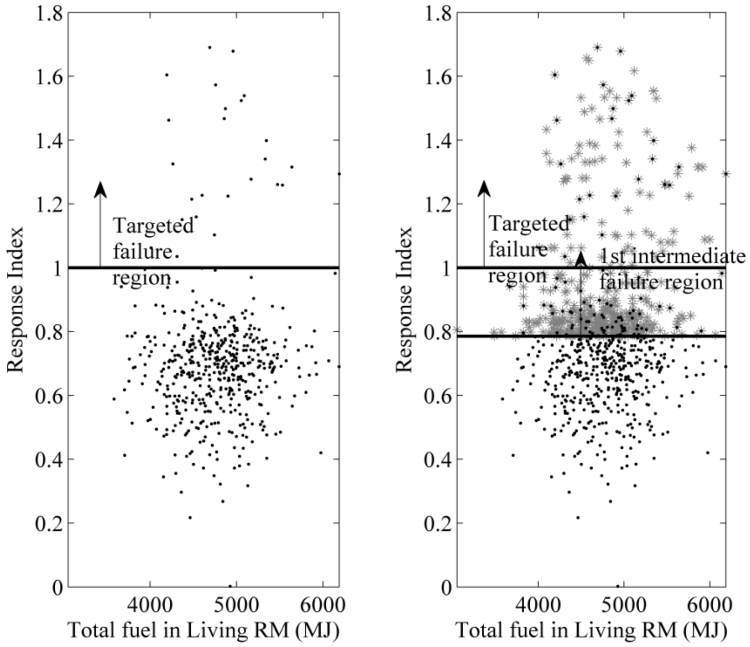

(a) (b)

Figure 5-19 Subset simulation: (a) step1, (b) step 2

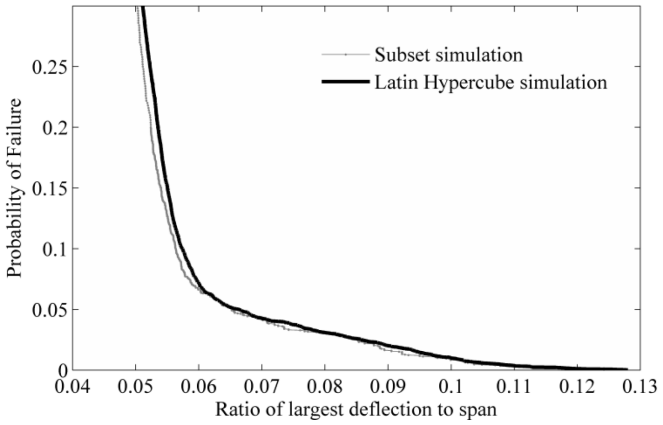

Figure 5-20 Probability of failure under different limiting values of deflection

The total simulation time of the Subset simulation was 43 hours one a single node with 2 CPUs whereas the Latin Hypercube simulation required more than 50 hours on 8 nodes. Although the total computing time is similar, the subset simulation required fewer resources as the calculation could be performed on a single node. This is significant because parallel computing systems are costly and not always available. Thus, the subset simulation is preferred to Latin Hypercube simulation. Moreover, the improvement on computational efficiency by using subset simulation will be more prominent in a system with an extremely small failure probability (e.g., less than 10^{-3}). Note that the failure probability is relatively high in this study as it is a conditonal probability based on the assumption that all suppression systems failed to work. Considering the annual fire occurance rate and the performance of fire suppression system in the fire simulation, the expected failure probability will be on the order of 10^{-5} (Phan 2010), making subset simulation even more attractive.

5.5 Conclusions

Under the framework for the evaluation of structural reliability under fire, the fire, heat transfer, and structural analyses were coupled to simulate the stochastic response of structures subjected to a realistic fire hazards. The reliability of an isolated structural column and a composite floor system were investigated. Subset simulation was introduced for the reliability assessment of structures in fire, and it was shown that the subset simulation required significantly less computational resources over Latin

Hypercube simulation. The cost savings will be amplified for systems that have small probabilities of failure.

The paper considers the reliability of a structural system rather than focusing on individual structural members. A fire spread model based on the latest NFPA survey data was combined with a zone fire to conduct a realistic fire simulation in a residential building with multiple compartments. The thermal and mechanical responses of the structure were simulated by 1D heat transfer analysis and a 3D structural analysis, respectively. Membrane action and thermally induced internal forces were considered in the structural model. The results showed that the unprotected composite floor system experienced a large deflection under severe fire exposure. Additionally, it was found that fire spread between multiple rooms has the potential to produce larger deflections that may lead to failure of the system. This finding challenges the current methodology that is based on the assumption that the fire is contained to a single compartment and justifies research on traveling fire.

This study successfully extended the Latin Hypercube simulation and the subset simulation to evaluate the system-level reliability of structures in fire. It was found that both methods yield consistent results. The relationship between the limiting deflection and the failure probability were also provided to help designers identify suitable failure criteria for structural systems. The quantification of structural reliability in fire allows the analyst to conduct a system-level design that is based on an acceptable level of risk, which is an essential component to performance-based design.

References

Ahrens, M. (2013). *Home Structure Fires***,** National Fire Protection Association, Quincy, MA.

AISC. (2011). "Steel Construction Manual Design Example v14.0." ⟨http://www.aisc.org/WorkArea/showcontent.aspx?id=29596⟩.

Au, S.K., and Beck, J.L. (2001). "Estimation of Small Failure Probabilities in High Dimensions by Subset Simulation," *Probabilistic Engineering Mechanics,* 16(4), 263-277.

Breeding, R.J., Helton, J.C., Gorham, E.D., and Harper, F.T. (1992). "Summary Description of the Methods Used in the Probabilistic Risk Assessments for NUREG-1150," *Nuclear Engineering and Design*, 135(1), 1-27.

Buchanan, A.H. (2001). *Structural Design for Fire Safety*, Wiley, New York.

Culver, C.G. (1976). "Survey Results for Fire Loads and Live loads in Office Buildings," *Building Science Series No. 85*, National Bureau of Standards, Washington, DC.

DiNenno, P. J. (2008). *SFPE Handbook of Fire Protection Engineering*, Fourth Edition, SFPE, Bethesda, Maryland.

Eamon, C.D., and Jensen, E. (2012). "Reliability Analysis of Prestressed Concrete Beams Exposed to Fire," *Engineering Structures*, 43, 69-77.

EC1 (2005). *Eurocode 1: Basis of Design and Action on Structures, Part 1-2: Actions on Structures-Actions on Structures Exposed to Fire*, British Standards Institution, London.

EC2 (2005). *Eurocode 2: Design of Concrete Structures, General Rules and Rules for Buildings and Structural Fire Design*, British Standards Institution, London.

EC3 (2005). *Eurocode 3: Design of Steel Structures, General Rules and Rules for*

Buidings and Structural Fire Design, British Standards Institution, London.

Elms, D.G., and Buchanan, A.H. (1981). "Fire Spread Analysis of Buildings," Research Report R35, Building Research Association of New Zealand.

Guo, Q., and Jeffers, A.E. (2014). "Finite-Element Reliability Analysis of Structures Subjected to Fire," *Journal of Structural Engineering*, doi: 10.1061/(ASCE)ST.1943-541X.0001082.

Guo, Q., Shi, K., Jia, Z., and Jeffers, A.E. (2013). "Probabilistic Evaluation of Structural Fire Resistance," *Fire technology*, 49(3), 793-811.

Helton, J.C., and Davis, F.J. (2003). "Latin Hypercube Sampling and the Propagation of Uncertainty in Analyses of Complex Systems," *Reliability Engineering & System Safety*, 81(1), 23-69.

Iqbal, S., and Harichandran, R.S. (2010). "Capacity Reduction and Fire Load Factors for Design of Steel Members Exposed to Fire," *Journal of Structural Engineering*, 136, 1554-1562.

Jeffers, A.E., and Sotelino, E.D. (2009). "Fiber Heat Transfer Element for Modeling the Thermal Response of Structures in Fire." *Journal of Structural engineering*, 135(10), 1191-1200.

Jensen, E., Van Horn, J., and Eamon, C.D. (2010). "Variability of Fire and Concrete Temperatures and the Associated Uncertainty in Structural Behavior", *Proceedings of 6th International Conference on Structures in Fire*, Kodur, V., and Franssen, J.M., Eds., DEStech Publications, USA, 959-966, 2010.

Kawagoe, K. (1958). "Fire Behaviour in Rooms," Building Research Institute, Report 27, Japan.

Koo, S.H., Fraser-Mitchell, J., Upadhyay, R., and Welch, S. (2008). "Sensor-Linked Fire Simulation using a Monte-Carlo Approach," *Proceedings of 9th*

International Symposium about Fire Safety Science, Karlsruhe, Germany.

Kumar, S., and Rao, C.V.S. (1995). "Fire Load in Residential Buildings", *Building and Environment*, 30(2), 299-305.

Lange, D., Devaney, S., and Usmani, A. (2014). "An Application of the PEER Performance Based Earthquake Engineering Framework to Structures in Fire," *Engineering Structures*, 66, 100-115.

Mckay, M.D., Beckman, R.J., and Conover, W.J. (1979). "A Comparison of Three Methods for Selecting Values of Input Variables in the Analysis of Output from a Computer Code," *Technometrics*, 21(2), 239-245.

Nayal, R., and Rasheed, H. (2006). "Tension Stiffening Model for Concrete Beams Reinforced with Steel and FRP Bars," *Journal of Materials in Civil Engineering*, 18, 831-841.

Nigro, E., Bilotta, A., Asprone, D., Jalayer, F., Prota, A., and Manfredi, G. (2014). "Probabilistic Approach for Failure Assessment of Steel Structures in Fire by means of Plastic Limit Analysis," *Fire Safety Journal*, 68, 16-29.

Olsson, A., Sabdberg, G., and Dahlblom, O. (2003). "On Latin Hypercube Sampling for Structural Reliability Analysis," *Structural Safety*, 25, 47–68.

Peacock, R.D., Reneke, P.A., Jones, W.W., Bukowski, R.W., Forney, G.P., *A User's Guide for FAST: Engineering Tools for Estimating Fire Growth and Smoke Transport,* NIST Special Publication 921, National Institute of Standards and Technology, Gaithersburg, MD.

Phan, L.T., McAllister, T.P., Gross, J.L., and Hurley, M.J. (2010). "Best Practice Guidelines for Structural Fire Resistance Design of Concrete and Steel Buildings," National Institute of Standards and Technology, Gaithersburg, MD.

Ramachandran, G. (1990). "Probability-Based Fire Safety Code", *Journal of Fire*

Protection Engineering, 3(2), 37-48.

Ravindra, M.K., and Galambos, T.V. (1978). "Load and Resistance Factor Design for Steel." *Journal of the Structural Division,* 104(9), 1337–1353.

Rein, G., Empis, C.A., and Carvel, R (2007). *The Dalmarnock Fire Tests: Experiments and Modelling*, School of Engineering and Electronics, University of Edinburgh, UK.

Van Coile, R., Caspeele, R., and Taerwe, L. (2014), "Reliability-Based Evaluation of the Inherent Safety Presumptions in Common Fire Safety Design," *Engineering Structures,* 77, 181-192.

Wang, Y., Burgess, I., Wald, F., and Gillie, M. (2012). *Performance-Based Fire Engineering of Structures*, CRC Press, Taylor & Francis Group, Boca Raton, FL.

Zio, E. (2013). *The Monte Carlo Simulation Method for System Reliability and Risk Analysis*. Springer, London.

CHAPTER 6 : SUMMARY, CONCLUSIONS, AND FUTURE WORK

With the development of the performance-based fire resistant design methodology, the evaluation of the structural performance in fire is needed in the design procedure. Compared to experimental tests, computational simulations are more attractive because are low-cost and capable of considering the system-level performance. However, most of the processes associated with fire-structure interaction are uncertain in nature. It becomes necessary to quantify the safety margin to ensure consistent reliability in the final application. In this study a framework for the reliability evaluation has been established to provide accurate and efficient structural reliability assessment under realistic fires. The reliability levels of both isolated structural members and composite structural systems have been calculated by extending reliability methods to the sequentially coupled structural-fire simulation. The investigations described herein have demonstrated that the proposed reliability evaluation framework is able to handle the large number of uncertain parameters that exist in the structural-fire simulation and thus promote further development of performance-based design with a quantified reliability level.

This chapter provides a summary of the work described in this dissertation. The first section in this chapter gives an overview of the methodology applied in previous chapters and a summary of key findings. The second section describes the limitations of the proposed approach and directions for future research.

6.1 Summary and Conclusions

The probabilistic framework described in the Chapter 2 is an innovative work to evaluate the structural fire resistance considering the uncertainty that exists in the fire behavior and the thermo-mechanical response of structures. The sensitivity analysis has been proposed to reduce the model dimensionality, and a deflection based limit state function was used to define the failure of the structural member. The deterministic analysis results have been compared with the probabilistic approach. Latin Hyper cube simulation has

been selected to sample uncertain parameters based on their distributions in the probabilistic analysis. The results shows that the protected beam with a 1-hour fire resistance rating under standard fire test still has a significant conditional failure probability when the wide range of uncertainties in the system are taken into account. The study demonstrates the importance of ensuring a consistent safety level in the fire resistant design of structures. Moreover, this study provides a method to help designers compare alternative design strategies based on the reliability level and identify the important factors in the structural fire protection.

The direct differentiation method (DDM) has been extended to the analysis of structures in fire in Chapter 3. The formulation of the structural sensitivity to parameters in the fire, thermal, and structural analyses was given by differentiating the governing finite element equations for the sequentially coupled nonlinear heat transfer and structural analysis. The proposed DDM method has been compared with the finite difference method (FDM) in the analysis of the response sensitivities of a protected beam exposed to a natural compartment fire. Significant cost savings have been observed in the DDM result as no additional simulations of perturbed parameters are needed. This work proposes a new approach to calculate the response sensitivity of structures exposed to fire with improved accuracy and efficiency, and both the reliability analysis and design optimization problem that needs to calculate the response gradient will benefit from this study.

In Chapter 4, the analytical reliability methods (i.e., first/second order reliability methods) have also been extended to the structural-fire problem. In the first/second order reliability methods (FORM/SORM), the limit state function is approached by the linear or quadratic equations around the design point. The methods transfer the task from determining the whole response surface to searching for the design point, which can significantly save computing time. A comparison between FORM/SORM and Latin Hypercube simulation has been conducted on a protected steel column. The results showed that the FORM can provide a very rapid estimation of the failure probability of structures subjected to fire; however, the error from FORM/SORM cannot be estimated without a careful error analysis. The direct differentiation method introduced in Chapter 3 has also been applied

in searching for the design point, which demonstrates significant improvement in computing cost especially when a large number of parameters exist.

The established reliability evaluation framework has investigated the performance of a protected steel column and a composite steel-framed floor system in Chapter 5. A probabilistic fire spread and development model was produced to consider more realistic fire behaviors using the zone model software CFAST. The thermal and mechanical analyses were conducted using Abaqus. A MATLAB code controlled and connected the three phases of analysis by transferring gas temperature and structural members' temperature. The macro structural model accounted for the membrane action and thermally induced internal forces in the structural system at elevated temperature, which has always been ignored in the standard fire tests and numerical simulations of the isolated structural members. The reliability assessment in the study considered the comprehensive structural performance under fire, and the analysis also showed that the failure pattern could be different by considering the real building partitions and it could cause more severe situations if the fire spread between rooms is considered.

In Chapter 5, the subset simulation was applied to investigate the structural reliability under fire for the first time. The system level reliability of structural fire resistance was assessed by applying both the Latin hypercube simulation and subset simulation, and the subset simulation showed a great saving in computational cost when the estimated failure probability is small. The analysis demonstrated that the failure probability is able to be quantified under the proposed reliability evaluation framework, which allows the analyst to efficiently evaluate the structural fire protection design based on the given reliability level and eventually help to realize a holistic performance-based fire resistance design.

6.2 Limitations and Future Work

This dissertation considers a framework to assess the structural reliability under fire. Under the reliability framework, the failure probability (or reliability index) can be calculated. The active fire protection systems including the automatic fire detection system, sprinkler system, and fire brigade performance are not considered at the current stage of the study. Involving the active fire protection system into the fire behavior

modeling makes the model closer to the realistic situation. In general, the critical stress cannot be determined for structures in fire because of non-uniform heating. Therefore, the structural failure criteria used in this study are displacement-based requirements. Additional work can be done to consider the localized failures when structures are subjected to fire.

The analyses conducted here are based on the statistical data reported in the literature. This data came from a variety of sources over a large time span and were not initially collected for the structural-fire reliability analysis. Thus the reliability calculated in this study may not necessarily reflect an actual building's behavior. It is recommended that future work should include more current and specific data that will lead to greater accuracy in the reliability models.

The compartments in this study were relatively small in size and limited primarily to post-flashover fires. As performance-based design is becoming increasingly common in high-rise office buildings and structures for special public functions (e.g., public transit centers, theaters, and stadiums), research is needed to evaluate the response of fires in large open spaces. Probabilistic traveling fire models are one potential way forward towards considering the reliability of these special types of structures. Moreover, this research considered only a portion of the structural system for computational efficiency. Therefore, the symmetric boundary conditions that were applied are not necessarily representative of the true restraint provided by the surrounding structure. With the development of more powerful computing technologies and the use of more efficient reliability methods, the consideration of full-scale structural systems may be possible.

.